2-12-2009

# Characterization of Putative Self-Resistance Genes in the Biosynthetic gene cluster of hygromycin A from Streptomyces hygroscopicus NRRL 2388

Vidya Dhote
*Portland State University*



Recommended Citation
Dhote, Vidya, "Characterization of Putative Self-Resistance Genes in the Biosynthetic gene cluster of hygromycin A from Streptomyces hygroscopicus NRRL 2388" (2009). *Dissertations and Theses*. Paper 6174.
https://doi.org/10.15760/etd.8034

# CHARACTERIZATION OF PUTATIVE SELF-RESISTANCE GENES IN THE BIOSYNTHETIC GENE CLUSTER OF HYGROMYCIN A FROM *STREPTOMYCES HYGROSCOPICUS* NRRL 2388

by

VIDYA DHOTE

A dissertation submitted in partial fulfillment of the
requirements for the degree of

DOCTOR OF PHILOSOPHY
in
CHEMISTRY

Portland State University
2009

DISSERTATION APPROVAL

The abstract and dissertation of Vidya Dhote for the Doctor of Philosophy in Chemistry were presented February 12, 2009, and accepted by the dissertation committee and the doctoral program.

COMMITTEE APPROVALS:

[redacted]
Kevin A. Reynolds, Chair

[redacted]
David H. Peyton

[redacted]
Dirk Iwata-Reuyl

[redacted]
Anna-Louise Reysenbach

[redacted]
Jason Podrabsky
Representative of the Office of Graduate Studies

DOCTORAL PROGRAM APPROVAL:

[redacted]
Kevin A. Reynolds, Director
Chemistry Ph.D. Program

# ABSTRACT

An abstract of the dissertation of Vidya Dhote for the Doctor of Philosophy in Chemistry presented February 12, 2009.

Title: Characterization of Putative Self-Resistance Genes in the Biosynthetic Gene Cluster of Hygromycin A from *Streptomyces hygroscopicus* NRRL 2388

*Streptomyces hygroscopicus* NRRL 2388 produces an aminocyclitol antibiotic called hygromycin A (HA), which targets bacterial protein synthesis by inhibiting the peptidyl transferase reaction. The *hyg6*, *hyg19*, *hyg21*, *hyg28*, and *hyg29* genes in the biosynthetic gene cluster of HA are predicted to confer self-resistance to the producer strain by different mechanisms. Targeted gene disruptions and *in vitro* characterization of recombinant proteins were carried out to elucidate the functions of these genes. The *hyg21* gene encodes an *O*-phosphotransferase with a proposed role in HA inactivation by phosphorylation. Disruption of *hyg21* led to a significant decrease in HA production but did not affect self-resistance. The recombinant Hyg21 phosphorylated HA and its analogs bearing a conserved fucofuranose moiety, using ATP or GTP as phosphoryl donor. The phosphorylated HA was inactive against HA-sensitive *E. coli* and *Streptomyces* strains, and also lacked the ability to inhibit *in vitro* protein synthesis.

The *hyg6* and *hyg29* genes are methyltransferase homologs and are predicted to confer resistance by ribosomal RNA methylation. Disruption of *hyg6* resulted in the

production of desmethylenehygromycin A and 5"-dihydrodesmethylenehygromycin A, which lacked the C4-C5 methylenedioxy bridge characteristic of HA. Desmethylenehygromycin A had higher protein synthesis inhibition activity than HA but significantly lesser antibiotic activity. Disruption of *hyg29* did not affect self-resistance but the antibiotic yield was reduced.

The *hyg19* and *hyg28* genes putatively encode a proton gradient-dependent transporter and an ATP-binding cassette transporter, respectively, and are hypothesized to confer resistance by antibiotic efflux. A Δ*hyg28* mutant resembled the wild type in antibiotic production and self-resistance levels. A Δ*hyg19* mutant produced lesser amounts of HA and also showed accumulation of 5"-dihydrohygromycin A, but there was no decrease in resistance. Disrupting *hyg19* together with *hyg21* significantly increased HA sensitivity, indicating that HA self-resistance in the producer strain arises by synergistic functioning of multiple gene products. Accumulation of 5"-dihydrohygromycin A in Δ*hyg19* also suggested that this compound is the immediate biosynthetic precursor of HA and that its dehydrogenation is coupled with efficient HA efflux. A short chain dehydrogenase encoded by *hyg26* was shown to reversibly catalyze the above reaction using NAD(H) as cofactor.

**Acknowledgements**

I wish to express my sincere gratitude to Dr. Kevin Reynolds for giving me the opportunity to work in his research group. It is his supervision, constant encouragement, and continual support that have made this thesis possible. I am also greatly indebted to all the members in the Reynolds group for sharing their expertise with me, and for creating such a stimulating, yet fun-filled environment of learning and growth. I especially extend my warmest thanks to Dr. Galina Florova, Dr. Nadaraj Palaniappan, and Dr. Mohini Ghatge for patiently advising me whenever I needed a sense of direction. My sincere thanks and appreciation are due to members of my advisory committee, Dr. David Peyton, Dr. Dirk Iwata-Reuyl, Dr. Anna-Louise Reysenbach, and Dr. Jason Podrabsky for their generous time, constructive criticism, and helpful suggestions during the different stages of my graduate career.

I would also like to thank Dr. Antonio Jimenez from Centra de Biología Molecular Severo Ochoa, Madrid, for providing with antibiotic A201A, and Dr. Daniel Wilson and Ms. Agata Starosta from Gene Center, Munich, for conducting the coupled transcription-translation assays.

My loving thanks go to all my friends, especially Sucheta Tripathy, Anupama Samuel, Sailaja and Krishna Mohan, Suji Uppalapati, and all in the Bremner family for always being there for me. Finally, and most importantly, I humbly offer my heartfelt thanks to my family. I dedicate this thesis to my parents, Ramesh Kumar and Suman Dhote, whose unconditional love and endless support have been the greatest

source of strength and inspiration for me. I also fondly thank my sister, Shivani, and my brother, Aditya, for their warmth and affection, which I will always cherish.

## Table of Contents

## List of Tables

## List of Figures

## List of Abbreviations

| | |
|---|---|
| ACP | Acyl carrier protein |
| Ala | Alanine |
| Arg | Arginine |
| Asp | Aspartate |
| AT | Acyltransferase |
| ATP | Adenosine triphosphate |
| bp | Base pair |
| C | Cytosine |
| CoA | Coenzyme A |
| COSY | Correlation spectroscopy |
| DH | β-hydroxyacyl ACP dehydratase |
| DNA | Deoxyribonucleic acid |
| EDTA | Ethylenediaminetetraacetic acid |
| ER | Enoyl ACP reductase |
| FAS | Fatty acid synthase |
| G | Guanine |
| Glu | Glutamate |
| GTP | Guanosine triphosphate |
| HA | Hygromycin A |
| HA-P | Phosphorylated hygromycin A |
| His | Histidine |

| | |
|---|---|
| HPLC | High performance liquid chromatography |
| hr | Hours |
| IPTG | Isopropyl thio-β-D-galactoside |
| KR | β-ketoacyl ACP reductase |
| KS | β-ketoacyl ACP synthase |
| LB | Luria broth |
| Lys | Lysine |
| MDH | Mannose dehydratase |
| min | Minutes |
| mRNA | Messenger RNA |
| MS | Mass spectrometry |
| $NAD^+$ | Nicotinamide adenine dinucleotide, oxidized form |
| NADH | Nicotinamide adenine dinucleotide, reduced form |
| $NADP^+$ | Nicotinamide adenine dinucleotide phosphate, oxidized form |
| NADPH | Nicotinamide adenine dinucleotide phosphate, reduced form |
| NDP | Nucleotide diphosphate |
| Ni-NTA | Nickel-nitrilotriacetate |
| NMR | Nuclear magnetic resonance spectroscopy |
| ORF | Open reading frame |
| PKS | Polyketide synthase |
| RNA | Ribonucleic acid |
| rRNA | Ribosomal RNA |

| | |
|---|---|
| SAM | S-adenosyl-L-methionine |
| SDS PAGE | Sodium dodecyl sulphate polyacrylamide gel electrophoresis |
| TCEP | Tris(2-carboxyethyl) phosphine |
| Thr | Threonine |

# 1. Introduction

## 1.1 General introduction to *Streptomyces* and secondary metabolic pathways

The *Streptomyces* genus, within the bacterial order Actinomycetales, is comprised of Gram-positive, filamentous, soil bacteria with a characteristically high G+C content (> 60%) in their genome [1]. These bacteria show complex morphological differentiation in their life cycle, similar to filamentous fungi, and therefore, are regarded as 'boundary organisms' between prokaryotes and eukaryotes [2]. The streptomycete life cycle begins with the germination of spores to form filamentous, branched, aseptate structures called hyphae. The hyphae spread out extensively on solid medium and form the substrate mycelium. Subsequently, some hyphae grow away from the substrate to form the aerial mycelium. When growth in the aerial mycelium ceases, they develop septa and form unigenomic compartments that mature into spores. The appearance of aerial mycelium coincides with the activation of secondary metabolic pathways (pathways that are not directly involved in the normal growth and development of an organism), which synthesize a large number of structurally diverse compounds. The function of these 'natural products' in the bacteria producing them is to serve as defense molecules, or as signals for cellular differentiation or cell-cell communication, thereby conferring ecological advantages to the producer species in their environmental niches [3]. The importance of these compounds to humans lies in the fact that they also possess interesting pharmacological properties and have found clinical applications as antibiotics (eg. erythromycin, tetracycline), antifungal compounds (eg. amphotericin B, nystatin),

anticancer agents (eg. doxorubicin, chromomycin), cholesterol-lowering drugs (eg. lovastatin, pravastatin), immunosuppressants (eg. rapamycin, FK506), livestock growth promoters (eg. monensin, tylosin), and insecticides (eg. spinosad) (FIGURE 1).

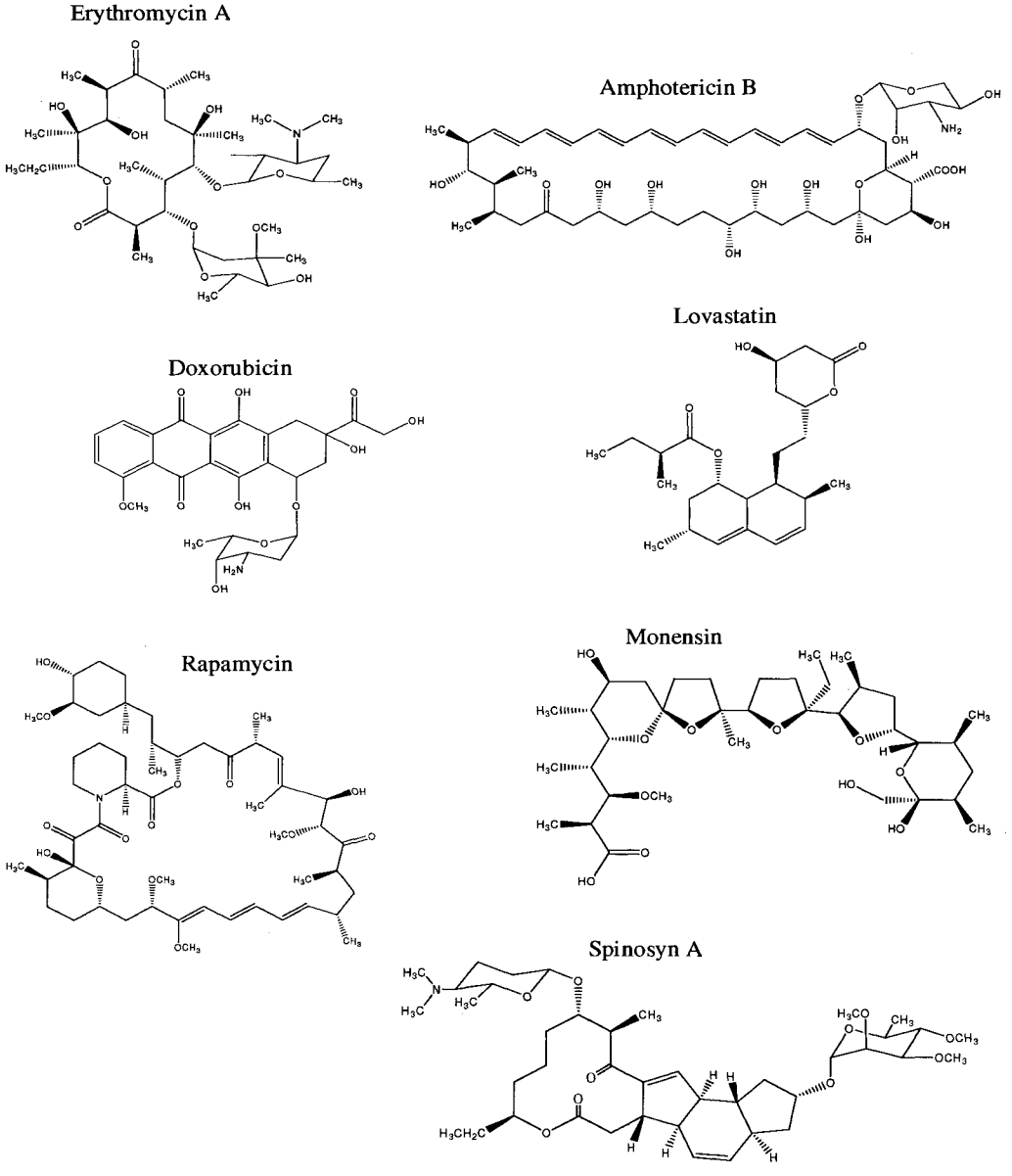


**FIGURE 1. Examples of commercially important compounds from streptomycetes**

The genes encoding the biosynthesis of a given secondary metabolite are typically clustered within the genome of the producing organism, and may have evolved by duplication of existing primary metabolic genes [4, 5]. Biosynthesis of the secondary metabolites proceeds from precursors that are intermediates or products of primary metabolism, and the enzymes involved show significant structural and functional similarities to primary metabolic enzymes. This is exemplified by the polyketide synthases (PKS) from which the largest class of secondary metabolites, namely the polyketides, is derived. Polyketide biosynthesis occurs in a manner analogous to fatty acid biosynthesis, and a component of the PKS can be functionally complemented, to some extent, by its counterpart in the fatty acid synthase (FAS) system [6-8]. Fatty acid synthases synthesize long-chain saturated fatty acids from acetyl-CoA and malonyl-CoA through a series of iterative decarboxylative condensation, ketoreduction, dehydration, and enoyl reduction steps. The FAS system is comprised of either a single multi-domain polypeptide carrying out several catalytic functions (Type I FAS) as in vertebrates, or a set of monofunctional proteins (Type II FAS) as in bacteria and higher plants. Similar to FASs, type I PKSs comprised of multimodular proteins, and type II PKSs comprised of multiple dissociable enzymes are present (FIGURE 2) [9]. A third type of PKS, type III, also exists, which is composed of iteratively-acting dimeric enzymes but is independent of the non-catalytic acyl carrier protein (ACP) component.

**A. Type I PKS (Modular, non-iterative) Eg. Erythromycin PKS**

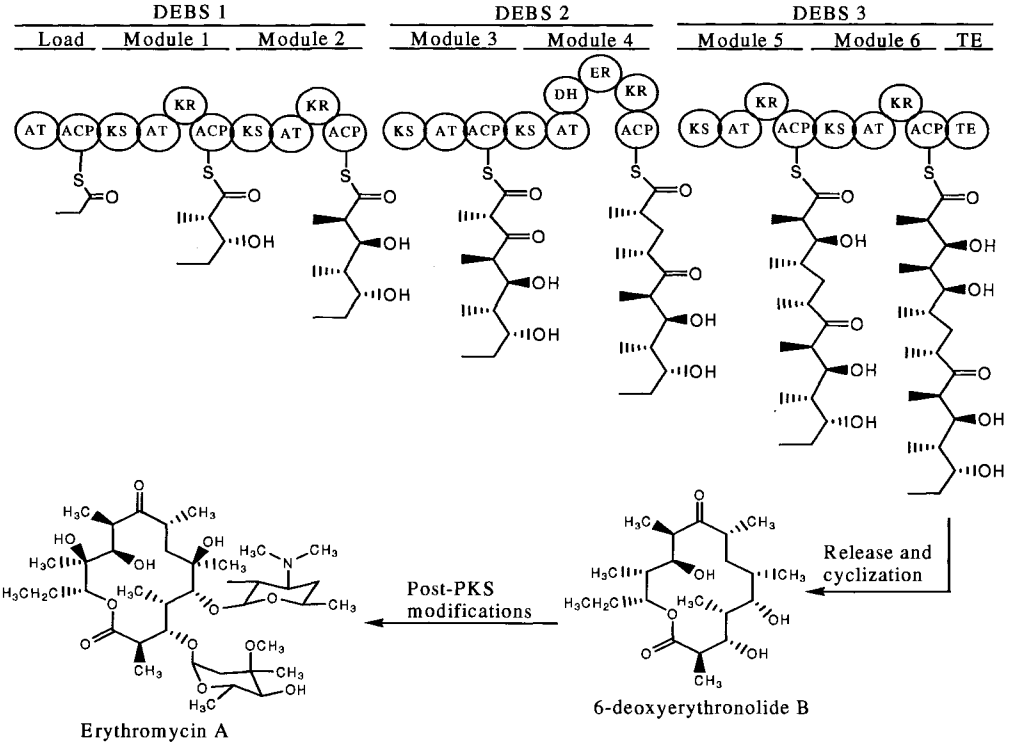


**B. Type II PKS (Non-iterative) Eg. Tetracenomycin PKS**

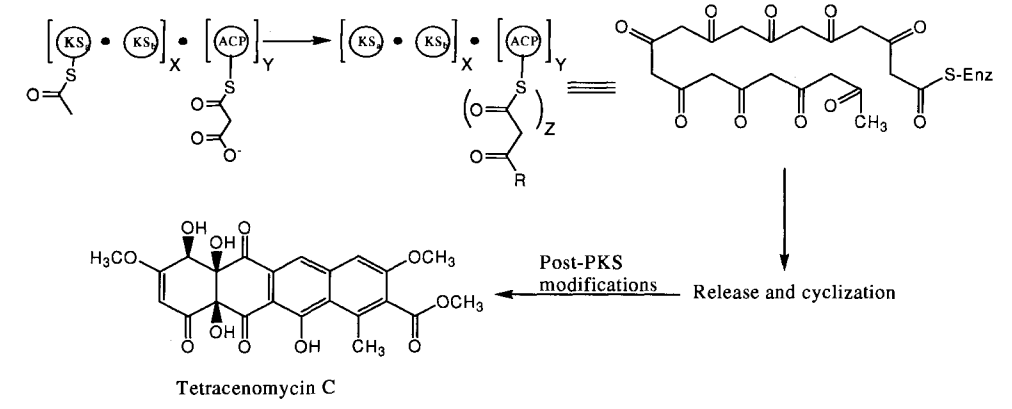


**C. Type III PKS (ACP-independent, Iterative) Eg. Flaviolin PKS**

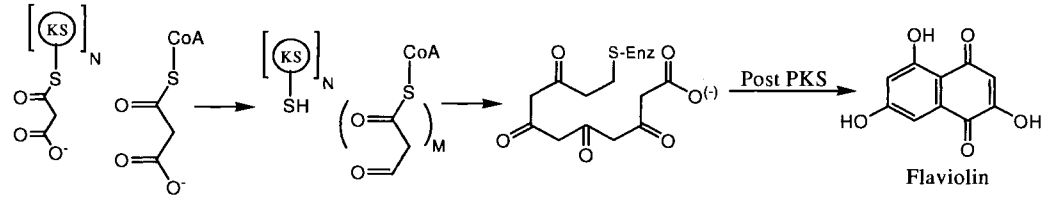


**FIGURE 2. Organization of type I, type II, and type III polyketide synthases**
ACP – Acyl carrier protein, AT – Acyltransferase, KS – Ketosynthase, KR – Ketoreductase, DH – Dehydratase, ER – Enoylreductase, TE – Thioesterase. Figure adapted from [9].

Structural diversity of the polyketides arises because the PKSs can utilize a wide range of acyl groups as starter and extender units. Moreover, the β–keto group may be reduced to different extents during chain elongation. The polyketide backbone also undergoes several modifications such as oxidation, methylation, and glycosylation (post-PKS tailoring steps), which give rise to further structural variations [10, 11].

Extensive genetic engineering of the secondary metabolite biosynthetic gene clusters has facilitated the production of several new compounds, thereby increasing the chemical diversity of available natural products [12, 13]. It is thought that the secondary metabolites isolated from *Streptomyces* so far represent only a small fraction of the total number of compounds that members of this genus are capable of producing [14]. Analysis of the completed *Streptomyces* genome sequences has revealed the existence of several additional gene clusters that synthesize compounds other than those already known [15-18]. Presently, there is an urgent need for new antibiotics because of the rapid onset of resistance that has rendered several antibacterials ineffective [19-21]. The *Streptomyces* species, being such prolific producers of natural products, can continue to be a rich source for the discovery and development of novel antibiotics and other bioactive compounds of therapeutic relevance.

### 1.2 Hygromycin A

Hygromycin A (HA, compound **1**) is a secondary metabolite produced by *Streptomyces hygroscopicus* NRRL 2388 (FIGURE 3). HA was initially isolated in

1953 and was shown to have moderate antibiotic activity against several Gram-positive and Gram-negative bacteria [22]. Several other interesting biological activities have been discovered for this compound. HA and an analog, methoxyhygromycin A (compound **3**, FIGURE 3) produced by the same strain, have been reported to inhibit the K88 fimbrial protein-mediated erythrocyte agglutination ability of enterotoxic *E. coli* [23]. HA has been found to be effective in controlling dysentery in pigs caused by *Serpulina hyodysenteriae* [24, 25]. Immunosuppressant properties have also been demonstrated for HA [26]. HA and **3** can also act as plant growth inhibitors / herbicides, and have been proposed as possible candidates for development into weed control agents [27, 28].

### 1.2.1 Antibacterial action of HA

Structurally, HA belongs to the aminocyclitol class of antibiotics that are characterized by the presence of a cyclohexane moiety with hydroxyl and amino or guanidino substituents. Some examples of this class of compounds are streptomycin, spectinomycin, gentamicin, and kanamycin. These antibiotics inhibit protein synthesis by binding to the 30S ribosomal subunit and preventing its interaction with mRNA [29]. The antibacterial activity of HA, however, is brought about by a different mechanism involving inhibition of the peptidyl transferase center within the 50S ribosomal subunit [30]. The presence of HA prevents the binding of chloramphenicol

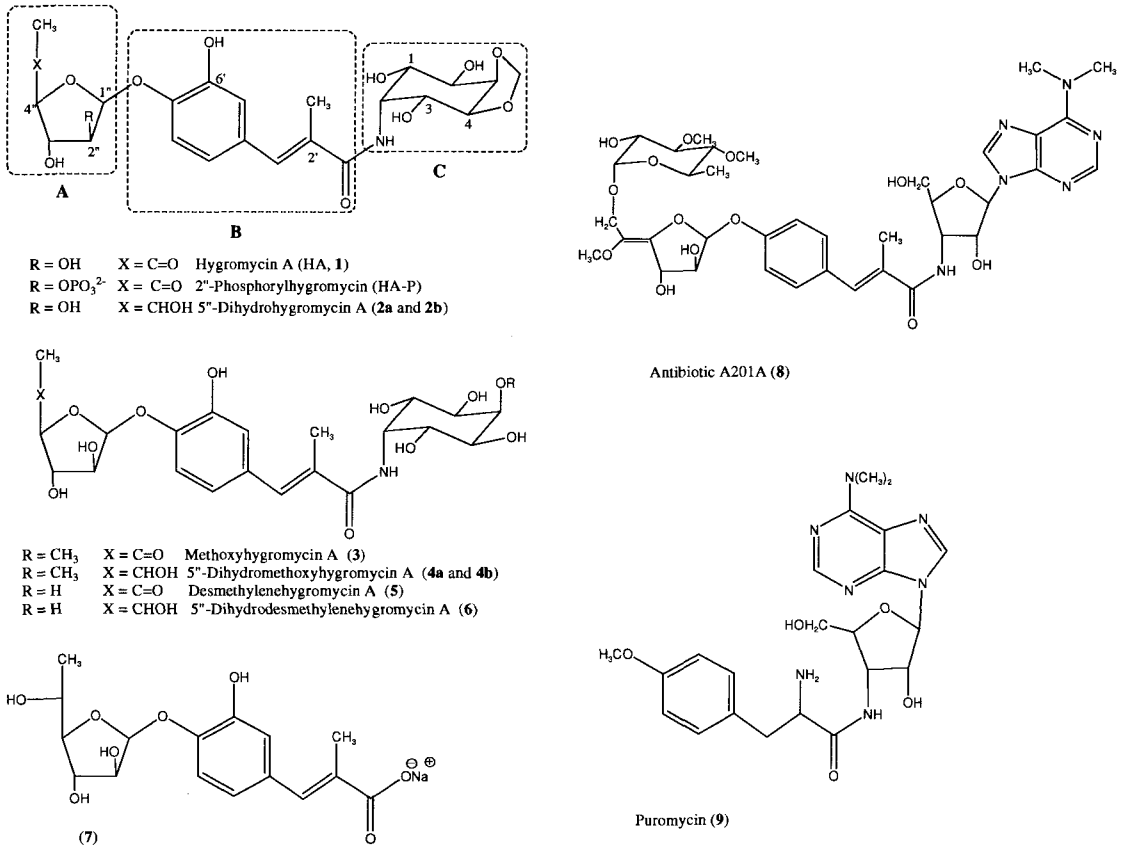


**FIGURE 3. Structures of hygromycin A and related compounds.** The three structural moieties in HA, 5-dehydro-α-L-fucofuranose (A subunit), (*E*)-3-(3,4-dihydroxyphenyl)-2-methylacrylic acid (B subunit), and 2L-2-amino-2-deoxy-4,5-*O*-methylene-*neo*-inositol (C subunit), are indicated. HA, **3**, and **5** also exist in small amounts as their corresponding C4" epimeric forms, which appear as 'shoulder peaks' with slightly earlier retention times in all HPLC traces.

or lincomycin, two other known peptidyl transferase inhibitors, suggesting that these antibiotics have overlapping binding sites or bind in close proximity to one another. HA binds more strongly to ribosomes than chloramphenicol, and hence is a more potent protein synthesis inhibitor. HA binding is precluded only by the 50S-targeting macrolides tylosin, carbomycin, and spiramycin that incorporate a disaccharide moiety

in their structure [31]. Thus, the structural features and binding mode of HA distinguish it from other ribosome-targeting antibiotics, offering possibilities for the development of new analogs to combat drug-resistant bacteria.

### 1.2.2 Structure and biosynthesis of HA

HA has a molar mass of 511, is highly soluble in water, and has an absorption maximum at 272 nm [23, 32]. Its structure is comprised of three very dissimilar moieties, namely 5-dehydro-α-L-fucofuranose, (*E*)-3-(3,4-dihydroxyphenyl)-2-methylacrylic acid, and the aminocyclitol 2L-2-amino-2-deoxy-4,5-*O*-methylene-*neo*-inositol, which will be referred to as the A, B, and C subunits, respectively (FIGURE 3). It is interesting to note that HA shows significant structural similarities to two other antibiotics, A201A (compound **8**) and puromycin (compound **9**) (FIGURE 3). HA resembles A201A in having similar A and B subunits, whereas with respect to puromycin, the structure of the B subunit is conserved. Structure-activity relationship studies showed that replacing the fucofuranose moiety in HA with a pyranose sugar significantly reduced the antibacterial activity, whereas substituting it with an allyl ether did not affect activity [33, 34]. An HA analog lacking the fucofuranose subunit or an allyl ether analog without the aminocyclitol completely lacked bioactivity [34]. Replacing the hydroxyl on the central phenyl ring with an amine group retained antibacterial activity, whereas substituting it with methyl or methoxy groups, or introducing functional groups at other positions on the phenyl ring reduced activity [34, 35]. Analogs with heteroaryl groups in place of the phenyl group were completely inactive [35]. Reduction in activity was observed when the methyl group in the B

moiety was replaced with propyl, allyl, or hydrogen [34]. The presence of the C4-C5 methylenedioxy bridge of the aminocyclitol subunit has been reported to be essential for optimal antibacterial activity of HA; compound **3**, the naturally occurring analog of HA with a methoxy group at C5, is significantly less active than HA [23, 36]. Introducing hydroxyl or methoxy groups at different positions on the aminocyclitol decreased *in vivo* activity in varying degrees [37, 38].

Detailed isotope-labeled precursor feeding studies were carried out by the Reynolds group to investigate the biosynthetic pathway of HA (FIGURE 4) [39]. Stable, isotopically labeled precursor compounds were fed to growing cultures of *S. hygroscopicus*. Following fermentation, HA was isolated and examined by $^{13}C$ NMR. The feeding experiments showed that both D-[1,2-$^{13}C_2$]glucose and D-[1-$^{13}C$]mannose were incorporated into the A subunit, suggesting that biosynthesis of the A subunit originates from glucose-6-phosphate, which is converted to fructose-6-phosphate and then to mannose-1-phosphate. The subsequent steps in the proposed pathway involve the generation of the nucleotide diphosphate (NDP)-activated mannose and conversion to NDP-L-fucose via a NDP-4-keto-6-deoxymannose intermediate. The NDP-L-fucose then undergoes ring contraction to form L-fucofuranose and a subsequent oxidation at C5 to form 5-dehydro-α-L-fucofuranose, or the A subunit.

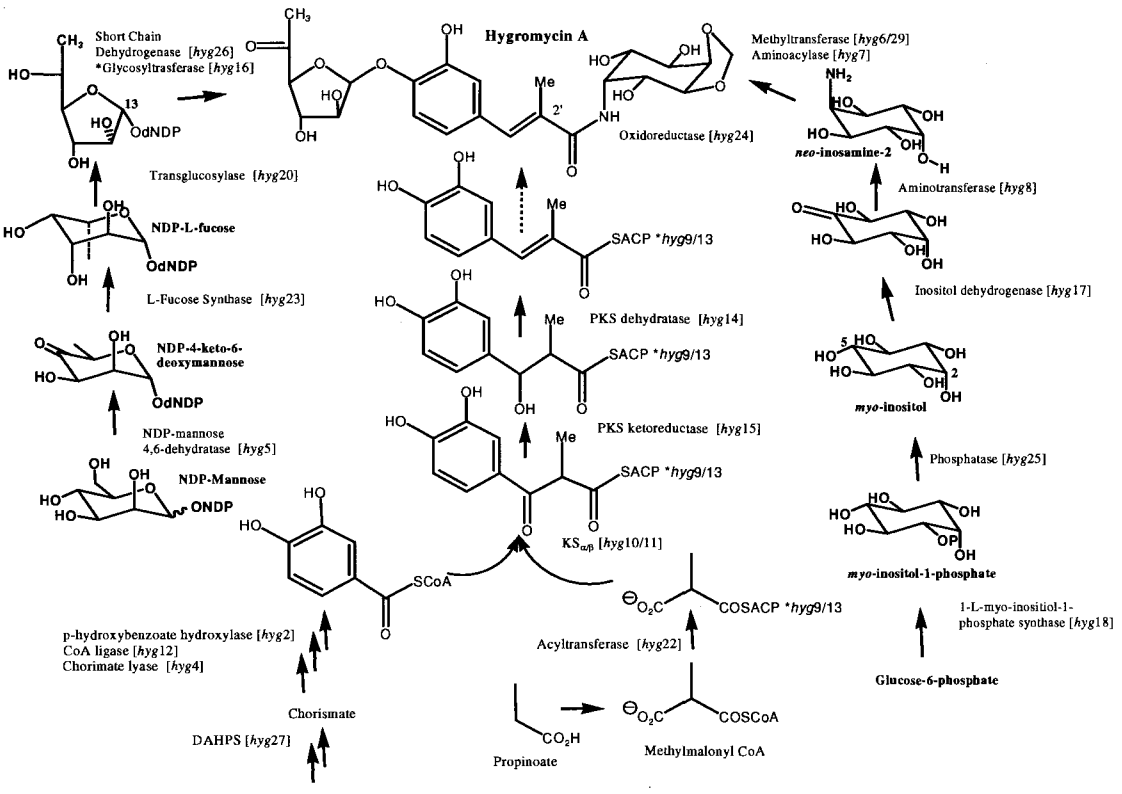


**FIGURE 4. Proposed pathway for hygromycin A biosynthesis.** The three structural moieties are synthesized by three distinct routes that converge to generate the final compound. Figure taken from [40].

Incorporation of [carboxy-$^{13}$C]-4-hydroxybenzoic acid and [2,3-$^{13}C_2$]propionate into the B subunit of HA suggested that this subunit is generated in a polyketide synthase-like manner. The proposed biosynthetic route for this branch of the pathway is initiated by the decarboxylative condensation of 4-hydroxybenzoyl-CoA starter unit with the propionate-derived methylmalonyl-CoA extender unit, followed by reduction and dehydration steps. The C subunit is also derived from glucose, but its biosynthesis is proposed to involve a *myo*-inositol intermediate. Oxidation of the C5 hydroxyl of *myo*-inositol and its subsequent transamination yields *neo*-inosamine-2, which makes the core aminocyclitol. The methylene group of the

C4-C5 methylenedioxy bridge is derived from *S*-adenosylmethionine, as suggested by feeding studies with L-[methyl-$^{13}$C]-methionine. These individual subunits of HA get linked to one another by a glycosidic bond between A and B, and an amide linkage between B and C subunits.

The putative biosynthetic pathway was subsequently used by the Reynolds group as a basis for developing a strategy to identify the biosynthetic gene cluster of HA in *S. hygroscopicus* (GenBank DQ314862) (FIGURE 5) [40]. Degenerate primers for a gene encoding a putative mannose dehydratase (MDH), which would convert NDP-mannose to NDP-4-keto-6-deoxymannose during A subunit biosynthesis, were used to amplify a MDH homolog from the *S. hygroscopicus* genome. This gene was next used to screen a cosmid library to identify the HA biosynthetic gene cluster.

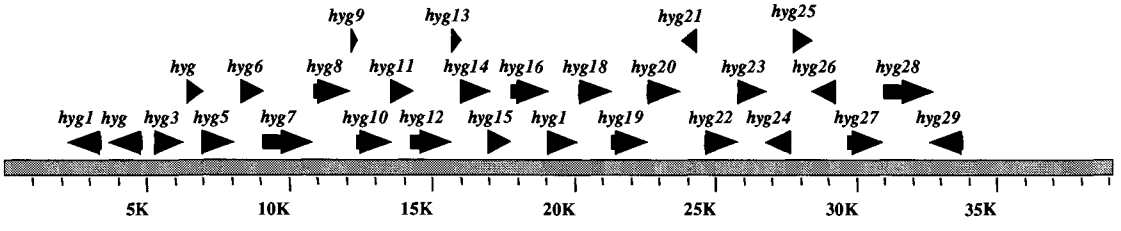


**FIGURE 5. Biosynthetic gene cluster of hygromycin A from *S. hygroscopicus* NRRL 2388.** The gene cluster is comprised of 29 open reading frames with predicted roles in HA biosynthesis, resistance, and pathway regulation (see TABLE 1).

Functional annotation of the 31.5 kb gene cluster recognized 29 open reading frames (ORFs), designated *hyg1-29*, whose protein products have been assigned to most of the reactions in the pathway (TABLE 1). Putative regulatory elements and resistance

determinants have also been identified in the gene cluster. A gene disruption experiment was carried out to confirm the function of the HA gene cluster [41]. Disruption of the *hyg26* gene, which encodes a putative short chain dehydrogenase proposed to convert L-fucofuranose to 5-dehydro-α-L-fucofuranose, resulted in the production of the reduced analogs of HA and **3**, namely 5"-dihydrohygromycin A (compound **2**) and 5"-dihydromethoxyhygromycin A (compound **4**) (FIGURE 3). This experiment confirmed that the gene cluster isolated was responsible for HA biosynthesis.

**TABLE 1. Genes in the hygromycin A biosynthetic gene cluster**

| Gene | Putative protein length | Proposed function |
|---|---|---|
| *hyg1* | 375 | AfsR regulatory protein |
| *hyg2* | 399 | p-hydroxybenzoate hydroxylase |
| *hyg3* | 323 | Regulatory protein |
| *hyg4* | 173 | Chorismate lyase |
| *hyg5* | 352 | Mannose dehydratase |
| *hyg6* | 249 | Methyltransferase |
| *hyg7* | 579 | Unknown |
| *hyg8* | 411 | Aminotransferase |
| *hyg9* | 83 | Acyl carrier protein |
| *hyg10* | 378 | β-ketoacyl synthase 1 |
| *hyg11* | 252 | Unknown |
| *hyg12* | 451 | CoA ligase |
| *hyg13* | 96 | Acyl carrier protein |
| *hyg14* | 347 | 3-hydroxyacyl ACP dehydratase |
| *hyg15* | 256 | 3-ketoacyl ACP reductase |
| *hyg16* | 431 | Glycosyltransferase |
| *hyg17* | 330 | *myo*-inositol dehydrogenase |
| *hyg18* | 363 | *myo*-inositol-1-phosphate synthase |
| *hyg19* | 416 | Transmembrane protein |
| *hyg20* | 370 | Transglucosylase |
| *hyg21* | 183 | Phosphotransferase |
| *hyg22* | 391 | Acyltransferase |
| *hyg23* | 325 | Fucose synthase |
| *hyg24* | 287 | Unknown |
| *hyg25* | 213 | *myo*-inositol-1-phosphatase |
| *hyg26* | 271 | Short chain dehydrogenase |
| *hyg27* | 401 | DAHP synthase |
| *hyg28* | 570 | ATP binding cassette transporter |
| *hyg29* | 378 | Methyltransferase |

### 1.3 Self-resistance mechanisms in antibiotic producers

*S. hygroscopicus*, like other bacteria that produce antibiotics, is equipped with mechanisms to protect itself from the lethal effects of its own destructive molecules. Generally, the genes responsible for self-resistance are found clustered with the antibiotic biosynthesis genes and are thought to have co-evolved with the latter to provide timely auto-immunity [42]. This appears to be the case for HA resistance genes also. The three most commonly encountered methods of self-resistance include 1) antibiotic inactivation by enzymatic modification, 2) modification of the cellular target for the antibiotic, and 3) exclusion of the antibiotic from the cell. Sequestration of the antibiotic by specific binding proteins, and changes in cell wall permeability also serve as additional means of self-protection in some strains. Many species use more than one method of resistance simultaneously, which provides them with multiple layers of protection.

#### 1.3.1 Self-resistance by antibiotic modification

Resistance by enzymatic inactivation of antibiotic is primarily mediated by *O*-phosphorylation of hydroxyl groups and *N*-acetylation of amino groups. In some cases, resistance is also brought about by *O*-glycosylation or amino acid addition. The donor groups for these modifications are ATP, acetyl-CoA, UDP-glucose, and L-leucine, respectively.

### 1.3.1.1 *O*-phosphorylation and *N*-acetylation

*O*-phosphorylation or *N*-acetylation as a means of antibiotic inactivation is widely observed in producers of the protein synthesis-inhibiting aminoglycoside antibiotics [42]. The ribosomes of these bacteria, which are the targets for the antibiotics, are not modified, and so remain sensitive throughout the bacterial life cycle. Covalent modification of the antibiotic by a functional group prevents or weakens its binding to the target, thus conferring resistance to the producer. It is frequently observed that the phosphotransferase and acetyltransferase activities function in conjunction with each other for maximum resistance. For example, the neomycin-producing *S. fradiae* possesses a 3'-*O*-phosphotransferase and a 3-*N*-acetyltransferase, and the resistance of a *S. lividans* expression host strain equals that of the producer only when the genes for both these enzymes are heterologously expressed in it (FIGURE 6) [43]. Similar observations have been made in the paromomycin-producer, *S. rimosus* [44]. Modification can occur not only on the final product, but also on pathway intermediates/precursors during antibiotic biosynthesis. This is best illustrated in streptomycin biosynthesis by *S. griseus* (FIGURE 6). The *strA* gene in the streptomycin biosynthetic gene cluster encodes streptomycin-6-phosphotransferase, which phosphorylates streptidine, an intermediate in the biosynthetic pathway. The remaining biosynthetic steps take place on this phosphorylated precursor, leading to the production of an inactive, phosphorylated form of streptomycin, 6'-phosphorylstreptomycin [45, 46]. An extracellular

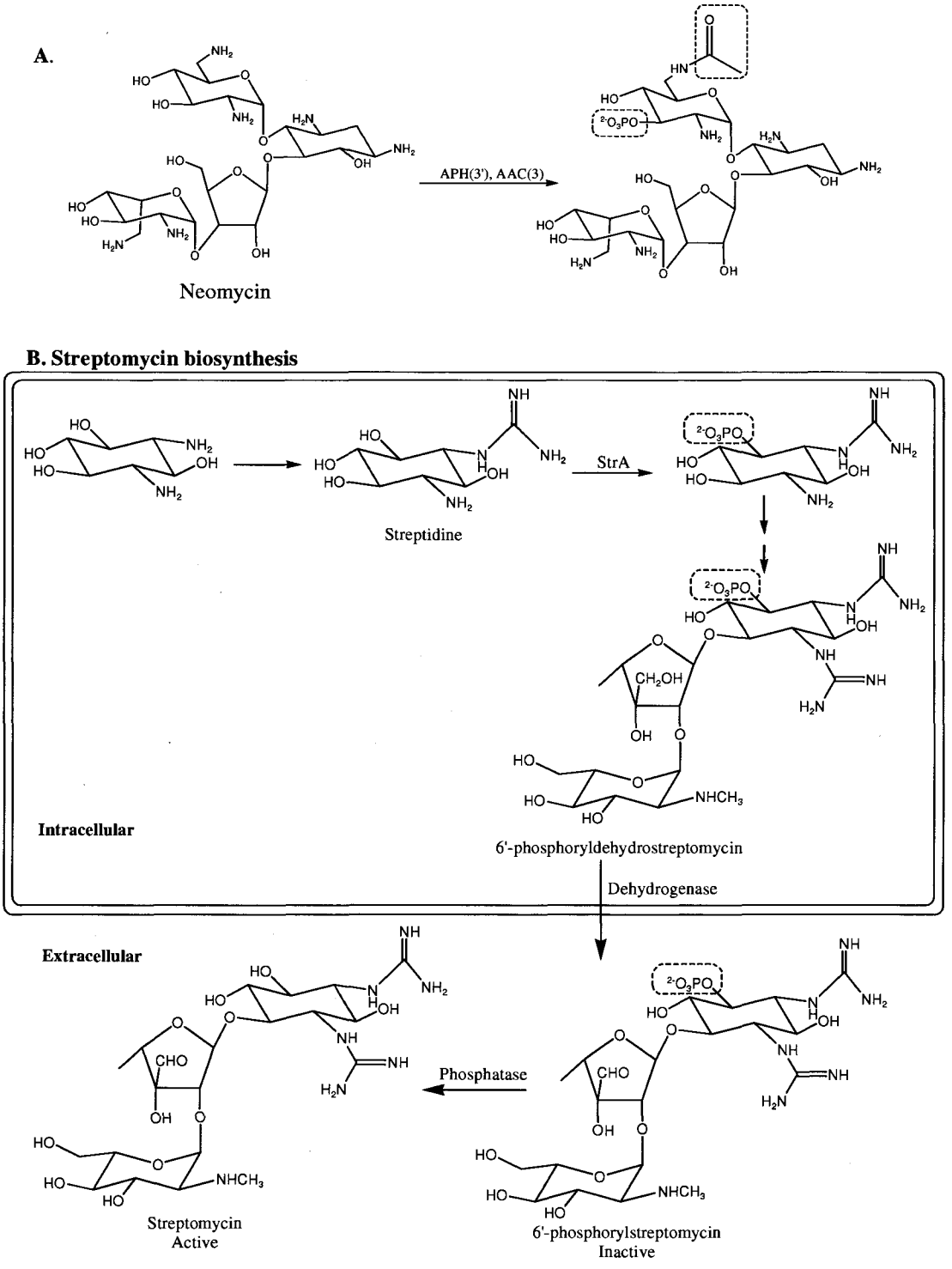


**FIGURE 6. Antibiotic modification by *O*-phosphorylation and *N*-acetylation.**
A. Neomycin is modified by both *O*-phosphorylation and *N*-acetylation.
B. Phosphorylation of streptomycin occurs on a pathway intermediate to form inactive 6'-phosphoryl streptomycin, which gets dephosphorylated extracellularly.

phosphatase dephosphorylates 6'-phosphorylstreptomycin to form the bioactive streptomycin [47]. Similarly, in the puromycin-producing *S. alboniger*, the puromycin-*N*-acetyltransferase acts on *O*-demethylpuromycin, a toxic intermediate in the biosynthetic pathway, such that puromycin is synthesized in its inactive acetylated form, which is deacetylated extracellularly [48].

#### 1.3.1.2 *O*-glycosylation

Antibiotic inactivation by *O*-glyosylation has been reported exclusively from the macrolide-producing *Streptomyces* sp. and has been well-characterized in the oleandomycin-producer, *S. antibioticus*. Macrolides including erythromycin, oleandomycin, pikromycin, and tylosin bind to the 50S ribosomal subunit and cause a premature termination of protein synthesis. The ribosomes of macrolide producers are normally modified by methylation, and therefore are resistant to antibiotic action [42]. However, the ribosomes of *S. antibioticus* are susceptible to oleandomycin throughout its life cycle [49]. Resistance to oleandomycin is conferred by synthesizing oleandomycin in an inactive glycosylated form (FIGURE 7) [50]. A glycosyl transferase encoded by the *oleI* gene in the oleandomycin gene cluster catalyzes this modification [51]. Glycosylated oleandomycin is exported out of the cell, where an extracellular glycosidase encoded by the *oleR* gene of the oleandomycin gene cluster deglycosylates it into active oleandomycin. A second glycosyltransferase, OleD, with an ability to glycosylate a broad range of macrolides, has also been characterized from *S. antibioticus*, but the gene encoding it is not a part of the oleandomycin gene cluster, and so OleD is considered to have a more general role in resistance that is not coupled

with antibiotic biosynthesis. A similar resistance mechanism involving glycosylation/ deglycosylation has also been observed in the biosynthesis of pikromycin by *S. venezuelae* [52].

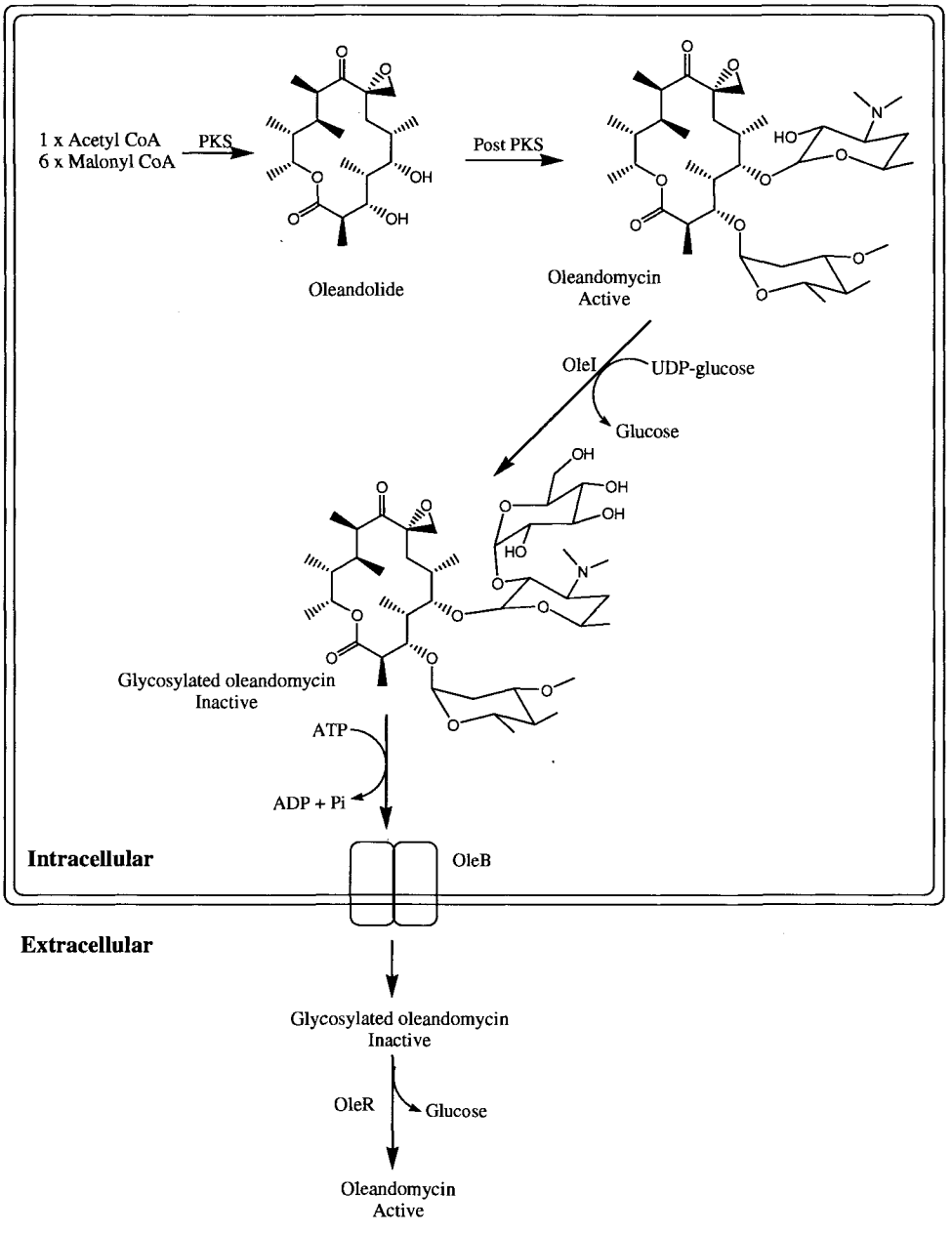


**FIGURE 7. Antibiotic modification by glycosylation.** Intracellular oleandomycin is made inactive by glycosylation and reactivated extracellularly by a glycosidase.

#### 1.3.1.3 Modification by leucine addition

Antibiotic inactivation by addition of a leucine residue has been reported only from *S. griseochromogenes*, which produces the peptidyl-nucleoside antibiotic blasticidin S [53]. Modification with leucine occurs on a toxic biosynthetic intermediate, demethylblasticidin S to form leucyldemethylblasticidin S, which has reduced antibiotic activity. Methylation of leucyldemethylblasticidin S yields leucylblasticidin S, which gets exported out of the cell and is hydrolyzed to form blasticidin S.

### 1.3.2 Modification of antibiotic target site

A second mode of resistance seen in bacteria is modification or replacement of the antibiotic target site. Depending on the target type, this can be classified as 1) ribosomal, involving the ribosomal RNA (rRNA), and 2) non-ribosomal, involving targets such as DNA gyrase, RNA polymerase, or elongation factor Tu.

#### 1.3.2.1 Methylation of ribosomal RNA

Resistance in bacteria that possess ribosomes tolerant to ribosome-targeting antibiotics is usually achieved by monomethylation or dimethylation of nucleotides on ribosomal RNA, and is the major route for self-protection in macrolide producers. Ribosomal methylation in an antibiotic producer was first studied in *S. azureus*, which produces thiostrepton [54]. The *tsr* gene product in this organism is a constitutively expressed *O*-methyltransferase that modifies the 2'-hydroxyl of an adenosine in the 23S rRNA (FIGURE 8) [55]. Self-resistance in *Saccharopolyspora erythraea* to

erythromycin is conferred by the *ermE* gene product, which is an adenine-dimethylating *N*-methyltransferase (FIGURE 9) [43]. In the tylosin producer, *S. fradiae*, a 23S rRNA dimethylase encoded by *tlrA*, along with two monomethylases encoded by *tlrB* and *tlrD*, provide resistance [56-58]. TlrA confers high levels of resistance by dimethylating an adenine residue. TlrD monomethylates at the same position as TlrA, while TlrB acts on a guanine residue. Experiments using a tylosin-sensitive *E. coli* strain showed that neither TlrB nor TlrD confers any appreciable levels of protection on its own, and that the two enzymes have to act synergistically for maximum resistance [58, 59]. RNA methylation is also observed in some aminoglycoside producers. An example is guanine monomethylation in the 16S rRNA of the gentamicin producer *S. tenebrarius* [60]. RNA modification prevents critical binding interactions between the drug and its target, which prevents or decreases drug binding and results in resistance.

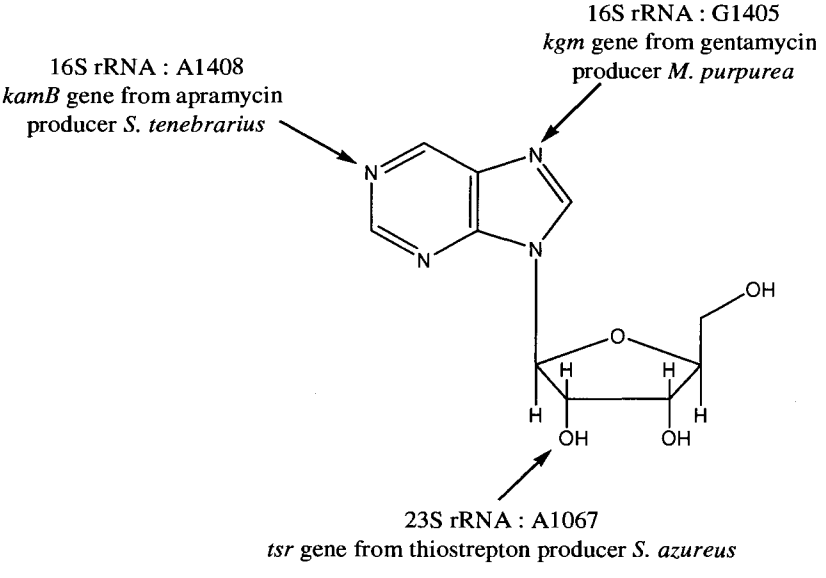


**FIGURE 8. Ribosomal RNA modification.** The different possible sites of modification on ribosomal RNA nucleotide are shown.

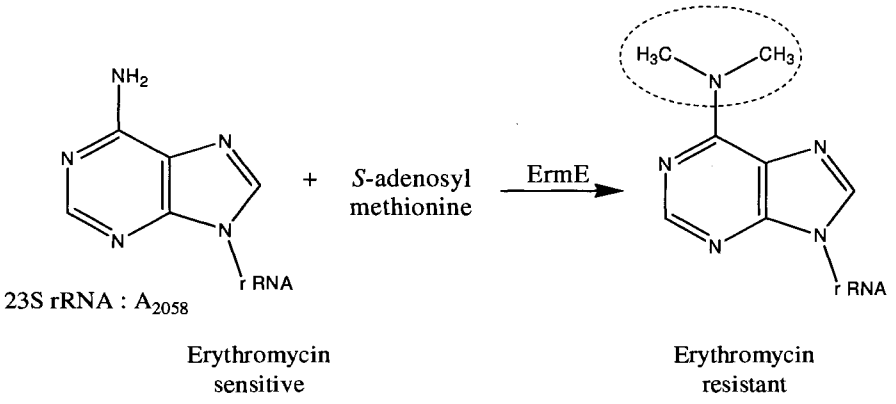


**FIGURE 9. Ribosomal RNA dimethylation.** ErmE-mediated adenine dimethylation confers erythromycin resistance in *Saccharopolyspora erythraea.*

### 1.3.2.2 Replacement of non-ribosomal target sites

Self-resistance in some antibiotic producers is mediated by expression of resistant forms of non-ribosomal targets. Three well-studied examples are 1) DNA gyrase inhibition by aminocoumarins, 2) elongation factor Tu (EF-Tu) inhibition by kirromycin, and 3) glyceraldehyde-3-phosphate dehydrogenase inhibition by pentalenolactone.

DNA gyrase is a bacterial topoisomerase that catalyzes ATP-dependent negative supercoiling of DNA. The enzyme is a heterotetramer comprised of two GyrA subunits and two GyrB subunits [61]. GyrA is responsible for the double strand breakage and re-ligation of DNA, whereas GyrB is responsible for ATP hydrolysis. The aminocoumarin antibiotics novobiocin, clorobiocin, and coumermycin A1 act by inhibiting the ATPase activity of GyrB [62]. The producer strains for these antibiotics, *S. spheroides*, *S. roseochromogenes* var. *oscitans,* and *S. rishiriensis,* respectively,

make themselves self-resistant by producing an alternate, resistant form of GyrB encoded by the *gyrB*$^{R}$ gene in the corresponding antibiotic biosynthetic gene cluster [63-65]. Studies in the novobiocin producer revealed that the predominant GyrB, termed GyrB$^{S}$, was novobiocin-sensitive, whereas GyrB$^{R}$ was novobiocin-resistant. It was observed that expression of *gyrB*$^{R}$ was induced by the antibiotic and that GyrB$^{R}$ replaced GyrB$^{S}$ from the gyrase tetramer once novobiocin production began [66-68].

*S. arenae*, the producer of pentalenolactone, also protects itself by synthesizing alternate isoforms of glyceraldehye-3-phosphate dehydrogenase, the target for the antibiotic [69]. Expression of the sensitive form of the enzyme is observed only in the absence of pentalenolactone production and is replaced by the resistant form once antibiotic production is initiated.

The kirromycin class of antibiotics inhibit protein synthesis by interacting with elongation factor Tu and immobilizing it on the ribosome [70]. The Ef-Tu identified in the kirrothricin producer, *S. cinnamoneus*, is intrinsically resistant to the antibiotic [71]. An alternate, sensitive form of EF-Tu has not been identified in this strain.

### 1.3.3 Antibiotic efflux pumps

Efflux pumps are often found in antibiotic biosynthetic gene clusters. These proteins are associated with the cell membrane and are involved in secretion of the antibiotic from inside the cell. They also contribute to self-resistance because active export prevents intracellular accumulation of the drug, thereby keeping the drug

concentration at levels that are tolerable for the bacterium. One of the types of efflux pumps found in antibiotic producers is the proton motive force pumps belonging to the major facilitator superfamily. These transporters have either 12 or 14 transmembrane segments and utilize a proton gradient across the membrane for transport [72, 73]. Proton gradient-dependent efflux pumps have been identified in the gene clusters of puromycin and actinorhodin [74, 75]. A second category of efflux pumps is the ATP binding cassette (ABC) transporters, which couple antibiotic export to ATP hydrolysis. Structurally, they are comprised of two hydrophilic ATP-binding domains and two hydrophobic transmembrane domains, which may be present on the same protein or on different polypeptides [76]. The ABC transporters in antibiotic-producing actinomycetes have been classified into three groups [77]. The Type I transporter system comprises two genes, one of which encodes a protein with a single ATP binding domain, and the second gene present immediately downstream encodes a membrane protein with six transmembrane segments. Type I ABC transporters have been identified in daunorubicin, tetronasin, mithramycin, and oleandomycin producers [78-81]. The Type II group is comprised of a single gene that encodes a protein with two ATP binding domains; a gene for the membrane component has not been identified in the corresponding biosynthetic gene cluster. Transporters of this type occur in carbomycin, tylosin, oleandomycin, A201A, and lincomycin producers [82-86]. The type III system is made of a single gene that encodes a protein with one ATP binding domain and one transmembrane domain. This type has been reported from the bleomycin and streptomycin producers [87, 88].

## 1.4 Antibiotic resistance in pathogens

Emergence of pathogenic bacteria with high levels of antibiotic resistance, often to multiple drugs, is a serious problem that is affecting not only the treatment of infectious diseases but also other medical areas where the risk of bacterial infection exists, such as organ transplantation, surgery, and chemotherapy. Drug resistance has now become a constant challenge for antibacterial drug development. One of the ways by which bacteria become refractory to drugs is through the independent evolution of point mutations in their genome, which creates resistance genes [89]. A second way, considered more effective for the acquisition and dissemination of resistance, is through the horizontal transfer of antibiotic resistance genes via gene cassettes, transposons, plasmids, and bacteriophages from other taxonomically distant bacteria in the environment, including antibiotic producing strains [90]. The resistance mechanisms in a pathogenic bacterium against a given antibiotic often have identical counterparts in the producer strain from which the antibiotic is derived. For example, the aminoglycoside-inactivating kinases in clinical strains are similar to the antibiotic-modifying kinases from the *Streptomyces* that produce these antibiotics [91]. Similarly, some glycopeptide- antibiotic producers harbor resistance genes that are homologous to the vancomycin resistance genes in *Enterococcus* [92]. Therefore, it is widely accepted that antibiotic resistance in pathogens has originated from the self-resistance mechanisms occurring in antibiotic producers [90, 93, 94]. However, the antibiotic producers are, obviously, not the only contributors for clinical resistance, especially for the semisynthetic and synthetic drugs. The general microbial population

in the soil ('soil antibiotic resistome'), living in the presence of antibiotic producers and also simultaneously exposed to man-made chemicals, forms a much larger reservoir of resistance genes [95]. Laboratory studies of resistance in non-pathogenic strains, including the producers, against a novel clinically relevant antibiotic can assist in the elucidation of resistance mechanisms that can potentially develop once its clinical use increases. Information gained from such studies can be used to develop better antibiotic analogs and also for developing inhibitors that would target the resistance mechanism itself.

### 1.5 Putative self-resistance mechanisms in *S. hygroscopicus* NRRL 2388

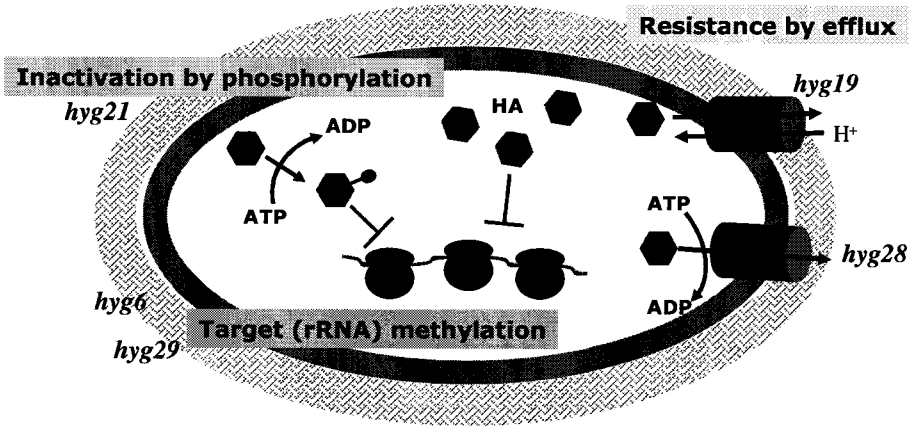


**FIGURE 10. Putative self-resistance mechanisms in *S. hygroscopicus* NRRL 2388.**

Analysis of the HA biosynthetic gene cluster identified four genes that are likely to contribute to self-resistance of the producer strain, *S. hygroscopicus* NRRL 2388 [40]. The *hyg21* gene shows similarity to *O*-phosphotransferases and is predicted to confer resistance by antibiotic inactivation. As HA is a ribosome-targeting antibiotic, a possible route of self-resistance in *S. hygroscopicus* can be target site

modification by rRNA methylation. A SAM-dependent methylation step is involved in biosynthesis of the methylenedioxy bridge of HA's aminocyclitol moiety. Two methyltransferase homologs, *hyg6* and *hyg29*, have been recognized in the HA gene cluster, and it is hypothesized that one of these encodes an *O*-methyltransferase for methylenedioxy bridge formation and the other encodes an rRNA methyltransferase for resistance. The *hyg19* gene shows similarity to proton gradient-dependent transporter genes. The *hyg28* gene resembles ABC transporter genes and putatively encodes a type II ABC transporter. It is proposed that Hyg19 and/or Hyg28 are responsible for efflux of HA, thereby conferring self-resistance.

### 1.6 Specific aims of current research

The objective of the present research is to investigate the mechanisms of self-resistance in *S. hygroscopicus* NRRL 2388 by characterizing the putative resistance determinants found in the biosynthetic gene cluster of HA. The specific aims are:

1) Characterize the *hyg21* gene product and test its role in HA inactivation.

2) Determine if either *hyg6* or *hyg29* contributes to self-resistance by rRNA methylation, and if the second gene encodes an *O*-methyltransferase that introduces the methyl group of the C4-C5 methylenedioxy bridge in HA.

3) Determine the roles of the two putative transporter systems encoded by *hyg19* and *hyg28* in HA efflux-mediated resistance.

## 2. Antibiotic resistance: An *O*-phosphotransferase catalyzes phosphorylation of hygromycin A in the producing organism, *Streptomyces hygroscopicus*

### 2.1 Summary

The *hyg21* gene in the hygromycin A (HA) biosynthetic gene cluster encodes an *O*-phosphotransferase with a proposed role in self-resistance of *S. hygroscopicus*. It was observed that insertional inactivation of *hyg21* leads to a greater than 90% decrease in HA production. The wild type and the *hyg21* mutant were comparably resistant to HA. Using *E. coli* as a heterologous host, Hyg21 was expressed and purified. Kinetic analyses revealed that the recombinant protein catalyzes phosphorylation of HA ($K_m$ 29.2 ± 4.4 μM) at the C2" position of the fucofuranose ring in the presence of ATP ($K_m$ 198.3 ± 19.1 μM) or GTP ($K_m$ 356.5 ± 62.1 μM) with a $k_{cat}$ of 2 $min^{-1}$. The phosphorylated HA is inactive against HA-sensitive Δ*tolC E. coli* and *Streptomyces lividans*, and also lacked the ability to inhibit *in vitro* protein synthesis. Hyg21 also phosphorylates methoxyhygromycin A and desmethylene hygromycin A with similar $k_{cat}$ and $K_m$ values to those observed for HA. Phosphorylation of the naturally occurring isomers of 5"-dihydrohygromycin A and 5"-dihydromethoxyhygromycin A was 8-10 times slower than for the corresponding non-natural isomers. These studies demonstrate that Hyg21 is an *O*-phosphotransferase with broad substrate specificity, tolerating changes in the aminocyclitol moiety more than in the fucofuranose moiety, and that phosphorylation by Hyg21 is one of several possible mechanisms of self-resistance in *S. hygroscopicus*

NRRL 2388. This chapter has been published as a paper in *Antimicrobial Agents and Chemotherapy*, 2008, 52 (10), 3580-8.

## 2.2 Introduction

As described in section 1.5, the *hyg21* gene in the hygromycin A (HA) biosynthetic gene cluster encodes a putative phosphotransferase that may inactivate HA by *O*-phosphorylation. To test this hypothesis, a genetic and biochemical investigation of *hyg21* and its gene product was pursued in the present study. This study showed that *hyg21* is not an absolute requirement for hygromycin biosynthesis and that Hyg21 is indeed a phosphotransferase that catalyzes the transfer of the γ–phosphoryl group of ATP to the 2"-hydroxyl group of HA, abolishing its antibacterial property. The steady state kinetic parameters for turnover of HA and its analogs have also been determined, which show that Hyg21 can phosphorylate HA and a range of analogous substrates bearing a fucofuranose moiety.

## 2.3 Materials and methods

### 2.3.1 Antibiotics and chemicals

All antibiotics and chemicals were purchased from Sigma-Aldrich (St. Louis, MO), unless otherwise indicated. Hygromycin A (HA) was kindly supplied by Pfizer Inc. Analogs of HA, **2a**, **3**, **4a**, and **7** (FIGURE 3) were isolated from the wild type and a Δ*hyg26* blocked mutant strain of *S. hygroscopicus* [40]. Compounds **5** and **6** were isolated from a *hyg6* deletion mutant (see chapter 3). A diastereomeric mixture of 5"-dihydrohygromycin A (**2a** and **2b**) was prepared by reduction of HA as described

previously [40]. A diastereomeric mixture of 5"-dihydromethoxyhygromycin A (**4a** and **4b**) was prepared from methoxyhygromycin A (**3**) in the same way. Antibiotic A201A (**8**) was a generous gift of Dr. A. Jimenez, Centro de Biologia Molecular 'Severo Ochoa', Madrid. [2-$^{3}$H] *myo*-inositol (20.0 Ci/mmol) was procured from Moravek Biochemicals (Brea, CA). Primers for PCR were obtained from Integrated DNA Technologies (Coralville, IA). Enzymes for DNA manipulations were purchased from New England Biolabs (Beverly, MA). Prestained protein molecular weight markers used in SDS PAGE analysis were obtained from Bio-Rad (Hercules, CA).

### 2.3.2 Bacterial strains, plasmids, and culture conditions

Cosmid 17E3, based upon the SuperCos1 vector, was the source for *hyg21* gene and has been described previously [40]. The pCR4®-TOPO® vector and One Shot® Mach1™-T1® chemically competent *E. coli* cells from Invitrogen (Carlsbad, CA) were used for cloning the *hyg21* PCR product. The pET-15b vector from EMD Biosciences (San Diego, CA) was used for expression of N-terminal His-tagged Hyg21 protein. The pET-15b vector with 0.5 kb *hyg21* ORF was designated as pET15b-*hyg21*. *E. coli* BL21-CodonPlus(DE3), obtained from Stratagene (La Jolla, CA), was the expression host for His-tagged Hyg21 protein. *E. coli* BW25113/pIJ790 (a strain with the λ-RED recombination plasmid), *E. coli* DH5α/pIJ773 (a strain with the *aac(3)IV* apramycin resistance cassette plasmid), and *E. coli* ET12567/pUZ8002 (a nonmethylating plasmid donor strain for intergeneric conjugation) have been described previously, and were provided by the John Innes Institute (UK) [41]. *S. hygroscopicus* NRRL 2388 is the wild type HA producer strain used to generate the

Δ*hyg21* mutant in which *hyg21* was replaced by the apramycin resistance cassette. The *E.coli* Δ*tol*C strain was procured from the *E. coli* Genetic Stock Center at Yale University. *E. coli* strains were normally grown at 37°C in Luria-Bertani (LB) medium supplemented with the required antibiotics. *S. hygroscopicus* wild type and deletion strains were propagated on ISP2 medium (0.4% yeast extract, 1.0 % malt extract, 0.4% dextrose, 2.0% agar, pH 7.2) at 30°C. Ampicillin (100 μg/ml final concentration), apramycin (50 μg/ml), carbenicillin (100 μg/ml), chloramphenicol (25 μg/ml), and kanamycin (50 μg/ml) were used as required.

### 2.3.3 DNA manipulations and analyses

Plasmid DNA was isolated using QIAprep Spin Miniprep kit from Qiagen (Valencia, CA). DNA fragments from agarose gels were isolated using Qiagen's QIAquick Gel Extraction kit. The QIAquick PCR purification kit was used for cleaning up the PCR product. Genomic DNA from *Streptomyces* strains was obtained using the Wizard Genomic DNA purification kit from Promega (Madison, WI). Automated DNA sequencing was performed at the DNA core facilities at Virginia Commonwealth University and Oregon Health and Science University. The DNA sequences were analyzed with Accelrys DS Gene software. The Hyg21 amino acid sequence was compared with sequences in the public domain using the BLASTP program at the NCBI server [96]. A motif search was carried out against the PROSITE database at the Expasy proteomics server [97].

### 2.3.4 Cloning of *hyg21* and construction of expression plasmid

The 552 bp *hyg21* gene was amplified from cosmid 17E3 using the GC-Rich PCR System from Roche Diagnostics following the manufacturer's instructions. Primers (5'-**CATATG**CCGGAAACTTCGTTCCAGGGC-3' and 5'-**GGATCC**TCAGCCGTTCGCCAGGAT-3') were designed to create an *Nde*I restriction site (bold font) at the initiation codon and a *Bam*HI restriction site (bold font) 3' to the termination codon. Amplification was performed with a GeneAmp PCR System 2700 (Applied Biosystems) using the following conditions: initial denaturation at 95 °C for 5 min, 30 cycles of amplification (45 s denaturation at 95 °C, 45 s annealing at 58 °C, and 45 s extension at 72 °C), and a final 7 min extension at 72 °C. The PCR product was cloned into pCR4®-TOPO® vector and was sequenced to ensure that no mutations occurred during amplification. The *hyg21* from the recombinant TOPO vector was then subcloned into the *Nde*I and *Bam*HI restriction sites of pET15b. The resulting pET15b-*hyg21* plasmid was introduced into the *E. coli* BL21-CodonPlus (DE3) expression host by transformation.

### 2.3.5 Expression and purification of His-tagged Hyg21 from *E. coli*

*E. coli* BL21 cells harboring the pET15b-*hyg21* plasmid were grown overnight in LB medium supplemented with 100 μg/ml ampicillin and 50 μg/ml chloramphenicol. 1000 ml of LB broth plus ampicillin and chloramphenicol, divided into two 4-liter fermentation flasks, was inoculated to 5% (v/v) with an overnight BL21 seed culture. The cells were allowed to grow at 37 °C for ~2 hr until an $A_{600\,nm}$ of 0.6 was reached. Expression of His-tagged protein was induced by adding 0.5 mM

isopropyl thio-β-D-galactoside (IPTG) and incubating at 30 °C for 5 hr. The cells were harvested by centrifugation and resuspended in 25 ml of lysis buffer (50 mM $NaH_2PO_4$, 300 mM NaCl, 10 mM imidazole, pH 8.0). His-tagged protein was purified under native conditions following the procedure outlined in Qiagen's Ni-NTA Spin protocol. All the protein purification steps were carried out at 4 °C. Cells were disrupted by sonication and the soluble fraction was applied to 1 ml of Ni-NTA agarose pre-equilibrated with lysis buffer. The column was washed with 50 ml of wash buffer (50 mM $NaH_2PO_4$, 300 mM NaCl, 20 mM imidazole, pH 8.0) and the protein was eluted with elution buffer containing 250 mM imidazole in fractions of 500 µl. Each fraction was analyzed by SDS-PAGE using a 13% acrylamide gel for the presence of Hyg21. The eluted protein was dialyzed for 14 hr against a buffer containing 50 mM Tris/HCl (pH 7.5), 20% glycerol, and 5 mM 2-mercaptoethanol, with a replacement with fresh buffer after 4 hr. Protein concentration was determined by Bio-Rad protein assay using bovine serum albumin as standard, and 50 µl aliquots of the purified protein were stored at -80 °C until further use.

### 2.3.6 Phosphorylation assay conditions

Initial enzyme assays were performed with ~10 µg purified enzyme in a 100 µl reaction of 50 mM Tris/HCl (pH 7.5), 5 mM 2-mercaptoethanol, 10 mM $MgCl_2$, 200 µM substrate, and 1 mM ATP. The reaction mixture was incubated at 30 °C for 2 hr and frozen at -20 °C. Hyg21 activity was studied by reverse-phase HPLC analysis by monitoring the appearance of phosphorylated product, which had a shorter retention time than the substrate. For kinetics studies, the reaction volume was scaled up to 600

μl with ~11 μg of enzyme. The assays were carried out for 15 min, during which phosphorylation activity was linear. The ATP concentration was fixed at 400 μM and the antibiotic concentration was varied from 5 μM to 100 μM. To determine kinetic parameters for ATP and GTP, the concentrations of these were varied and the concentration of HA was fixed at 90 μM. In all cases the samples were analyzed by HPLC and the amount of product formed was determined from its peak area using a HA standard curve as reference. The rate of phosphorylation was reported as the nmoles of product formed per minute. The data were plotted in GraFit 4 to determine the kinetic parameters. The pH profile was obtained using 100 μM HA and 1000 μM ATP at 30 °C for 15 min in the following buffers: 50 mM potassium acetate, pH 5.0; 50 mM Tris/maleate, pH 6.0, 6.5; 50 mM Tris/HCl, pH 7.0, 7.5, 8.0, 9.0. The effect of temperature on Hyg21 activity was checked using 100 μM HA and 1000 μM ATP in 50 mM Tris/HCl, pH 7.5 at room temperature (23 °C), 30 °C, 37 °C, and 50 °C in a 15 min assay.

### 2.3.7 Purification and characterization of phosphorylated hygromycin A

Ten reaction mixtures (5 ml each) with a final composition of 200 μM HA, 1000 μM ATP, 10 mM $MgCl_2$, 5 mM 2-mercaptoethanol, and 0.5 mg enzyme in 50 mM Tris/HCl, pH 7.5 were incubated overnight at 30 °C. The assay mixtures were pooled and filtered using Millex®-LCR 0.45 μm filter unit from Millipore, and the phosphorylated HA was purified by semipreparative reverse phase HPLC. Fractions containing the purified product were pooled and dried by evaporation. The dried sample was dissolved in deuterium oxide for structural elucidation by NMR. $^1$H NMR

spectra were recorded on Nicolet NM-500 MHz (modified with a Tecmag Libra interface) instruments calibrated using residual undeuterated solvent as an internal reference. 2D COSY correlation spectra were recorded on a Bruker AMX-400 NMR spectrometer. A standard HA sample was run under identical conditions for comparison. Coupling constants (*J*) were expressed in Hertz. Abbreviations for multiplicities are: s = singlet, d = doublet, t = triplet, q = quartet, m = multiplet.

**Hygromycin A.** $^1$H NMR (500 MHz, $D_2O$) δ 7.23 (d, *J* = 8.5 Hz, 1H), 7.10 (s, 1H), 7.03 (s, 1H), 7.01 (s, 1H), 5.82 (d, *J* = 4.5 Hz, 1H), 5.25 (s, 1H), 4.92 (s, 1H), 4.73 (m, 1H), 4.58 (t, *J* = 4.5 Hz, 1H), 4.50-4.46 (m, 1H), 4.37-4.35 (m, 1H), 4.31-4.25 (m, 2H), 4.14 (dd, *J* = 3.5, 9.5 Hz, 1H), 4.02 (dd, *J* = 5.5, 9.5 Hz, 1H), 3.90 (dd, , *J* = 3.5, 6.0 Hz, 1H), 2.15 (s, 3H), 2.07 (d, , *J* = 1.5 Hz, 3H).

**Phosphorylated hygromycin A.** $^1$H NMR (500 MHz, $D_2O$) δ 7.34 (d, *J* = 8.5 Hz, 1H), 7.16 (s, 1H), 7.08 (s, 1H), 7.06 (s, 1H), 5.95 (d, *J* = 2.5 Hz, 1H), 5.31 (s, 1H), 4.97 (s, 1H), 4.69 (m, 1H), 4.63 (t, *J* = 4.5 Hz, 1H), 4.58 (d, *J* = 6.5 Hz, 1H), 4.36-4.31 (m, 2H), 4.20 (dd, *J* = 3.5, 9.5 Hz, 1H), 4.08 (dd, *J* = 5.0, 9.5 Hz, 1H), 3.95 (t, *J* = 4.5 Hz, 1H), 2.25 (s, 3H), 2.12 (s, 3H).

### 2.3.8 HPLC and LC-MS conditions

Reverse phase HPLC analyses of the phosphorylation assays and the fermentation broths were carried out using an Agilent 1100 Series HPLC system with either an analytical 5 μm Eclipse XDB-C18 (4.6 * 150 mm) column or a

semipreparative 5 μm Phenomenex C18 column (250 * 10 mm). Solvents used were A (10% methanol, 90% water, 0.05% formic acid) and B (90% methanol, 10% water, 0.05% formic acid). Gradient conditions for the analytical column were 100% A for 2 min, 100 – 36% A for 16 min, 36 – 0% A for 2 min, 0% A for 8 min, 0 – 100% A for 2 min, 100% A for 10 min, at a flow rate of 1 ml/min. Gradient conditions for the semi preparative column were 100% A for 2 min, 100 – 44% A for 16 min, 44 – 0% A for 2 min, 0% A for 6 min, 0 – 100% A for 1 min, 100% A for 5 min, at a flow rate of 3 ml/min. HA and related compounds were detected at 272 nm. Analysis of radiolabeled HA production by feeding [2-$^{3}$H] *myo*-inositol was carried out on a Beckman System Gold instrument equipped with a radiodetector. MS characterization was performed using a Perkin-Elmer SCIEX API 2000 mass spectrometer in the positive mode.

### 2.3.9 Targeted gene disruption of *hyg21*

The *hyg21* gene in the wild type was replaced with the apramycin resistance cassette using the PCR-targeted *Streptomyces* gene replacement method [41]. The Expand High Fidelity kit from Roche was used for PCR amplification of apramycin resistance cassette from pIJ773 with primers *hyg21*_KO_Forw (5'-**ACCGTTGACCGAGAATGGGTAAAGGAGCAGAAAACAATG***ATTCCGGGG ATCCGTCGACC*-3') and *hyg21*_KO_Revr (5'-**TCCACCGGGCCCCGCGCGGACCCGCCGCCCGGCGGATCA***TGTAGGCTG GAGCTGCTTC* 3') (bold font indicates homology to the nucleotide sequence flanking *hyg21* while italicized font is homologous to pIJ773). Gene replacement was carried out first in cosmid 17E3 and then in the genome of *S. hygroscopicus*. Gene

replacement in the resulting mutant strain, Δ*hyg21*, was confirmed by PCR amplification of the apramycin cassette from the chromosomal DNA using the outer primers, *hyg21*_Out_Forw (5'-CCGCTTTCCGTCACAACGGAT-3') and *hyg21*_Out_Revr (5'-CATGCGCACCTGGCTGAC-3') and by sequencing the PCR product.

### 2.3.10 Fermentation conditions for *S. hygroscopicus* strains

*S. hygroscopicus* wild type and Δ*hyg21* mutant strains were cultivated as reported earlier [39]. Briefly, 50 – 100 µl of spore suspension were inoculated into 50 ml of seed culture medium containing 13.0 g glucose, 7.0 g corn starch, 7.0 g NZ amine YTT, 3.0 g of corn steep solid, 1.3 g of $MgSO_4$. $7H_2O$, 0.7 g of $(NH_4)_2PO_4$, 0.7 g $KH_2PO_4$, 2 mg of $CoCl_2.6H_2O$, 2 drops of soybean oil, and 1 drop of polypropylene glycol (P2000) in 1 liter of tap water, pH 7.0. The seed culture was grown for 2 days at 30 °C and 280 rpm, and 4 ml of it was inoculated into 100 ml of production medium (50 g glucose, 10 g soy flour, 5.0 g of NZ amine YTT, 5.0 g of NaCl, 1.0 g of $CaCO_3$, 2 drops of soybean oil, and 1 drop of P2000 in 1 liter of tap water, pH 7.0). After 6 days of growth at 30 °C and 280 rpm, the mycelium was removed by centrifugation at 10000 rpm for 10 min at 4 °C and the filtered supernatant was analyzed directly by HPLC. To obtain cell lysates, mycelium was collected from 100 ml of culture, suspended in 5 ml of methanol and shaken on an orbital shaker at room temperature for 6 hr. The suspension was then subjected to a brief sonication and cell debris was removed by centrifugation.

### 2.3.11 Feeding of [2-$^3$H] labeled *myo*-inositol

Feeding studies using radiolabeled precursors were carried out in 5 ml of production medium inoculated with 200 µl of seed culture. [2-$^3$H] *myo*-inositol was added after 24 hr to a final concentration of 0.4 µCi/ml.

### 2.3.12 Assays to test the bioactivity of phosphorylated hygromycin A

The bioactivity of phosphorylated HA (HA-P) was tested by antibiotic diffusion method using an efflux pump deficient Δ*tol*C *E. coli* strain as test organism. 15 ml of LB agar was overlaid with 1.5 ml of soft agar (0.3% agar) seeded with 2 µl of an overnight culture of Δ*tol*C *E. coli*. Filter paper discs (5 mm diameter) were placed on the plate, to which 30 µg and 60 µg of purified HA-P were applied. Similar amounts of HA were used as positive control. The plate was incubated for 15 hr at 37 °C and examined for the appearance of zones of inhibition. The assay was also repeated with *S. lividans*. 25 µl of spores were spread on ISP2 agar plate and filter paper discs were placed as before. The plate was examined for zones of inhibition after 15 hr of incubation at 30 °C.

The ability of HA and HA-P to inhibit protein synthesis was verified by coupled transcription-translation experiments, which were performed by Daniel Wilson's group at the Center for Integrated Protein Science, Munich. The assays were carried out using an *E. coli* lysate-based system (RTS100 *E. coli* HY kit from Roche) for the expression of green fluorescent protein (GFP) in the presence and absence of antibiotics [98, 99]. GFP was quantitated under native and denaturing conditions using

ImageQuaNT (Molecular Dynamics, Inc.) and represented graphically using SigmaPlot (Systat Software, Inc.).

### 2.3.13 Hygromycin sensitivity of *S. hygroscopicus* and the Δ*hyg21* strain

The $MIC_{95}$ of HA for wild type and Δ*hyg21* mutant was determined by the agar plate dilution method. 30 µl of spore suspensions of both the strains (2000 CFU/ml) (CFU - colony forming unit) were plated on 3 ml ISP2 agar plates containing 200 µg/ml, 300 µg/ml, and 400 µg/ml of the antibiotic. The plates were incubated at 30 °C for 48 hr. The $MIC_{95}$ was the lowest concentration of HA that prevented visible growth of 95% or more of the CFUs on the plate.

## 2.4 Results

### 2.4.1 Sequence analysis of Hyg21

The *hyg21* ORF is 552 nucleotides long with a putative translation product of 183 amino acids and a theoretical molecular weight of 19.87 kDa. A search of the NCBI protein sequence database using the web-based BLASTP program revealed that the deduced amino acid sequence has highest similarity of 73% to the Ard2 protein from *Saccharothrix mutabilis* subsp. *capreolus*, the producer of antibiotic A201A (compound **7**) (FIGURE 3). A201A is structurally homologous to HA, and cell free extracts from *S. capreolus* wild type and *S. lividans* harboring a recombinant Ard2 have been shown to phosphorylate A201A at the C-2 hydroxyl of the hexafuranose moiety leading to loss of antibiotic activity [100]. There have been no published reports of purification or characterization of Ard2. No significant overall similarity of

Hyg21 to any other known antibiotic modifying kinases could be detected. A BLAST/Conserved Domain search instead retrieves the gluconate kinase domain proteins, indicating that Hyg21 and Ard2 may represent a new class of antibiotic modifying kinases. A search of PROSITE protein domain database indicated the presence of a ATP/GTP binding site motif, also known as Walker A motif or P-loop, [(A/G)XXXXGK(S/T)], near the *N*-terminus of Hyg21 within residues 24-31 (GIPGSGKS) [97]. This glycine-rich motif is often found in nucleotide-binding proteins and is known to form a flexible loop that interacts with ATP or GTP [101, 102]. On the basis of these observations, it is hypothesized that the *hyg21* gene encodes a kinase involved in *O*-phosphorylation of HA.

### 2.4.2 Hyg21-catalyzed phosphorylation of hygromycin A

The PCR amplified *hyg21* ORF was cloned into *E. coli* expression vector pET15b to give the pET15b-*hyg21* plasmid and overexpressed in BL21-CodonPlus cells as an *N*-terminal $His_6$-tagged protein. A large fraction of the expressed protein formed inclusion bodies under the given expression conditions but it was possible to recover substantial amounts of soluble protein using a 1-liter culture and affinity chromatography purification on a Ni-NTA agarose column. SDS-PAGE analysis of the purified preparation demonstrated a prominent protein band with a relative molecular mass of 22 kDa, consistent with the mass of Hyg21 (~20 kDa) containing a hexahistidine tag (~2 kDa) (FIGURE 11).

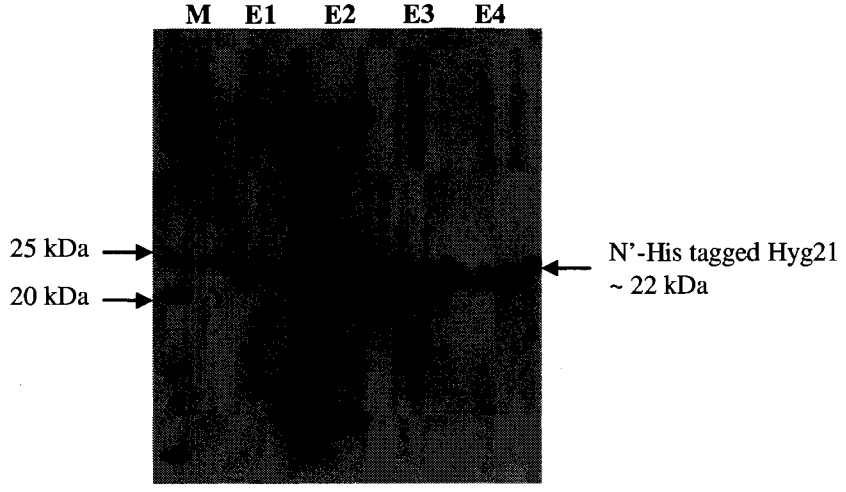


**FIGURE 11. SDS PAGE analysis of Hyg21 from Ni-NTA purification.**
Lane M – Standard protein marker; Lanes E1-E4 – Hyg21 elution fractions

In order to determine the biochemical function of Hyg21, the recombinant protein was incubated with HA and ATP at 30 °C for 2 hr. Reverse-phase HPLC analysis of the reaction mixture after incubation revealed a significant decrease in the HA peak and the appearance of a new peak with a shorter retention time (FIGURE 12B). In a control incubation without Hyg21, this new peak was absent and the levels of HA did not alter (FIGURE 12A). The shorter retention time for the new peak was consistent with increased polarity of HA through addition of a phosphoryl group. Mass spectrometric analysis of the reaction mixture showed that the compound under the new peak had a molecular mass of 592 ($[M+H]^+$) (FIGURE 12C). This increase of 80 AMU from that of HA (512 $[M+H]^+$) corresponds to the addition of a single phosphoryl group to the molecule. These data support the hypothesis that *hyg21* encodes a phosphotransferase that carries out mono-phosphorylation of HA.

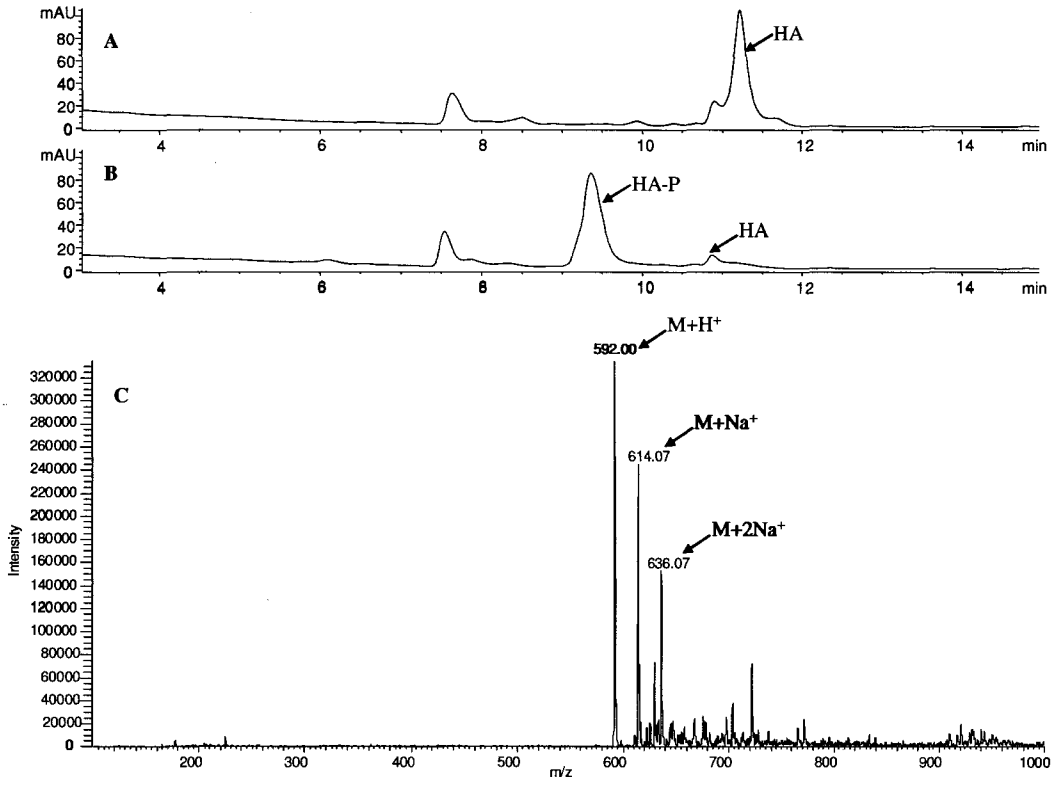


**FIGURE 12. Reverse phase HPLC – MS analyses of phosphorylation of hygromycin A by Hyg21.** Panel A.- HPLC chromatogram of a control reaction of hygromycin A (HA) and ATP without Hyg21. Panel B - HPLC chromatogram of a reaction of hygromycin A and ATP after incubation with Hyg21. The resulting phosphorylated HA (HA-P) product has a shorter retention time than HA under the tested HPLC conditions. Panel C represents mass spectral analysis (in positive mode) of the HA-P.

The presence of 5 mM 2-mercaptoethanol in assays of Hyg21 was found to be necessary for maintaining optimal activity. The optimal pH for Hyg21 activity was measured across a range of pH values from 6 to 9 (FIGURE 13A). The fastest rate of reaction, determined by the amount of product formed per min, was in the range of pH 7.5 and 8. Activity was markedly decreased at lower pH values and almost absent at

pH 5. The effect of temperature on activity was also studied across a range of 23 °C – 50 °C. In a 15 minute assay, product formation was maximal at 30 °C. The enzyme retained two-thirds of its activity at room temperature and 37 °C, but very little at 50°C (FIGURE 13B).

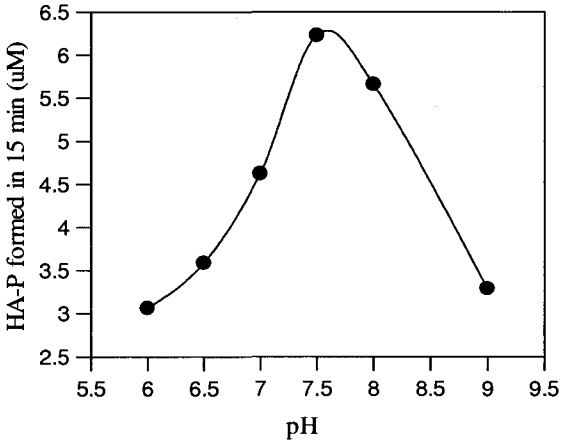


**FIGURE 13A. pH dependence of Hyg21 activity.** Assays were done with 100 μM HA and 1000 μM ATP at 30 °C for 15 min and the amount of phosphorylated HA (HA-P) was determined.

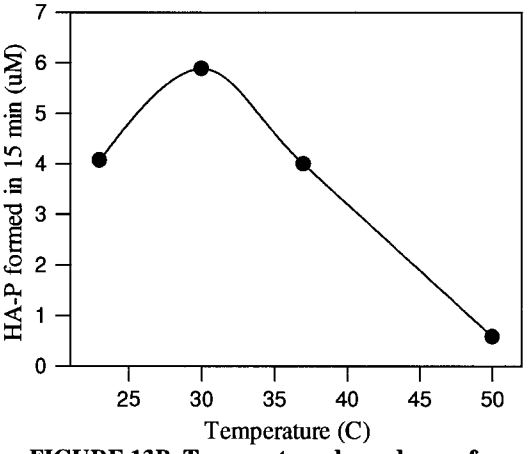


**FIGURE 13B. Temperature dependence of Hyg21 activity.** Assays were done with 100 μM HA and 1000 μM ATP at pH 7.5 for 15 min and the amount of phosphorylated HA (HA-P) was determined.

### 2.4.3 Activity of phosphorylated HA

The activity of phosphorylated HA (HA-P) was tested in a disc diffusion assay against HA-sensitive Δ*tolC E. coli* strain that has an impaired efflux mechanism due to the absence of the outer membrane component of the efflux pump [103]. As seen in FIGURE 14A, distinct zones of inhibition were seen with HA. In contrast, no zones of inhibition were seen with the phosphorylated HA even at 60 μg. Similar observations of antibacterial activity for HA but not HA-P were observed in disc diffusion assays against HA-sensitive *Streptomyces lividans*. HA-P was also tested for its ability to inhibit *in vitro* protein synthesis in a coupled transcription-translation assay. The $IC_{50}$

and $IC_{90}$ of HA-P for green fluorescent protein synthesis inhibition were observed to 28 μM and 70 μM, respectively. These values are 13-16 times higher than those for HA, which showed an $IC_{50}$ of 2.2 μM and an $IC_{90}$ of 4.2 μM. These observations are consistent with the hypothesis that phosphorylation abolishes the antibiotic potency of HA and also indicate the likely function of *hyg21* as a self-resistance determinant in *S. hygroscopicus* NRRL 2388.

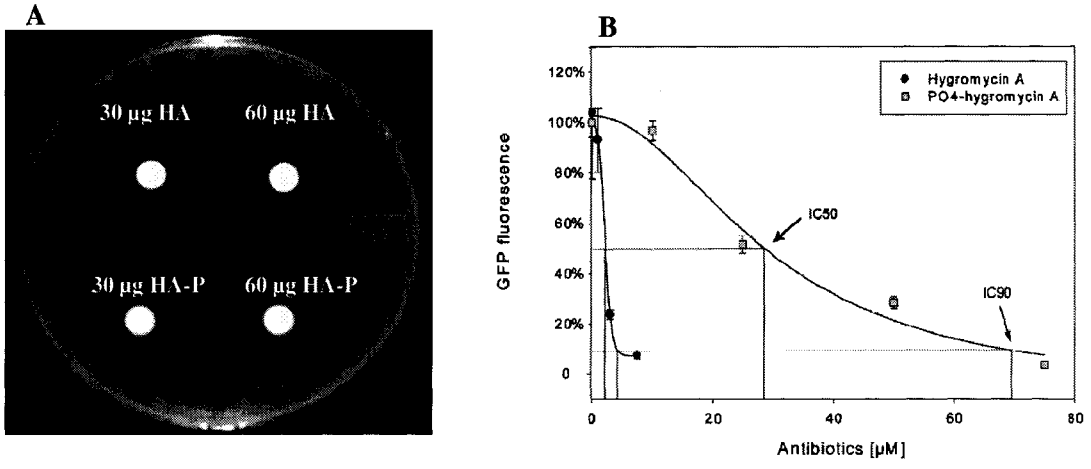


**FIGURE 14. Activity of hygromycin A (HA) and its phosphorylated form (HA-P).** A. Filter paper discs with HA or HA-P were placed on agar plate seeded with Δ*tolC E. coli*. Only HA and not HA-P showed bioactivity, as indicated by the absence of growth around the filter paper discs with HA-P.
B. *In vitro* green fluorescent protein synthesis was carried out in the presence of HA and HA-P. The $IC_{50}$ of HA-P was 15 times higher than that of HA.

### 2.4.4 Site of phosphorylation in HA

$^1$H NMR analyses of purified HA (5 mg) and HA-P (2 mg) were carried out to determine the site of phosphorylation by Hyg21. The chemical shifts of the two samples were virtually identical, with the exception of the proton signal for the C2" methine (H2"), which is shifted downfield from δ 4.36 ppm for HA to δ 4.69 ppm in

HA-P. In each case the H2" assignment was confirmed by a COSY experiment, which revealed a strong cross peak with the distinctive anomeric H1" resonance (FIGURE 15). The chemical shift change for the H2" alone is consistent with phosphorylation of the C2" hydroxyl substituent.

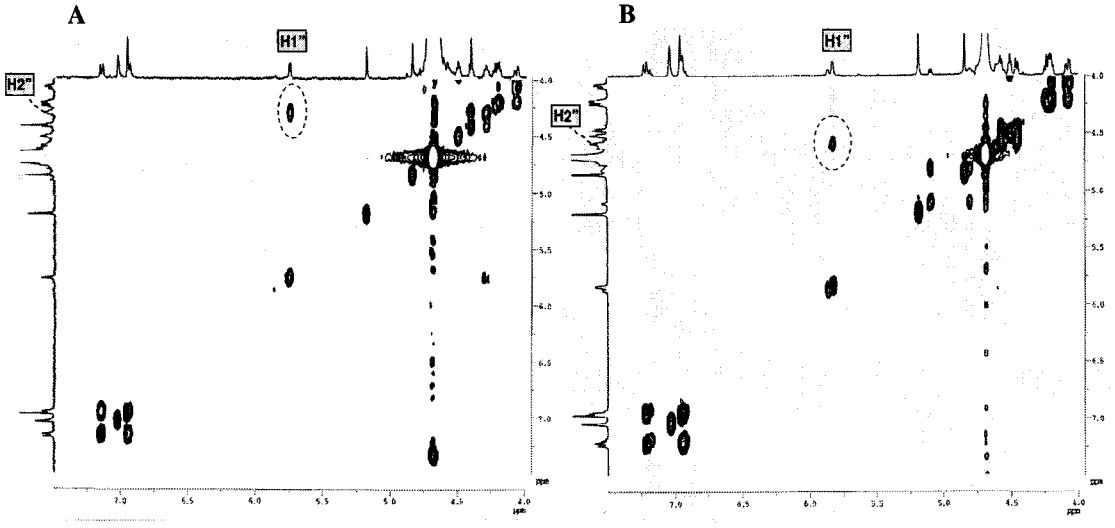


**FIGURE 15. Expansion of 2D $^{1}H$-$^{1}H$ COSY spectra of hygromycin A (A) and its phoshorylated form (B) in $D_2O$.**

### 2.4.5 Substrate specificity of Hyg21

The substrate specificity of Hyg21 was explored by carrying out enzyme assays with various analogs of HA **(2-6),** A201A (**8**), and puromycin (**9**) (FIGURE 3). HPLC-MS analyses revealed that, with the exception of **9**, all of these compounds were partially or completely converted to new products with shorter retention times and with masses increased by 80 AMU (TABLE 2). Notable among these observations was that antibiotic A201A (**8**), which is much larger than HA but has structurally similar fucofuranose and (*E*)-3-hydroxyphenyl)-2-methylacrylic acid moieties, was

also a substrate for Hyg21. In addition, **7**, which lacks the aminocyclitol and thus is significantly smaller than HA, is also a substrate. In both cases the substrate contains a fucofuranose with a C2-hydroxyl substituent. This moiety is missing in **9**, despite its structural similarities with both HA and A201A, and in this case phosphorylation with Hyg21 is not observed. These observations demonstrate that Hyg21 exhibits broad substrate specificity and that the fucofuranose moiety with C2-hydroxyl group is a key structural element required for phosphorylation. The latter inference is consistent with the observation that in HA, Hyg21 catalyzes phosphorylation at C2 of this moiety.

HA phosphorylation was also carried out by substituting ATP with guanosine triphosphate (GTP), thymidine triphosphate (TTP) and cytidine triphosphate (CTP). Besides ATP, product formation was seen only with GTP. There was no reaction with either TTP or CTP.

The rate of phosphorylation for different substrates was determined by measuring the amount of product formed per minute (TABLE 2). The reaction was linear during the first 15 min of incubation under the given assay conditions. Under these conditions $k_{cat}$ values of 2.2 $min^{-1}$ and $K_m$ values of approximately 30 μM were obtained for HA (FIGURE 16). The enzyme had a lower $K_m$ value for ATP than for GTP (FIGURE 17). Similar but slightly slower $k_{cat}$ rates were observed for ATP-dependent phosphorylation of **3** and **5** by Hyg21. These data and similar $K_m$ values indicated that the methylene group of HA, which is present as a methyl group in **3** and absent in **5,** is not important for binding and catalysis.

**TABLE 2. Summary of the kinetic data for Hyg21 phosphorylation**

| **Substrate** (see FIGURE 3 for structures) | **Substrate mass** $[M+H]^+$ | **Product mass** $[M+H]^+$ | $k_{cat}$ ($min^{-1}$) | $K_m$ (μM) |
|---|---|---|---|---|
| Hygromycin (HA) | 512 | 592 | 2.2 | 29.2 ± 4.4 |
| Methoxyhygromycin A (**3**) | 514 | 594 | 2.0 | 29.7 ± 5.8 |
| Desmethylenehygromycin A (**5**) | 500 | 580 | 1.9 | 35.6 ± 3.9 |
| 5"-Dihydrohygromycin A (Natural isomer) (**2a**) | 514 | 594 | 0.2 | 8.5 ± 3.0 |
| 5"-Dihydrohygromycin A (Non-natural isomer) (**2b**) | 514 | 594 | 1.6 | 16.5 ± 2.8 |
| 5"-Dihydromethoxyhygromycin A (Natural isomer) (**4a**) | 516 | 596 | 0.13 | 10.0 ± 2.6 |
| 5"-Dihydromethoxyhygromycin A (Non-natural isomer) (**4b**) | 516 | 596 | 1.3 | 12.3 ± 1.8 |
| 5"-Dihydrodesmethylenehygromycin A (Natural isomer) (**6**) | 502 | 582 | ND* | ND |
| 5"-Dihydro AB subunit (**7**) | 363 | 443 | ND | ND |
| A201A (**8**) | 803 | 883 | ND | ND |
| ATP | - | - | - | 198.3 ± 19.1 |
| GTP | - | - | - | 356.5 ± 62.1 |

* ND – Not determined

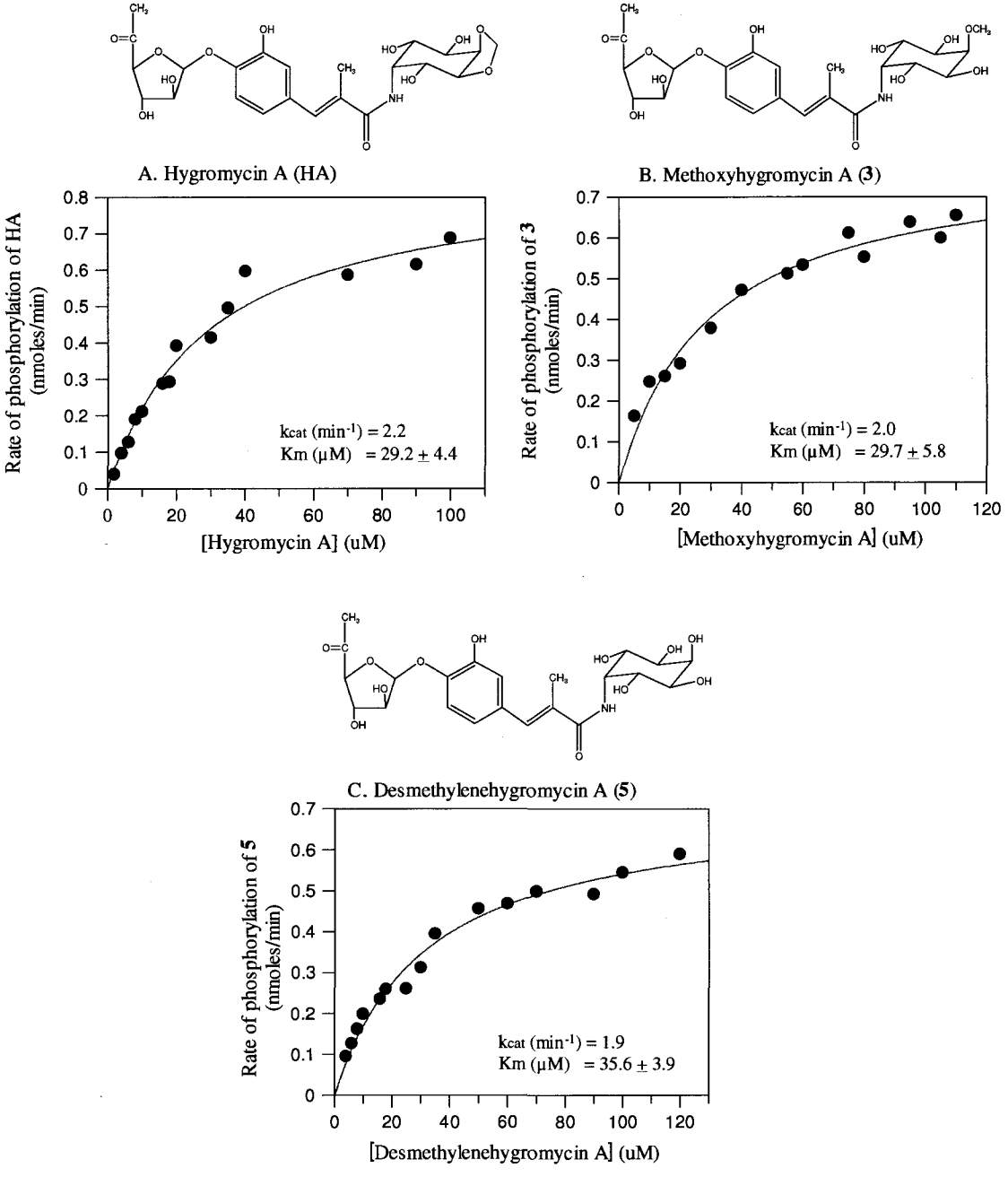


**FIGURE 16. Kinetic analysis of Hyg21 using varying concentrations of HA, 3, or 5, and 400 μM of ATP.**

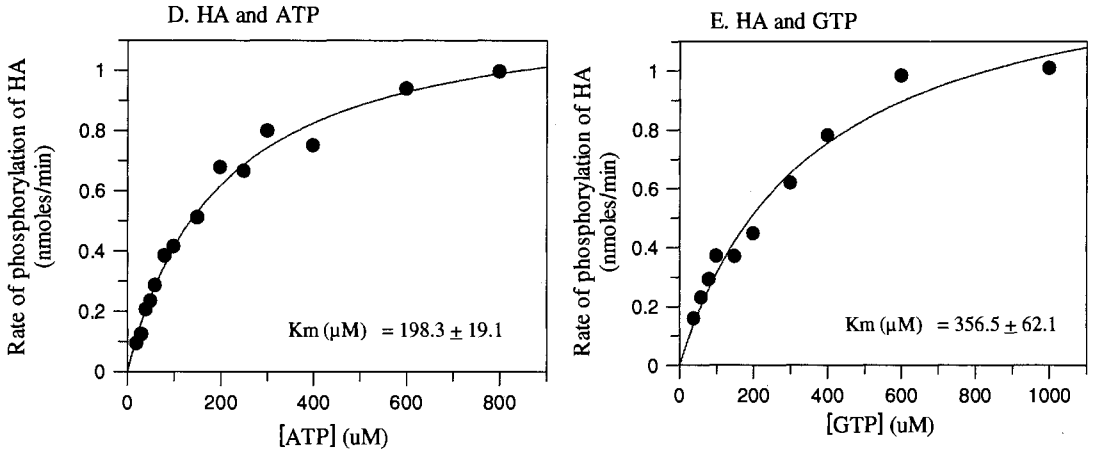


**FIGURE 17. Kinetic analysis of Hyg21 using varying concentration of ATP or GTP, and 90 μM of HA.**

Compounds **2a** (a 5"-dihydro analog of HA) and **4a** (a 5"-dihydro analog of methoxyhygromycin A, **3**) have previously been identified in fermentation of the *Δhyg26 S. hygroscopicus* mutant [40]. A diastereomeric mix of **2a** and the other 5"-dihydroisomer (**2b**) was produced by chemical reduction of HA. HPLC analysis of Hyg21-catalyzed phosphorylation of this mixture revealed much faster reaction rates with **2b** than with **2a** (FIGURE 18). Apparent kinetic values for the reaction of each isomer in the mixture were obtained, which revealed that **2b** was processed with similar reaction rate ($k_{cat}$ 1.6 $min^{-1}$) to HA, **3**, and **5**. In contrast, the reaction rate is 8-fold slower ($k_{cat}$ 0.2 $min^{-1}$) with the isomer **2a**, which appears to be either a shunt metabolite or an intermediate in the HA biosynthetic pathway (see chapter 4) (TABLE 2) (FIGURE 19).

A similar set of observations was made with a diastereomeric mixture of **4a** and **4b** (obtained by chemical reduction of **3**). The phosphorylation rate for the **4a**

isomer is slow ($k_{cat}$ 0.13 $min^{-1}$), but much faster ($k_{cat}$ 1.3 $min^{-1}$) for **4b** (TABLE 2) (FIGURE 19).

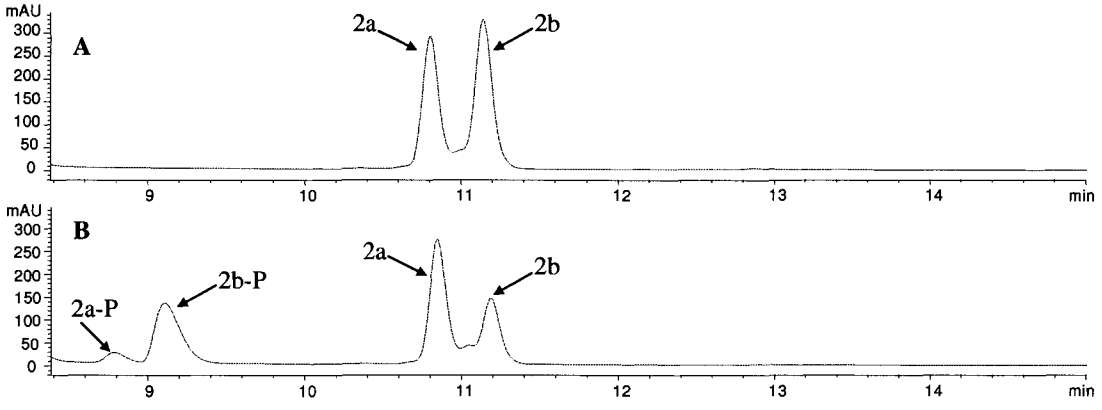


**FIGURE 18. Hyg21-catalyzed phosphorylation of a diastereomeric mixture of 5"-dihydrohygromycin A (2a and 2b).** Panel A - HPLC chromatogram of a control reaction of dihydrohygromycin A and ATP without Hyg21. Panel B - HPLC chromatogram of a reaction of dihydrohygromycin A and ATP after incubation with Hyg21. **2a** is the naturally occurring isomer also detected in fermentation broths of the wild type and the *hyg26* blocked mutant. **2b** is the non-natural isomer observed only in the diastereomeric mixture after chemical reduction of HA. The phosphorylated products of **2a** and **2b** are labeled as **2a-P** and **2b-P** respectively.

In contrast to the $k_{cat}$ values, much smaller changes in $K_m$ were observed for the various substrates. These kinetic data indicate that Hyg21 can process HA analogs in which the 5"-keto group is reduced, but the efficiency of the process is determined by the stereochemistry at the C5". Kinetic studies for substrates **6**, **7**, and **8** were precluded because of low availability of the substrates and/or presence of impurities. A comparison of reaction completion with HA and **8** carried out under standard conditions indicated that the rate of conversion of **8** was at least 5-fold slower.

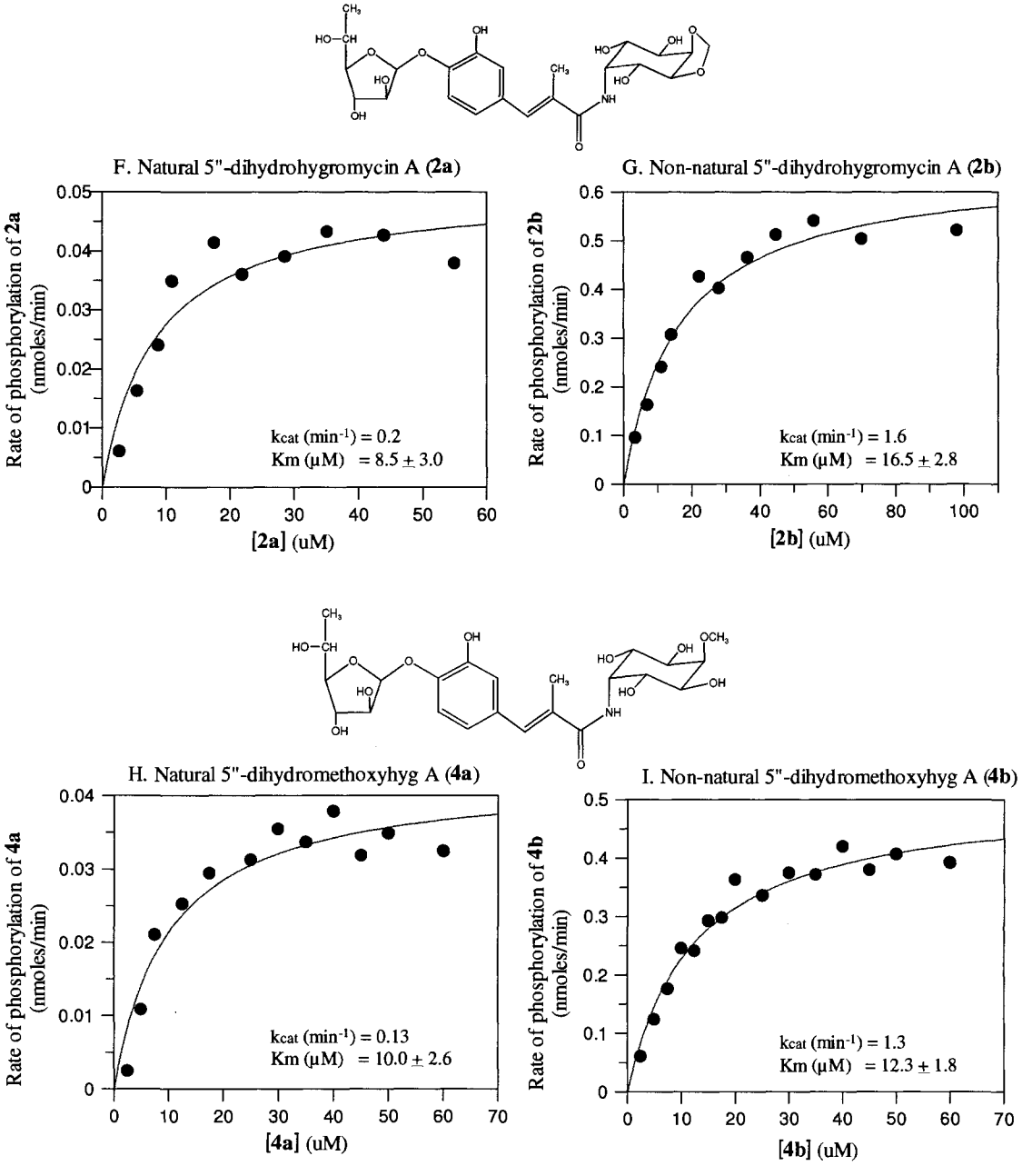


**FIGURE 19. Kinetic analysis of Hyg21 with natural and non-natural 5"-dihydro compounds.**

### 2.4.6 Generation and analysis of a Δ*hyg21 S. hygroscopicus* mutant

The *hyg21* gene in *S. hygroscopicus* was replaced with the apramycin resistance gene to assess its role in HA biosynthesis and resistance. A gene replacement strategy was used because the *hyg21* is well-separated from its flanking genes, and its orientation relative to these indicates that it is not part of a polycistronic transcript (FIGURE 20).

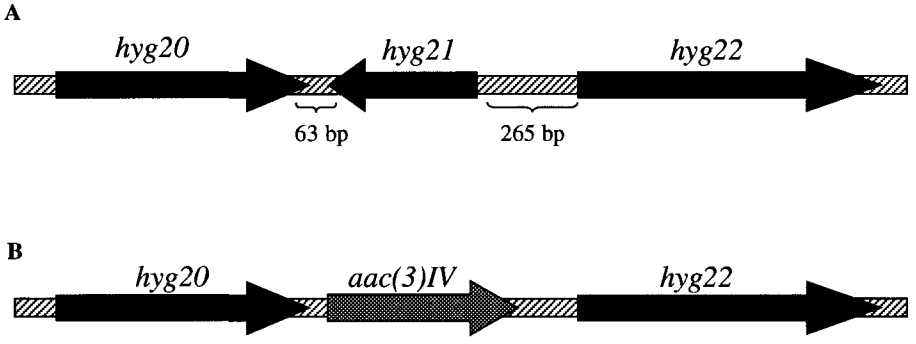


**FIGURE 20. Schematic representation of *hyg20-22* region in the genome of *S. hygroscopicus* wild type (Panel A) and Δ*hyg21* mutant (Panel B).** The *hyg20* and *hyg22* gene products are homologous to transglucosylases and acyltransferases respectively, and have been proposed to be involved in HA biosynthesis. The *hyg21* gene is replaced with the apramycin resistance gene, *aac3(IV)*, in Δ*hyg21* strain.

The Δ*hyg21* mutant strain was cultured and the fermentation broth was analyzed for the production of HA. HA was detected indicating that *hyg21* was not essential for the biosynthetic process. Nonetheless, the yields were dramatically reduced (>90%) from the 0.8 g/L of HA obtained in the wild type strain. Detailed LC-MS analyses of fermentation broth of Δ*hyg21* also revealed the presence of **3**, **4a**, **5** and **6**. The same compounds could be detected by radioactive scintillation counting when the mutant was grown in the presence of tritiated *myo*-inositol (which is

converted into the aminocyclitol portion of HA) (FIGURE 11). While the levels of **3**, **4a**, **5** and **6** could not be quantitated, the analyses indicated that they were similar in both the wild type and Δ*hyg21* mutant, contrasting the observations made for the levels of HA.

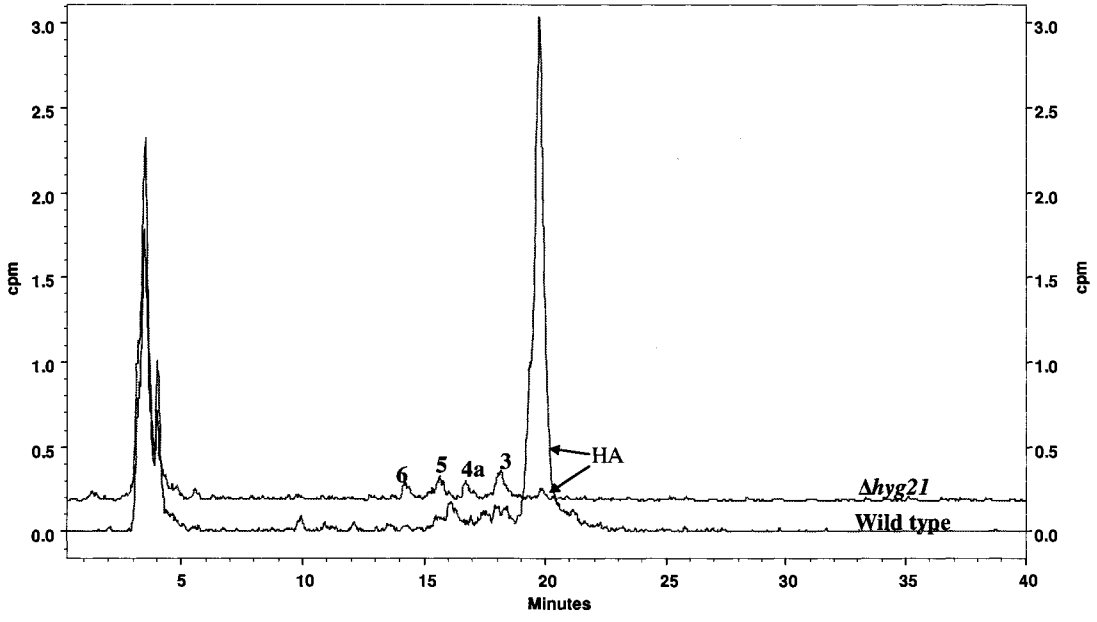


**FIGURE 21. Reverse-phase HPLC analyses and radiolabel detection of wild type and Δ*hyg21* culture broths grown in the presence of [2-$^3$H] *myo*-inositol.** Production of hygromycin A (HA) was significantly decreased in the mutant. Radiolabeled analogs of HA are present in fermentation broths of both the wild type and Δ*hyg21* strains (see FIGURE 3 for structures).

The low amounts of HA in the fermentation broth of Δ*hyg21* raised the possibility that it is HA-P that is exported from *S. hygroscopicus* by an efflux pump and subsequently converted to HA by an extracellular phosphatase. In such a case HA might be expected to accumulate inside the cells of Δ*hyg21*. To investigate this possibility the mycelium of Δ*hyg21* was lysed by methanol treatment and the lysate was analyzed by HPLC. However, HA could not be detected in the cell lysate and it

was estimated that nearly all of the HA made by this strain is found in the fermentation broth. Also, no HA-P could be detected in either the cell lysate or the fermentation broth of the wild type strain. An agar plate dilution assay was carried out to assess whether the Δ*hyg21* strain had increased sensitivity to HA as compared to the wild type strain. The $MIC_{95}$ for both the strains was found to be 400 μg/ml.

## 2.5 Discussion

Analysis of the deduced amino acid sequence of the *hyg21* gene in the HA biosynthetic gene cluster led to a hypothesis that it encodes a protein that phosphorylates HA and thus provides a resistance mechanism to the producing organism by antibiotic inactivation. The first component of this hypothesis has been unequivocally verified by *in vitro* assays in which Hyg21 phosphorylated HA selectively at the C2"-OH position. Hyg21 also phosphorylates a number of HA analogs, and the site of modification in these may also be the C2"-OH. Some of these analogs are observed at various levels in fermentations of the wild type *S. hygroscopicus* [39, 40]. It was also observed that these analogs, in particular methoxyhygromycin A and desmethylenehygromycin A, have some level of antibacterial activity, albeit less than that observed for HA. Presumably, resistance to these compounds as well as HA can be provided in part by the Hyg21-catalyzed phosphorylation.

Although Hyg21 phosphorylated HA, the rate of reaction was very slow ($k_{cat}$ of ~2 $min^{-1}$). Analyses of *S. hygroscopicus* fermentations reveal that the majority of the

HA product is found in fermentation media indicating an efficient export process. No evidence for any HA-P in the fermentation broth or in the cell lysate is seen, and sequence analyses of the HA biosynthetic gene cluster to date have not revealed a candidate phosphatase that would convert HA-P to HA (the *hyg25* gene product appears to be involved in conversion of *myo*-inositol-1-phosphate to *myo*-inositol, a step in the biosynthesis of the aminocyclitol moiety of HA, chapter 3). Thus, all evidence indicates that it is HA that is exported and that HA-P may be generated from residual HA in the cell. In such a case, a slow rate of phosphorylation by Hyg21 would allow most of the HA biosynthetic product to be exported rather than become trapped intracellularly as HA-P.

The results from these studies do not provide unequivocal evidence for the hypothesis that phosphorylation of HA is a resistance mechanism in the producing organism. It is observed that HA and not HA-P has antibacterial activity against other bacteria. The loss of antibacterial activity has further been shown to be due to inhibition of binding to the ribosomal target than due to poorer penetration into the organisms. However, the Δ*hyg21* mutant retains significant resistance to HA. This observation likely reflects the presence of other operational mechanisms of resistance. The most likely of these are methylation of the ribosomal RNA, catalyzed by the *hyg29* gene product, and an efficient HA export process, catalyzed by the *hyg19* and *hyg28* gene products. Characterization of the remaining putative resistance determinants in the HA biosynthetic gene cluster are reported in the later part of this thesis. Finally, the observation that insertional inactivation of *hyg21* reduces the

production of HA to almost negligible amounts is curious. A polar effect from replacement of the gene cannot be ruled out, but seems unlikely given the strategy used and the organization of genes surrounding *hyg21* (FIGURE 20). This result was consistently observed in all the four mutant colonies that were examined. A significant decrease in HA production would be predicted in this mutant if the Hyg21-catalyzed phosphorylation process occurred at an earlier step in the biosynthetic process, with the later stages occurring with phosphorylated intermediates. Early modification would ensure that the resistance mechanism is in operation prior to assembly of the final product and has precedent in the biosynthesis of streptomycin and paromomycin [44, 45]. The slow turnover of HA might also indicate that a pathway intermediate, and not the final product, may be the preferred substrate for Hyg21. However, there is no genetic evidence for a phosphatase that would be responsible for the conversion of HA-P to HA, and HA-P is not detected in fermentations of the wild type strain. These observations argue against Hyg21-catalyzed phosphorylation of a pathway intermediate as a step in the biosynthetic process. In the case of tylosin biosynthesis it has been shown that disruption of any of the four genes involved in the biosynthesis of the mycaminose sugar, which is the first sugar that gets attached to tylactone (the polyketide aglycone), abolishes not just tylosin production but also the accumulation of tylactone [104]. In a similar way, HA-P may be required for stimulating the HA biosynthetic pathway by positive feedback regulation, accounting for the decreased production in the Δ*hyg21* mutant.

In conclusion, it has been shown in this study that Hyg21 catalyzes phosphorylation of HA and related compounds, leading to loss of antibacterial activity due to poorer binding to the ribosomes. Thus, *hyg21* is the first of the several possible resistance determinants in *S. hygroscopicus* NRRL 2388 that has been functionally characterized. The roles of Hyg6 and Hyg29 (methyl transferases), and Hyg19 and Hyg28 (antibiotic efflux proteins) as additional resistance determinants are described in the subsequent sections of this thesis.

## 3. Characterization of two methyltransferase homologs, *hyg6* and *hyg29*, from the biosynthetic gene cluster of hygromycin A

### 3.1 Summary

Hygromycin A (HA) exerts its antibiotic activity by binding to the 23S rRNA and inhibiting the peptidyl transferase reaction. The structure of HA is characterized by the presence of a methylene bridge between the C4 and C5 hydroxyl groups in the aminocyclitol subunit, which is derived from *S*-adenosylmethionine. The gene cluster for HA biosynthesis contains two methyltransferase homolog genes, *hyg6* and *hyg29*. Targeted disruption of *hyg6* abolished the production of HA and methoxyhygromycin A. Instead, the *hyg6* mutant strain produced two new metabolites, desmethylene hygromycin A and 5"-dihydrodesmethylenehygromycin A, which lacked the methylenedioxy bridge. The structures of the desmethylene compounds were confirmed by mass spectrometry and NMR analysis. Antibacterial activity assays against an efflux pump-deficient *E. coli* strain (Δ*tolC E. coli*) showed that the biological activity of desmethylenehygromycin A was 15 times reduced in comparison to HA. This activity is comparable to that of methoxyhygromycin A, indicating that an intact methylenedioxy bridge is essential for optimum antibacterial activity. At the same time, the *in vitro* protein synthesis inhibition activity of desmethylene hygromycin A was nearly 4 times greater than that of HA or methoxyhygromycin A, suggesting that the loss in biological activity due to disruption of the methylenedioxy ring is likely to be due to reduced uptake of the compounds into the cell and not due to their inability to bind to the ribosomes. Disruption of *hyg29* did not affect the

resistance of *S. hygroscopicus* to HA or the antibiotic production profile, although the antibiotic yield was reduced. Ribosomal RNA methylation is a possible route of self-resistance in *S. hygroscopicus*, which could be performed by the *hyg29* gene product. It is currently not known whether the ribosomes of *S. hygroscopicus* are modified or not, but the results of *hyg29* disruption indicate that this gene is dispensable for antibiotic production and resistance, presumably due to the presence of other putative self-resistance determinants.

### 3.2 Introduction

Bacteria protect themselves from ribosome-targeting antibiotics chiefly by 1) mutations in the genes for ribosomal RNA (rRNA) or ribosomal proteins, or 2) by methylation of rRNA at specific positions. Genes for rRNA methylases conferring intrinsic resistance are frequently found in the biosynthetic gene clusters of antibiotics that bind to the ribosome. Macrolide antibiotics such as erythromycin, clarithromycin, oleandomycin, pikromycin, and tylosin bind to the 50S ribosomal subunit The crystal structure of the 50S ribosomal subunit complexed with macrolides revealed the manner in which the macrolactone and the sugar substituents of the antibiotic interact with the ribonucleotides lining the binding pocket in 23S rRNA [105-107]. Specifically, the 2'-hydroxyl and the 3'-dimethylamino groups of the common desosamine sugar make hydrogen bonds with N1 and N6 of $A_{2058}$ in 23S rRNA. Mono- or dimethylation of the exocyclic amine at N6 of $A_{2058}$ results in loss of these contacts and prevents drug binding, leading to resistance. The rRNA methylases in macrolide producers use *S*-adenosylmethionine as methyl group donor and are either

constitutively or inducibly expressed. In *S. fradiae*, the producer of tylosin, expression of the genes encoding the TlrA dimethyltransferase, acting on $A_{2058}$, and the TlrB monomethyltransferase, which methylates $G_{748}$, is induced by tylosin, whereas the *tlrD* gene for a $A_{2058}$-monomethyltransferase is constitutively expressed [56, 57, 59]. A stepwise response to tylosin was proposed to explain the presence of multiple rRNA methylases in *S. fradiae* [59]. $A_{2058}$ monomethylation by the constitutively-expressed *tlrD* provides protection from low amounts of tylosin diffusing in from older mycelium. When tylosin production begins in the local regions of the mycelium, expression of *tlrB* is induced, leading to $G_{748}$ methylation and enhanced resistance. Further increase in tylosin production induces *tlrA* expression and $A_{2058}$ dimethylation, resulting in maximum resistance.

A different category of methyltransferases associated with antibiotic gene clusters is comprised of those that modify the structure of the antibiotic by methylation, such as the post-polyketide synthase (post-PKS) methyltransferases. Depending on the site of reaction, these enzymes are classified as *O*-, *N*-, or *C*-methyltransferases. Methylation can take place either on the polyketide backbone or on the non-PKS moieties such as sugars before or after their attachment to the PKS core. Multiple methyltransferases are functional in the biosynthesis of tylosin. An *N*-methyltransferase, TylM, dimethylates the 3-amino group during biosynthesis of the mycaminose moiety of tylosin, while a *C*-methyltransferase, TylCIII, acts on the mycarose moiety [108]. While these enzymes act before glycosyl transfer onto the lactone occurs, there are additional methylases that catalyze *O*-methylation in the final

two steps of tylosin biosynthesis, and thus can be called true post-PKS enzymes. Demethylmacrocin *O*-methyltransferase methylates the C2"' hydroxyl and converts demethylmacrocin to macrocin, the penultimate product in tylosin biosynthesis [109]. Macrocin is acted upon by macrocin *O*-methyltransferase at C3"' hydroxyl to form tylosin [110]. Both these enzymes are highly selective for their respective substrates and neither of them is capable of methylating the alternative demethylated compound, an observation that established that the 2"'-*O*-methylation step precedes 3"'-*O*-methylation. In biosynthesis of tetracenomycin, three consecutive SAM-dependent methylations take place on the polycyclic aromatic scaffold. A C3 *O*-methyl transferase, TcmN, transforms tetracenomycin D3 to tetracenomycin B3, which is further *O*-methylated at C8 by TcmO into tetracenomycin E. A different enzyme, TcmP, now carboxymethylates tetracenomycin E and forms the penultimate biosynthetic product, tetracenomycin A2 [111, 112].

Heterologous expression and gene inactivation experiments of methylases have been carried out to verify their roles in self-resistance and antibiotic biosynthesis, and also to produce intermediates or analogs with higher biological activity. The latter objective has been achieved in the case of avermectin biosynthesis in *S. avermitilis*. The avermectins are produced as a mixture of two categories of compounds – the A components that have a methoxy group at C5, and the B components with a C5 hydroxyl group. The unmethylated B components have higher biological activity than the methylated A compounds. Conversion of the B type to the A type is catalyzed by avermectin B 5-*O*-methyltransferase encoded by the *aveD* gene. When an insertional

inactivation of *aveD* was performed, it resulted in a mutant strain that accumulated only the more active avermectin B components [113, 114].

As described in chapter 1, hygromycin A (HA) prevents protein synthesis by inhibiting peptidyl transferase reaction [30]. RNA footprinting experiments showed that HA binds in the central loop region of domain V of 23S rRNA, which is the region for peptidyl transferase activity [31]. Sequence analysis of the biosynthetic gene cluster of HA identified *hyg6* and *hyg29* as putative methyltransferase genes [40].

Since HA binds to the ribosomes, it is hypothesized that rRNA methylation by the activity of either the *hyg6* or *hyg29* gene products may exist as a self-resistance mechanism in *S. hygroscopicus*. The aminocyclitol moiety of HA has a unique methylene bridge between the C4 and C5 hydroxyl groups, whereas the non-bridge analog, methoxyhygromycin A (**3**), has a methoxy group at C5 (FIGURE 3). Feeding studies had indicated that the methylene bridge was derived from *S*-adenosyl methionine and it was proposed that the bridge formation involves methylation of the C5 hydroxyl group of *neo*-inosamine 2 by a SAM-dependent methyltransferase, followed by cyclization [39]. Thus, either *hyg6* or *hyg29* is hypothesized to encode a C5 *O*-methyltransferase acting on the aminocyclitol. In the present chapter, the results of targeted gene disruption experiments performed to verify the proposed roles of *hyg6* and *hyg29* are reported. The study revealed that methylation of the C5 hydroxyl group is performed by Hyg6 and not by Hyg29. An analog of HA without the

methylenedioxy bridge, produced by the Δ*hyg6* mutant, was observed to have significantly reduced antibacterial activity, but retained considerable *in vitro* protein synthesis inhibition activity. Disruption of *hyg29* showed that it is not essential for antibiotic production or self-resistance of *S. hygroscopicus*.

## 3.3 Materials and methods

### 3.3.1 Chemicals, bacterial strains and growth conditions

All chemicals were purchased from Sigma unless stated otherwise. Hygromycin A and 2L-2-amino-2-deoxy-4,5-*O*-methylene-*neo*-inositol (C subunit) were kindly supplied by Pfizer Inc. The SuperCos1 vector-derived cosmids 17E3 and 15A10 were the sources for *hyg6* gene and *hyg29* gene, respectively. Δ*hyg6* and Δ*hyg29* are mutant strains derived from *S. hygroscopicus* wild type in which the respective genes have been replaced with the apramycin resistance cassette. Fermentation conditions for *S. hygroscopicus* strains are described in section 2.3.10. The Δ*hyg6* strain was fed with the C subunit by adding the compound after 24 hr of fermentation to a final concentration of 5 mM. The Δ*tol*C *E. coli* strain was procured from the *E. coli* Genetic Stock Center at Yale University.

### 3.3.2 Targeted disruption of *hyg6* and *hyg29* genes

The *hyg6* and *hyg29* genes were independently replaced with the apramycin resistance cassette using the PCR-targeted *Streptomyces* gene replacement method [41]. The gene knockout primers and outer primers for verification of the gene disruption are given in TABLE 3. Because of the 8 nucleotide overlap between *hyg6*

and the succeeding *hyg7* gene, only 705 out of 750 bases of *hyg6* were targeted. Similarly, in order to not affect *hyg28*, with which *hyg29* shares 68 bases, only 1007 out of 1137 nucleotides of *hyg29* were replaced with the apramycin resistance cassette (FIGURE 22). The resulting mutant strains were termed Δ*hyg6* and Δ*hyg29*. The DNA sequence data were analyzed with Accelrys DS Gene software. Public domain sequence database searches were performed using tools at the NCBI server and at the Expasy proteomics server.

**TABLE 3. Primers used for disruption of *hyg6* and *hyg29***

| | |
|---|---|
| **Primers for *hyg6* gene disruption** | |
| *hyg6*_KO_Forw | 5'**CGCCCCTCGACCGCGAAGACCTTCTGGGGGCAGCGGATG***ATTC CGGGGATCCGTCGACC*-3' |
| *hyg6*_KO_Revr | 5'**ATGGTGGTCCGGCCTCCTCGTGTCGTCTGCGTGCCACTG***TGTA GGCTGGAGCTGCTTC*-3' |
| **Outer primers for verification of *hyg6* gene disruption** | |
| *hyg6*_Out_Forw | 5'-CTCGCGCAACGCCTGCGCCA-3' |
| *hyg6*_Out_Revr | 5'-GCCGTGGTTGACCGCGACG-3' |
| **Primers for *hyg29* gene disruption** | |
| *hyg29*_KO_Forw | 5'**GCCGCCCGACCCGAGGCGCCCGGAGACGCCGCCGCGATG***ATT CCGGGGATCCGTCGACC*-3' |
| *hyg29*_KO_Revr | 5'**GCCGTCCGGCCTCTGTGGACCAGCTGTGCGCCGCCTCCA***TGTA GGCTGGAGCTGCTTC*-3' |
| **Outer primers for verification of *hyg29* gene disruption** | |
| *hyg29*_Out_Forw | 5'-CTGGAGGGAGACCCTCGTGG-3' |
| *hyg29*_Out_Revr | 5'-CGCGCCCGGACAACGGTCCC-3' |

Bold font indicates homology to the nucleotide sequence flanking *hyg6* or *hyg29* while italicized font is homologous to pIJ773 plasmid bearing the $Apra^R$ cassette.

### 3.3.3 HPLC/MS analysis and quantitation of antibiotic production yields

Reverse phase HPLC analysis of fermentation broths of *S. hygroscopicus* strains were carried out using a methanol-water gradient system as described in

section 2.3.8. Mass spectrometric analysis was carried out in negative mode on a Bruker Daltonics MicroTOF-Q system. For a quantitative analysis of production of HA and its analogs, cultures of the wild type and mutant strains were set up in triplicate. Using HA provided by Pfizer Inc, a standard curve was generated of peak area *vs* amount in μg with a range between 5 μg and 50 μg. 50 μl of filtered fermentation broth from each culture were injected. The amounts of HA and related products in each injection sample were determined from their individual peak areas using the standard curve as reference and extrapolated to estimate the total production per liter of fermentation.

### 3.3.4 Extraction and characterization of desmethylene analogs

For extraction of desmethylene compounds, Amberlite XAD-4 (Sigma) was added to the fermentation broth of Δ*hyg6* (1:20 ratio by volume) and stirred overnight at 4 °C. The XAD column was washed first with water and then with methanol to elute the bound compound. The eluted fraction was concentrated by evaporation and the solid was re-dissolved in methanol. Further purification was carried out by semipreparative HPLC (see section 2.38). $^1$H-NMR spectra were recorded on a Bruker AMX-400 NMR. 2D COSY correlation spectra were recorded on a Bruker AMX-600 NMR spectrometer. Coupling constants (*J*) were expressed in Hertz. Abbreviations for multiplicities are: s = singlet, d = doublet, t = triplet, q = quartet, m = multiplet.

**Hygromycin A (1).** $^1$H-NMR (400 MHz, $D_2O$) $\delta$ 7.10 (1H, d, $J$ = 8.0, H-9′), 7.01 (1H, s, H-3′), 6.88 – 6.91 (2H, m, H-5′, H-8′), 5.69 (1H, d, $J$ = 4.4, H-1″), 5.18, 4.83 (2H, -

$OCH_2O$-), 4.50 – 4.48 (1H, m, H-2), 4.40 – 4.18 (5H, m, H-2″, H-4″, H-4, H-5, H-6), 4.08 (1H, t, $J$ = 2.8, H-3″), 3.95 (1H, dd, $J$ = 5.2, H-1), 3.82 (1H, dd, $J$ = 3.6, H-3), 2.16 (3H, s, H-6″), 2.02 (3H, s, α-$CH_3$).

**Desmethylenehygromycin A (5).** $^1$H-NMR (400 MHz, $D_2O$) $\delta$ 7.14 (1H, d, $J$ = 8.4, H-9′), 6.99 (1H, s, H-3′), 6.94 (1H, s, H-5′), 6.93 (1H, d, $J$ = 8.4, H-8′), 5.72 (1H, d, $J$ = 4.4, H-1″), 4.74 – 4.62 (1H, m, H-2), 4.41 – 4.40 (2H, m, H-3″, H-4″), 4.30 – 4.22 (1H, m, H-2″), 4.02 (1H, t, $J$ = 2.8, H-5), 3.95 – 3.92 (2H, m, H-1, H-3), 3.72 (2H, dd, $J$ = 10.0, 2.8, H-4, H-6), 1.99 (6H, s, α-$CH_3$, H-6″).

**5″-Dihydrodesmethylenehygromycin A (6).** $^1$H-NMR ($D_2O$, 400 MHz) $\delta$ 7.17 (1H,d, $J$ = 8.2, H-9′), 7.08 (1H, s, H-3′), 7.01 (1H, s, H-5′), 6.99 (1H, d, $J$ = 8.2, H-8′), 5.69 (1H, d, $J$ = 4.4, H-1″), ~4.7 (1H, partially obscured by solvent peak, H-2), 4.33-4.29 (2H, m, H-2″, H-3″), 4.11 (1H, t, $J$ = 2.8, H-5), 4.03 (2H, dd, $J$ = 10.0, 4.2, H-1, H-3), 3.87-3.80 (3H, m, H-4, H-6, H-5″), 3.74 (1H, t, $J$ = 6.0, H-4″) 2.08 (3H, s, α-$CH_3$), 1.13 (3H, d, $J$ = 6.8, H-6″).

### 3.3.5 $MIC_{90}$ of HA and analogs for Δ*tolC E. coli*

5 µl of an overnight culture of Δ*tolC E. coli* were added to 200 µl final volume of fresh LB supplemented with HA or its analogs. The tubes were grown with shaking for 2 hr at 37°C and the absorbance at 600 nm was measured. The $MIC_{90}$ is defined as the lowest concentration of the antibiotic at which 90% of *E. coli* growth is inhibited compared to a control *E. coli* culture grown in the absence of any antibiotic.

### 3.3.6 Coupled transcription-translation assay

All coupled transcription-translation experiments were carried out by Daniel Wilson's group at the Center for Integrated Protein Science, Munich.using an *E. coli* lysate-based system for the expression of green fluorescent protein (GFP) in the presence and absence of antibiotics [98, 99]. GFP was quantitated under native and denaturing conditions using ImageQuaNT (Molecular Dynamics, Inc.) and represented graphically using SigmaPlot (Systat Software, Inc.).

### 3.3.7 Hygromycin sensitivity of Δ*hyg29* strain

The $MIC_{95}$ of HA for the Δ*hyg29* mutant was determined by the agar plate dilution method as described in section 2.3.13. Briefly, spores were plated on ISP2 agar plates containing varying amounts of HA, incubated at 30°C for 48 hr, and scored for growth. The $MIC_{95}$ was defined as the lowest concentration of HA that prevented visible growth of 95% or more of the colony forming units on the agar plate.

## 3.4 Results

### 3.4.1 Sequence analysis of *hyg6* and *hyg29*

The *hyg6* gene is comprised of 750 bases. Its predicted protein product consists of 249 amino acids with a calculated molecular mass of 27.62 kDa, and shows similarity to the FkbM family of methyltransferases. This protein family is represented by 31-*O*-demethyl-FK506 methyltransferase (FkbM) involved in biosynthesis of the macrocyclic polyketide immunosuppressants FK506 and FK520 [115]. Heterologous expression and targeted gene disruption had demonstrated that FkbM catalyzed C31

*O*-methylation leading to FK506 and FK520. Like FkbM, Hyg6 also does not show any conserved sequence motifs characteristic of SAM-binding proteins. The *hyg29* gene has 1137 bases, and its predicted protein product has 378 amino acids and a molecular mass of 40.45 kDa. Interestingly, the sequence of Hyg29 shows high similarity (53 %) to carboxyl *O*-methyltransferases of the protein-L-isoaspartate(D-aspartate) *O*-methyltransferase (PCMT) family. No authentic rRNA methyl transferases were retrieved in the BLAST search, although a Conserved Domain Database search also retrieved the KsgA/Dim1 family of rRNA adenine dimethyltransferases along with the PCMT family. Conserved SAM-binding motifs were, however, not identified in Hyg29.

### 3.4.2 Targeted disruption of *hyg6* and *hyg29*

To determine the roles of *hyg6* and *hyg29* in HA biosynthesis and self-resistance, the genes were independently replaced with apramycin resistance cassette in the wild type *S. hygroscopicus* genome by PCR targeting method [41]. Care was taken to avoid the regions of overlap of *hyg6* and *hyg29* with their neighboring genes (FIGURE 22). The Δ*hyg6* and Δ*hyg29* mutant strains thus obtained were cultured along with the wild type, and the fermentation broths were analyzed by HPLC and LC-MS for antibiotic production. Analyses of the fermentation broth of Δ*hyg29* mutant showed that it produced HA, **3**, and their corresponding C5"-hydroxyl analogs **2** and **4**. The level of HA production had, however, decreased by ~60% (400 mg/l) compared to that in the wild type (~1 g/l). In contrast, the production of HA was completely abolished in Δ*hyg6* strain. Instead, the HPLC trace of this mutant showed a

dominant new peak at 12.5 min and an additional minor peak at 11.5 min under the existing HPLC conditions (FIGURE 23).

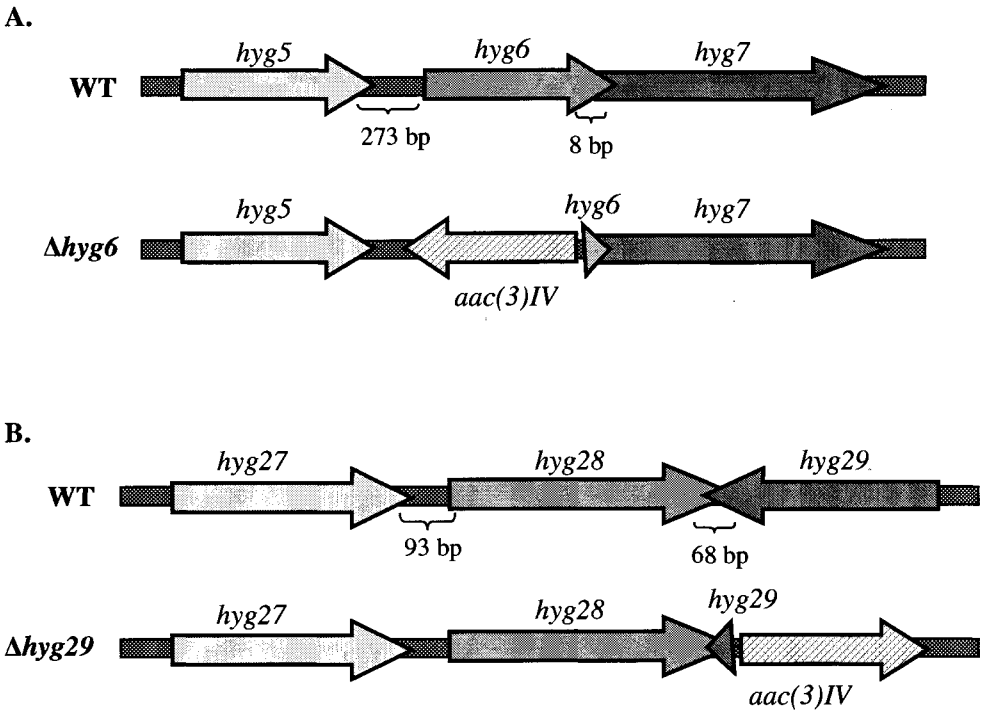


**FIGURE 22. Arrangement of *hyg6* (panel A) and *hyg29* (panel B) genes in the hygromycin A biosynthetic gene cluster.** The *hyg5* gene in panel A is a mannose dehydratase homolog while *hyg7* is a gene with an unknown function. The *hyg27* and *hyg28* genes in panel B are homologous to DAHPS synthase and ABC transporter, respectively.

The major peak showed a mass in negative mode of m/z = 498 $[M - H]^-$ and the minor peak showed a mass of m/z = 500 $[M - H]^-$. A mass of 499 is consistent with the mass of HA that is missing the methylene group bridging O-4 and O-5. A mass of 501 corresponds to a C5"-reduced derivative of the major peak. Therefore, the two peaks are indicative of desmethylene HA analogs (**5, 6**) (FIGURE 3).

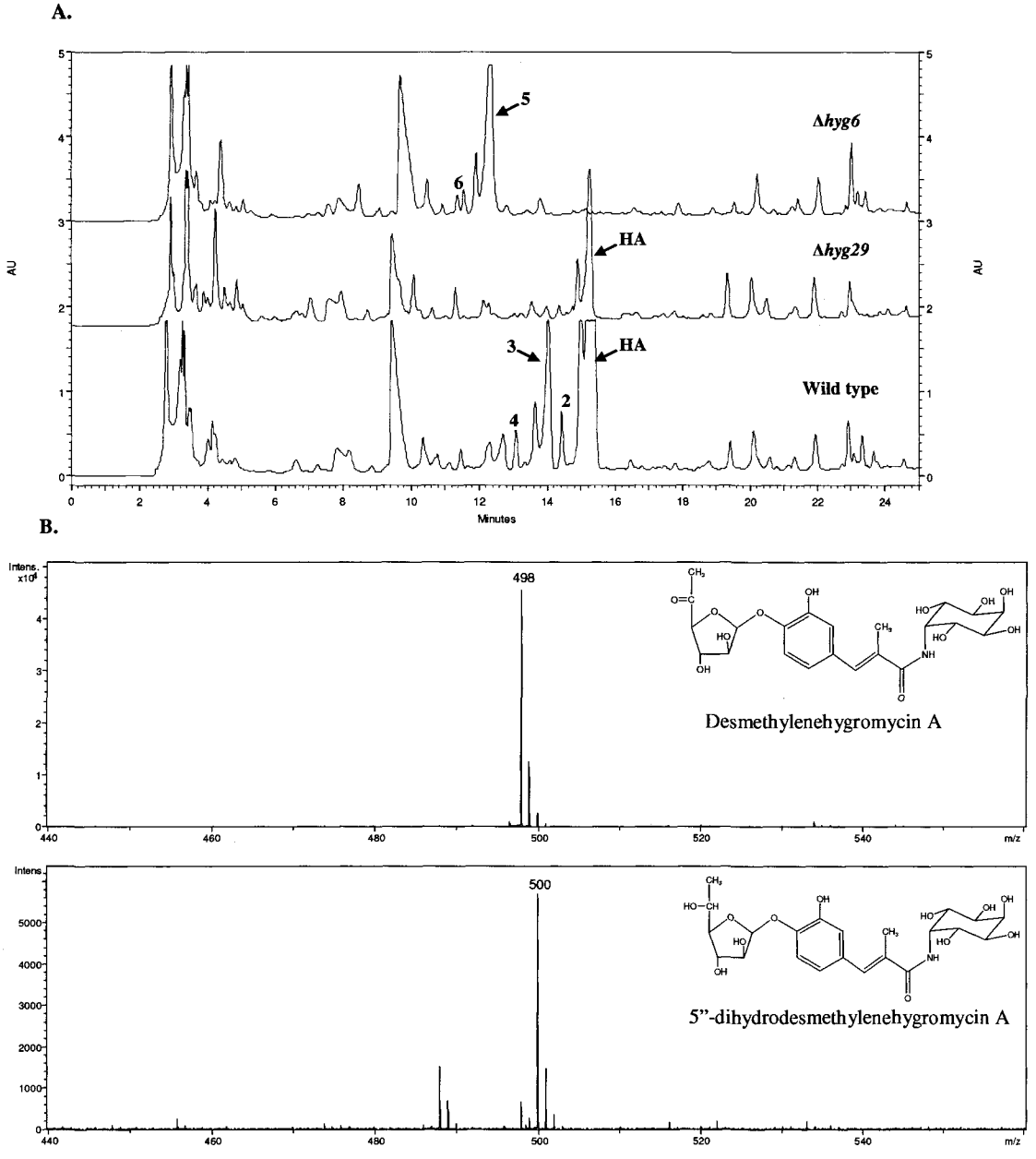


**FIGURE 23. Effect of *hyg6* and *hyg29* disruptions on hygromycin A production.**
A. Disruption of *hyg29* caused a decrease in hygromycin production whereas disruption of *hyg6* resulted in the production of new metabolites **5** and **6**.
B. Mass spectrometric analysis (negative mode) of Δ*hyg6* fermentation broth. Two new species were identified with $[M-H]^-$ values of 498 and 500 corresponding to desmethylenehygromycin A (**5**) and 5"-dihydrodesmethylenehygromycin A (**6**), respectively.

The amount of production of the major compound was estimated to be approximately 400 mg/L. When the C subunit was provided to this strain, a low amount of HA could be observed, but the level of **5** was not significantly altered. Thus, the above data provide evidence that methylation of C5-OH of the aminocyclitol in the biosynthesis of HA is carried out by the *hyg6* gene product.

### 3.4.3 Structural elucidation of desmethyleneHA analogs

To further characterize the two new compounds isolated from the Δ*hyg6* strain, they were purified by semi-preparative HPLC and their structures were elucidated by NMR. The most compelling data from the $^1$H-NMR spectra of **5** and **6** was the absence of either a three-proton singlet at ~3.5 ppm (for the O-5 methyl group of **3**), or two one-proton singlets at ~5.18 ppm and 4.83 ppm (for the methylene group bridging O-4 and O-5 of HA). Therefore, the MS and $^1$H-NMR data show that compounds **5** and **6** are nearly identical to HA and **3** except that their aminocyclitol moiety has not been methylated (FIGURE 24).

The differences in the $^1$H-NMR spectra between **5** and **6** involve the fucofuranose moiety. The H-6″ signal for **5** is a singlet at 1.99 ppm (overlapping with protons from α–$CH_3$), while the H-6″ signal for **6** is a doublet at 1.20 ppm. The H-4″ signal is also shifted from ~4.4 ppm in **5** to 3.74 ppm in **6** (shifts are approximate for H-4″ in **5** because this signal is obscured by other signals at the same chemical shift). There is also a new signal for **6** that appears at approximately 3.79 ppm, which is obscured by other signals.

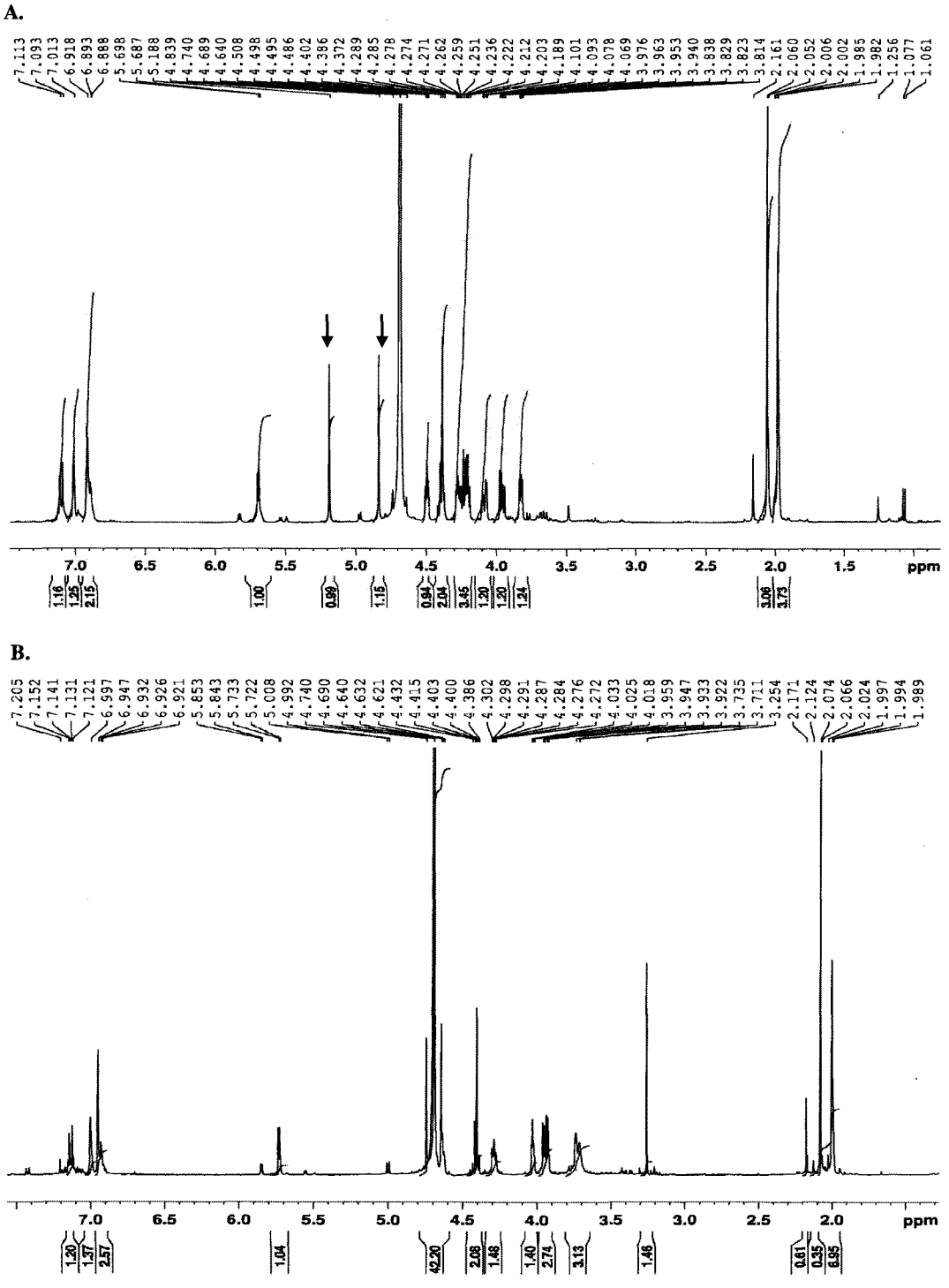


**FIGURE 24. $^{1}$H-NMR spectra of hygromycin A (panel A) and desmethylenehygromycin A (panel B).** The methylene bridge protons in hygromycin A, indicated by arrows in panel A, are absent in desmethylenehygromycin A.

The upfield shifts for H-4″ and H-6″ of compound **6** are explained by the fact that these protons are not adjacent to a carbonyl group, while in **5**, these protons are adjacent to the C-5″ ketone. The signal for H-6″ for **6** is split into a doublet due to coupling with a "new" proton at C-5″. The new signal at ~3.79 ppm (partially obscured) is due to H-5″, which is not present in **5**. The H-5″ assignment was confirmed by a COSY experiment, which revealed a crosspeak with H-6″. These data show that compound **6** is the reduced form of compound **5**. The compounds were therefore named desmethylenehygromycin A (**5**) and 5″-dihydrodesmethylene hygromycin A (**6**).

### 3.4.4 Activity of desmethylenehygromycin A

The antibacterial activity of **5** was determined using Δ*tolC E. coli* as test organism and compared with that of HA, methoxyhygromycin A (**3**), and 5"-dihydroAB (**7**) to determine the importance of the methyl / methylene group on the cyclitol. The $MIC_{90}$ of HA for Δ*tolC E. coli* was determined to be 10 μg/ml. Compounds **3** and **5** had much less activity, with the $MIC_{90}$ for both being 150 μg/ml. Compound **7** lacked inhibitory activity even at a concentration of 250 μg/ml. Next, the compounds were assessed for their ability to inhibit the synthesis of green fluorescent protein (GFP) using an *E. coli in vitro* coupled transcription-translation system (assays were conducted in Munich) [98, 99]. HA was shown to be highly active *in vitro*, having an $IC_{50}$ and $IC_{90}$ of 2.2 μM and 4.2 μM, respectively, whereas compound **7** was inactive (as expected from the MIC values), exhibiting no effect on translation at 100 μM. In contrast to the poor MIC values for **3** and **5**, both compounds displayed

excellent inhibitory activity *in vitro*. Based on the $IC_{50}$ values, **3** was at least as effective as HA, whereas **5** was ~4-fold more potent (TABLE 4) (FIGURE 25).

**TABLE 4. Comparison of $MIC_{90}$ and $IC_{50/90}$ data for hygromycin A and analogs**

| | HA | 3 | 5 | 7 |
|---|---|---|---|---|
| **$MIC_{90}$ (μg/ml)** | 10 | 150 | 150 | >250 |
| **$IC_{50}$ (μM)** | 2.1 | 1.8 | 0.5 | >100 |
| **$IC_{90}$ (μM)** | 5.2 | 6.2 | 1.6 | >100 |

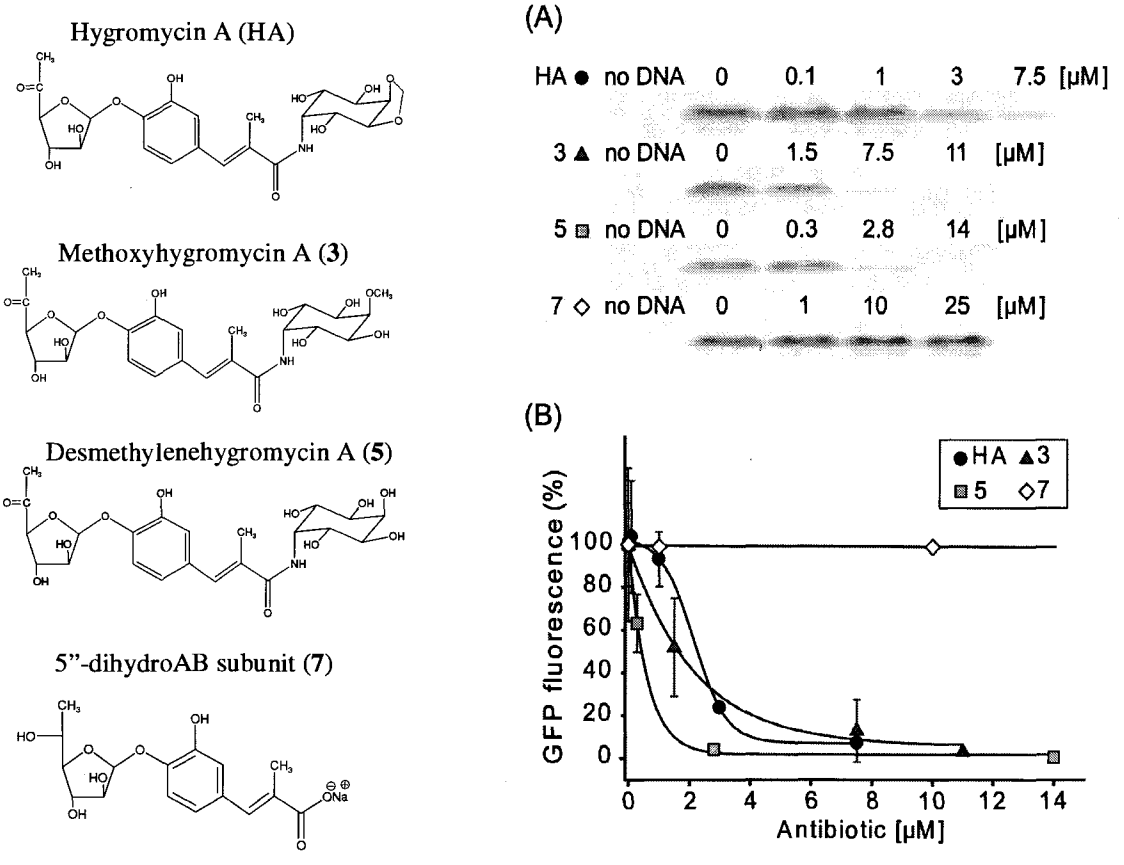


**FIGURE 25. Effect of hygromycin A and derivatives on *in vitro* transcription-translation.** A. Detection of green fluorescent protein (GFP) using native PAGE and fluorescence without or with HA, **3**, **5**, or **7**. B. Quantitation of (A) performed in triplicate with error bars indicating the standard deviation. GFP fluorescence is given as a percentage where 100% is defined as the fluorescence detected in the absence of the antibiotic. Assays carried out in Munich by Daniel Wilson's group.

### 3.4.5 Resistance of Δ*hyg29* mutant strain to HA

In order to verify if the *hyg29* gene contributed to self-resistance of *S. hygroscopicus*, spores of the wild type and Δ*hyg29* strains were grown on agar plates with different HA concentrations. The $MIC_{95}$ of HA for the wild type was found to be 400 μg/ml. The mutant also showed high level of self-resistance, with an $MIC_{95}$ value of 300 μg/ml.

## 3.5 Discussion

The structure of hygromycin A is uniquely characterized by the presence of a methylenedioxy bridge. Natural products with a methylenedioxy bridge have been identified more commonly from plants and less commonly from actinomycetes. Examples of secondary metabolites from actinomycetes possessing a methylenedioxy bridge include dioxapyrrolomycin, simaomicin, and the streptovaricins, which have a six-membered 1,3-dioxine ring [116-118]. FR-900109, the dioxolides, and pseudoverticin possess a five-membered 1,3-dioxolane ring similar to that seen in HA [119-121]. In the present study, the gene responsible for the *O*-methylation step of methylene bridge formation in HA was identified by gene inactivation experiments. Two methyltransferase homologs, *hyg6* and *hyg29*, are present in the biosynthetic gene cluster of HA. Inactivation of *hyg6* completely abolished the production of HA and led to the accumulation of two new products, desmethylenehygromycin A (**5**) and its C5"-reduced analog, 5"-dihydrodesmethylenehygromycin A (**6**), which lacked the C4-C5 methylenedioxy bridge on the aminocyclitol (FIGURE 3). This work provided conclusive evidence that the C4-C5 methylene group in HA is contributed by the *O*-

methylation activity of Hyg6 and not by Hyg29. The desmethylene analogs have not been detected in the wild type fermentations so far. The MIC data showed that antibacterial activity of **5** against the Δ*tolC E. coli* strain was 15 times less than that of HA. Interestingly, the MIC value of **5** was the same as that of methoxyhygromycin A (**3**), which has a C5-$OCH_3$ group instead of the methylenedioxy bridge. The lower antibacterial activity of **3** has been reported previously [23, 122]. A study of the activities of HA analogs modified on the cyclitol and lacking the methylenedioxy ring has also underlined the significance of this functional group in enhancing the biological activity of HA [38]. The present data is, thus, in agreement with the existing information. However, removal of the methylenedioxy ring did not lead to a loss in the ability to inhibit *in vitro* protein synthesis. Compound **7**, which lacks the C subunit, is totally inactive, as has been reported in previous studies [34]. In contrast, compounds **3** and **5**, where the methylenedioxy ring is absent, retained potent protein synthesis inhibitory activity, with **5** being ~4 times more active than **3** (TABLE 4) (FIGURE 25). These data suggest that the aminocyclitol ring is indeed essential for translation inhibition activity, whereas an intact methylenedioxy ring is not. It appears that the loss in biological activity due to disruption of the methylenedioxy ring stems from another factor, such as uptake of the drug into the cell, rather than abolishing the ribosome binding ability of the compound.

The formation of **3** and **5** suggests that the enzyme catalyzing the amide bond formation that connects the AB- and C- fragments has relaxed substrate specificity and is able to recognize the unmethylated (C5-OH) aminocyclitol, the C5-$OCH_3$

aminocyclitol, and also the C4-C5 methylenedioxy-bridged aminocyclitol as substrates (FIGURE 26). As suggested in an earlier report, the cyclization step of methylene dioxy bridge formation cannot occur once the aminocyclitol gets attached to the AB subunit, and so **3** represents a byproduct and not a precursor of HA [40]. The exact placement of Hyg6-catalyzed C5-*O*-methylation in the pathway sequence still could not be determined. The order of the biosynthetic steps leading from glucose-6-phosphate to *myo*-inositol is conserved across other aminocyclitol antibiotics such as streptomycin, bluensomycin, spectinomycin, and diverges only from the steps subsequent to *myo*-inositol formation [123]. As has already been stated, **5** has not been detected in the wild type fermentation. Compound **5** has also not been found in a Δ*hyg7* mutant that was blocked in the cyclization step of methylenedioxy bridge formation, and so, produced only **3** (data unpublished). These observations may imply that, under physiological conditions, methylation happens only on free *neo*-inosamine 2 before its attachment to the AB subunit. This means that **5** is not a precursor of **3**, and that formation of **5** is facilitated due to the relaxed substrate specificity of the amide bridge-forming enzyme only when the normal progression of the pathway is blocked, as in the Δ*hyg6* mutant. An alternate explanation could also be that the C5-*O*-methylation must be taking place at a much faster rate than amide bond formation. However, failure to detect even trace levels of **5** in wild type fermentation lends more support to the former possibility than to the latter.

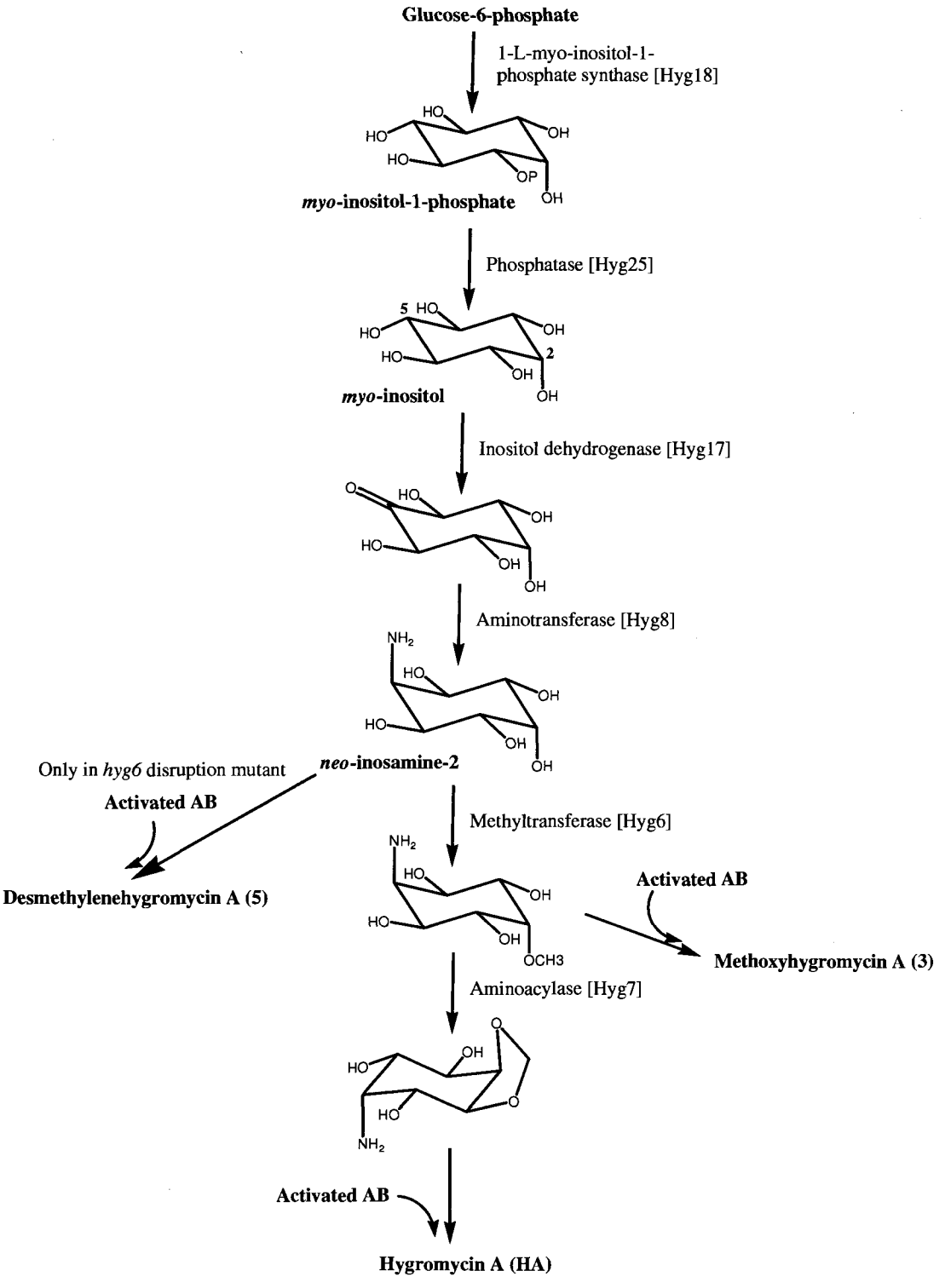


**FIGURE 26. Routes for biosynthesis of desmethylenehygromycin A and methoxyhygromycin A during the course of HA biosynthesis**

Inactivation of the second methyltransferase homolog, *hyg29*, resulted in a decrease in the yield of HA, although the antibiotic production profile and self-resistance were not affected. The present study did not provide any information that would support the proposed role of *hyg29* as an rRNA methylase-encoding gene. At the time of this study, it was not known whether the ribosomes of *S. hygroscopicus* are resistant to HA or not. Moreover, ribosomal self-resistance is not always observed for ribosome-targeting antibiotics. If the *hyg29* gene product is indeed an rRNA methylase, the high level of HA resistance of the Δ*hyg29* mutant suggests that in the absence of target-site modification by *hyg29*, self-resistance is possibly being conferred by the other resistance determinants in the HA gene cluster, namely the putative efflux pumps and the HA inactivating *O*-phosphotransferase. It will be interesting to study if a difference in rRNA methylation and HA-binding patterns exists between the ribosomes extracted from the wild type and the Δ*hyg29* strain.

In summary, the present study has unambiguously identified *hyg6* as the methyltransferase gene responsible for the C5-*O*-methylation step of HA biosynthesis and has also led to the isolation of two previously unidentified HA analogs. The function of the other methyltransferase gene, *hyg29*, remains presently unresolved and can only be verified by more specific studies such as *in vitro* rRNA methylation assays.

# 4. Involvement of a short chain dehydrogenase, a putative ABC transporter, and a putative proton-gradient dependent transporter in the biosynthesis and efflux of hygromycin A

## 4.1 Summary

The *hyg19* and *hyg28* genes in the biosynthetic gene cluster of hygromycin A (HA) putatively encode a proton gradient-dependent transporter and an ATP-binding cassette (ABC) transporter, respectively, and either or both the gene products are hypothesized to confer intrinsic HA resistance to the producer strain, *S. hygroscopicus* NRRL 2388, by antibiotic efflux. A Δ*hyg28* mutant, resulting from disruption of the ABC transporter gene, produced the same amount of HA as the wild type and also demonstrated similar levels of self-resistance. On the other hand, a Δ*hyg19* mutant, generated by disrupting the proton gradient-dependent transporter gene, produced lesser amounts of HA and accumulated 5"-dihydrohygromycin A, but showed no decrease in self-resistance due to loss of *hyg19*. Interestingly, a strain in which *hyg19* was disrupted together with *hyg21* (*O*-phosphotransferase gene) was significantly more sensitive to HA. This observation indicated that HA self-resistance in the producer strain arises by synergistic functioning of multiple gene products. Accumulation of 5"-dihydrohygromycin A in Δ*hyg19* also suggested that this compound is the immediate precursor of HA in the biosynthetic sequence, and further indicated that the dehydrogenation of 5"-dihydrohygromycin A to HA is coupled to efficient HA efflux. A short chain dehydrogenase encoded by *hyg26* was expressed

and purified from *E. coli*, and was shown to reversibly catalyze the above reaction using NAD(H) as cofactor.

## 4.2 Introduction

The antibiotic efflux system, comprised of membrane transporter proteins, is considered to have evolved in antibiotic producers primarily for effective secretion of the completely synthesized metabolite. It contributes to intrinsic resistance by keeping the intracellular drug concentrations at subtoxic levels and by excreting any drug molecules that re-enter the cell after initial export [42]. Both primary active transporters, which couple molecular transport to ATP hydrolysis, and secondary active transporters, which use the energy of the membrane electrochemical gradient for efflux, occur in antibiotic producers.

The ATP hydrolysis-dependent transporters belong to the ATP-binding cassette (ABC) transporter superfamily. This is one of the largest families of transporter proteins, with members occurring ubiquitously in all phyla of organisms from prokaryotes to humans [124-126]. These proteins bring about transport of a wide variety of substrates that includes small molecules like sugars, amino acids, antibiotics, as well as macromolecules like proteins and polysaccharides. Structurally, they are comprised of two hydrophilic ATP-binding domains and two hydrophobic transmembrane domains, which may be present on the same protein or on different polypeptides [76]. A two-site model has been proposed for transport by ABC proteins, according to which the transmembrane domains possess an intracellular high-affinity

drug binding site and an extracellular low affinity site, and ATP hydrolysis induces conformational changes that interconvert these sites, resulting in efflux of the drug [127]. As described in section 1.3.3, the ABC transporters in antibiotic-producing actinomycetes have been classified into three groups [77]. The Type I transporter system comprises two genes, one of which encodes a protein with a single ATP binding domain, and the second gene present immediately downstream encodes a membrane protein with six transmembrane segments. Type I ABC transporters have been identified in daunorubicin, tetronasin, mithramycin, and oleandomycin producers [78-81]. The Type II group is comprised of a single gene that encodes a protein with two ATP binding domains; a gene for the membrane component has not been identified in the corresponding biosynthetic gene cluster. Transporters of this type occur in carbomycin, tylosin, oleandomycin, A201A, and lincomycin producers [82-86]. The type III system is made of a single gene that encodes a protein with one ATP binding domain and one transmembrane domain. This type has been reported from the bleomycin and streptomycin producers [87, 88].

The electrochemical gradient-dependent transporters involved in antibiotic efflux in actinomycetes typically belong to the major facilitator superfamily (MFS). These proteins bring about transport of only small molecules, and together with the ABC transporters, form nearly 50% of all transporter proteins [73, 124-126, 128]. The MFS transporters for drug efflux are chiefly proton-gradient dependent antiporters composed of a single polypeptide with either 14 transmembrane segments (drug:$H^+$ antiporter, 14 spanner (DHA14) family), or 12 transmembrane segments (drug:$H^+$

antiporter, 12 spanner (DHA12) family). Members of DHA14 family have been identified in producers of tetracenomycin, puromycin, cephamycin, and mitomycin C [74, 129-131]. MFS transporters with 12 membrane-spanning domains have been reported from producers of lincomycin and valanimycin [132, 133]. The N-termini of MFS proteins are more conserved and are thought to be involved in transport, while the C-termini are more variable in sequence for specificity of ligand recognition [73, 128].

The majority of these efflux pumps are specific for the antibiotic with which they are associated in the biosynthetic gene cluster, but transporters from antibiotic producers that confer multidrug resistance phenotype are also known, as in the case of pristinamycin producer [134]. The expression of genes encoding transporter proteins is often tightly linked to one or more genes present in the biosynthetic gene cluster of the corresponding antibiotic and can also be induced by biosynthetic pathway intermediates / antibiotic precursors. This was reported for actinorhodin export in *S. coelicolor* A3(2), in which it was observed that expression of *actA*, the gene for the transmembrane pump in the actinorhodin biosynthetic gene cluster, is regulated by a repressor protein encoded by *actR* in the gene cluster, and that the repression is relieved by an antibiotically inactive precursor of actinorhodin [135]. This phenomenon, referred to as a 'feed-forward' mechanism for activation of antibiotic export, ensures that the transporter is made available as soon as the final biosynthetic product is generated and needs to be removed from inside the cell.

As mentioned in chapter 1, there are two putative HA efflux/resistance genes, *hyg19* and *hyg28*, in the HA biosynthetic gene cluster. In the study reported in this chapter, the proposed roles of these two genes and their functional association with the *hyg26* gene that encodes a short chain dehydrogenase have been investigated. Disruption of *hyg28*, which encodes a putative ABC transporter, revealed that this gene is not essential for HA export. Disruption of *hyg19*, which encodes a putative proton gradient-dependent transporter, reduced HA production and also caused accumulation of its reduced analog, 5"-dihydrohygromycin A. This observation suggested that HA biosynthesis is associated with Hyg19-dependent efflux. Studies on *hyg26* showed that the enzyme encoded by it is a NAD-dependent dehydrogenase with reversible activity, and further indicated that the conversion of 5"-dihydrohygromycin A to HA, catalyzed by Hyg26, is the final step of HA biosynthesis prior to efflux.

## 4.3 Materials and methods

### 4.3.1 Chemicals, bacterial strains, and growth conditions

All antibiotics and chemicals were purchased from Sigma Aldrich. PCR primers were obtained from Integrated DNA Technologies. Enzymes for DNA manipulations were obtained from New England Biolabs. Hygromycin A (HA) was kindly provided by Pfizer Inc. Dihydrohygromycin A (**2**), 5"-dihydromethoxy hygromycin A (**4**), and (*E*)-3-(3-hydroxy-4-*O*-α-fucofuranosylphenyl)-2-methylacrylic acid (dihydroAB subunit) (**7**) were purified from fermentation broth of the *S. hygroscopicus* SCH30 mutant strain by semi-preparative HPLC method as described earlier [40]. A *hyg7* (D-aminoacylase homolog) disruption strain of *S. hygroscopicus*

was the source for methoxyhygromycin A (**3**) (data unpublished), and the *hyg6* (C5 *O*-methyltransferase) disruption strain was the source for desmethylenehygromycin A (**5**) and 5"-dihydrodesmethylenehygromycin A (**6**) (chapter 3). *S. hygroscopicus* strains were propagated as described earlier [39, 40]. *E. coli* strains were cultured using standard protocols [136]. The Δ*tol*C *E. coli* strain was procured from the *E. coli* Genetic Stock Center at Yale University.

### 4.3.2 Nucleotide and protein sequence analysis

Homology searches for sequences of *hyg19*, *hyg26*, and *hyg28* genes were carried out using the BLAST suite of programs at the National Center for Biotechnology Information website [96]. Protein motif searches were carried out using the PROSITE database [97]. Hydropathy analysis for Hyg19 was based on the amino acid hydropathy values of Kyte and Doolittle, and carried out at the Transporter Classification Database server [137, 138]. The MEMSAT3 program was also used for secondary structure and topology prediction of Hyg19 [139].

### 4.3.3 Gene disruption experiments

The *hyg19* and *hyg28* genes, and also a segment of the HA biosynthetic gene cluster comprised of *hyg19*, *hyg20*, and *hyg21* genes, were individually replaced by apramycin resistance cassette using the PCR targeted *Streptomyces* gene replacement method [41]. The primers used to amplify the disruption cassette from pIJ773 plasmid are listed in TABLE 5. Primers for *hyg28* disruption were designed such that the 68-nucleotide overlap between the 3'-end of *hyg28* and the 5'-end of the downstream

*hyg29* gene was unaffected. The *hyg19* and *hyg19+hyg20+hyg21* disruptions were carried out in cosmid 17E3, while *hyg28* gene disruption was done in cosmid 15A10 [40]. The recombinant cosmids were introduced into *S. hygroscopicus* wild type by conjugation and selected for apramycin resistance. The genotype of the mutant strains was confirmed by PCR amplification of apramycin cassette from chromosomal DNA and by verifying the sequence of the PCR product. Automated DNA sequencing was done at the MMI research core facility at Oregon Health and Science University. The DNA sequence data were analyzed using Accelrys DS Gene software.

**TABLE 5: Primers used for disruption of *hyg19* and *hyg28***

| | |
|---|---|
| **Primers for *hyg19* gene disruption** | |
| *hyg19*_KO_Forw | **GATCCGACCCGTGCCGGGCGGAAGGGAGCACCAGTGATG***ATTC CGGGGATCCGTCGACC* |
| *hyg19*_KO_Revr | **GGTGATGAGCGGGGCGCTGAGCCAGAGGAACATCACGAC***TGTA GGCTGGAGCTGCTTC* |
| **Outer primers for verification of *hyg19* gene disruption** | |
| *hyg19*_Out_Forw | ATGAAGTCGCCACCCGAGC |
| *hyg19*_Out_Revr | GTCGGCGAAGTGGTCCAGGC |
| **Primers for *hyg28* gene disruption** | |
| *hyg28*_KO_Forw | **CTGATGACTGCCACTCTCGTCGCCAAGGATCTGGCCGCC***ATTCC GGGGATCCGTCGACC* |
| *hyg28*_KO_Forw | **CTCGGTGACCCGGCCGTCCGCCACCTCCAGGCGGCGGGT***TGTA GGCTGGAGCTGCTTC* |
| **Outer primers for verification of *hyg28* gene disruption** | |
| *hyg28*_Out_Forw | CTCAATCGGGCGCAGGCC |
| *hyg28*_Out_Revr | TGGACAGAGGCCGGACGG |
| **Primers for (*hyg19+hyg20+hyg21*) gene disruption** | |
| Forward | **GATCCGACCCGTGCCGGGCGGAAGGGAGCACCAGTGATG***ATTC CGGGGATCCGTCGACC* |
| Reverse | **ACCGTTGACCGAGAATGGGTAAAGGAGCAGAAAACAATG***TGTA GGCTGGAGCTGCTTC* |
| **Outer primers for verification of (*hyg19+hyg20+hyg21*) gene disruption** | |
| Outer_Forw | ATGAAGTCGCCACCCGAGC |
| Outer_Revr | CATGCGCACCTGGCTGAC |
| **Expression primers for *hyg26* gene encoding short chain dehydrogenase** | |
| Forward | **CATATG**AGTGGACTGATGCGGGAC |
| Reverse | **GGATCC**TCAGAATTCGCTGACGC |

The 39-nucleotide homologous region flanking the targeted gene is indicated in bold. The italicized primer region is homologous to pIJ773. The *Nde*I and *Bam*HI sites in *hyg26* expression primers are indicated in bold.

### 4.3.4 Analysis of antibiotic production in *S. hygroscopicus* strains

Fermentation broths of *S. hygroscopicus* disruption strains were analyzed for antibiotic production by high performance liquid chromatography (HPLC) and liquid chromatography – mass spectrometry (LC-MS) methods on a Bruker Daltonics MicroTOF-Q instrument fitted with Agilent 1100 series HPLC system. Cell-free extracts were generated by methanol lysis of mycelia and examined by HPLC [140]. The production yields of HA and related metabolites were estimated from their corresponding peak areas in the chromatograms using a standard curve of HA as reference.

### 4.3.5 Sensitivity of *S. hygroscopicus* strains to hygromycin A

HA sensitivity of *S. hygroscopicus* wild type and mutant strains was determined by agar plate dilution method as described previously [140]. Briefly, spores were plated on ISP2 agar plates containing varying amounts of HA, incubated at 30 °C for 48 hr, and scored for growth. The $MIC_{95}$ was defined as the lowest concentration of HA that prevented visible growth of 95% or more of the colony forming units on the agar plate.

### 4.3.6 Bioactivity of 5"-dihydrohygromycin A and other dihydro analogs

The Δ*tolC E. coli* strain was used as test organism to determine the antibiotic activity of **2**, **4**, **6**, and **7**. The strain was grown in 200 µl LB at 37 °C for 2 hr in the presence of different concentrations of antibiotic, and the $A_{600}$ was measured. The $MIC_{90}$ was defined as the lowest concentration of the antibiotic at which 90% of

bacterial growth was inhibited compared to a control *E. coli* culture grown in the absence of any antibiotic.

### 4.3.7 Coupled transcription-translation assay

All coupled transcription-translation experiments were performed using an *E. coli* lysate-based system in the presence and absence of antibiotics as described in chapters 2 and 3 [98, 99]. Native and SDS gels were quantitated using ImageQuaNT (Molecular Dynamics, Inc.) and represented graphically using SigmaPlot (Systat Software, Inc.).

### 4.3.8 Cloning, overexpression, and purification of recombinant Hyg26

The 816-bp *hyg26* gene was amplified from cosmid 17E3. Primers were designed to introduce an *Nde*I restriction site at the initiation codon and a *Bam*HI restriction site 3' to the termination codon (TABLE 5). Amplification was performed using the following temperature program: initial denaturation at 95 °C for 5 min, 25 cycles of amplification (45 s denaturation at 95 °C, 45 s primer annealing at 56 °C, 1 min extension at 72 °C), and a final 7 min extension at 72 °C. The gene was subsequently cloned into the *Nde*I and *Bam*HI restriction sites of pET15b vector (Novagen). The resulting pET15b-*hyg26* construct was introduced into *E. coli* BL21-CodonPlus (DE3) expression host (Stratagene) by transformation. For protein expression, cells were grown at 37 °C in LB medium containing 100 μg/ml ampicillin and 50 μg/ml chloramphenicol. When an $A_{600}$ of 0.6 was reached, the culture flask was brought to room temperature (~23 °C), and expression was induced by adding 0.5

mM isopropyl thio-β-D-galactoside (IPTG). After further 6 hr incubation, cells were harvested by centrifugation and stored at -80 °C.

The N-terminal His-tagged Hyg26 was purified under native conditions according to Qiagen's Ni-NTA protocol. Cells were resuspended in BugBuster Master Mix protein extraction reagent (Novagen) and lysed by incubating at room temperature for 30 min. The lysate was cleared by centrifugation and the supernatant was loaded onto Ni-NTA agarose prequilibrated with buffer containing 50 mM $NaH_2PO_4$, 300 mM NaCl, and 10 mM imidazole [pH 8.0]. The column was washed with wash buffer (50 mM $NaH_2PO_4$, 300 mM NaCl, 20 mM imidazole [pH 8.0]) and the protein was eluted with elution buffer (50 mM $NaH_2PO_4$, 300 mM NaCl, 250 mM imidazole [pH 8.0]). The eluted protein was dialyzed overnight against a buffer containing 50 mM Tris-HCl (pH 7.5), 20% glycerol, and 5 mM 2-mercaptoethanol, and stored at -80 °C until further use.

### 4.3.9 Determination of molecular mass of Hyg26

The molecular mass of purified His-tagged Hyg26 was determined by size-exclusion chromatography using a Phenomenex BioSep-SEC-S4000 size exclusion column fitted to an Agilent 1100 series HPLC system. The column was equilibrated and eluted with 20 mM sodium phosphate (pH 7.2) at a flow rate of 0.5 ml/min. Carbonic anhydrase (25 kDa), bovine serum albumin (66 kDa), β-amylase (200 kDa), apoferritin (443 kDa), and thyroglobulin (669 kDa) were used as standards. The void

and total column volumes were calculated from the elution volumes of blue dextran (2000 kDa) and 2,4-dinitrophenyl aspartate (299 Da), respectively.

### 4.3.10 Hyg26 enzyme assays and kinetic analyses

Initial enzyme assays were performed at 30 °C with 4 μg of purified enzyme in a 100 μl reaction mixture of 50 mM Tris-HCl (pH 7.5) and 2 mM tris(2-carboxyethyl) phosphine (TCEP). The dehydrogenase activity was studied by incubating Hyg26 with 100 μM of the 5"-dihydro analogs **2**, **4**, **6**, or **7**, and 1000 μM NAD or NADP. For lactate dehydrogenase coupled assays, 1000 μM sodium pyruvate and 5 units of lactate dehydrogenase were added. The reductase activity was detected using 100 μM HA, **3**, or **5**, and 1000 μM NADH or NADPH. After incubation for 2 hr at 30 °C, the sample was loaded onto a reverse-phase HPLC column (Agilent Eclipse XDB-C18) to detect the oxidized products (with longer retention times) in the dehydrogenase assay or the reduced products (with shorter retention times) in case of the reductase assay. Samples were separated at a flow rate of 1 ml/min with a methanol:water gradient as described earlier [140]. The optimal temperature and pH for Hyg26 reductase activity were determined with 100 μM HA and 1000 μM NADH in a 15 min assay followed by quantitating the amount of product (**2**) formed from its peak area. The temperatures used were 23 °C (room temperature), 30 °C, 37 °C, and 42 °C. For pH studies the following buffers were used: 50 mM potassium acetate, pH 4.0, 5.0; 50 mM potassium phosphate, pH 6.0, 7.0; 50 mM Tris-HCl, pH 7.5, 8.0, and 9.0. The metal requirement was similarly checked by conducting the assay in the presence of 5 mM and 10 mM ethylenediamine-tetraacetic acid (EDTA). Kinetic analyses of reductase activity were

carried out at 37°C for 15 min with 800 ng Hyg26 in 100 µl assay buffer comprised of 50 mM phosphate (pH 6) and 2 mM TCEP. The NADH concentration was fixed at 60 mM while the antibiotic concentration was varied from 2 mM upto 60 mM where needed. For kinetic studies of NADH, HA was fixed at 20 mM while NADH was varied from 0.25 mM to 10 mM. Each assay was performed in duplicate and the average values of the two measurements were plotted in GraFit 4 to determine the kinetic parameters.

## 4.4 Results

### 4.4.1 Predicted roles of *hyg19* and *hyg28* genes in the HA biosynthetic gene cluster

The biosynthetic gene cluster of hygromycin A has two genes, *hyg19* and *hyg28*, that encode putative transporter proteins. The predicted translation product of *hyg19* has 416 amino acids with a theoretical molecular mass of 43.85 kDa. A search of the NCBI protein sequence database using the deduced Hyg19 sequence returns several transmembrane proteins belonging to the major facilitator superfamily (MFS). The highest sequence similarity (66%) is observed with a putative transmembrane protein, Ata9, from the biosynthetic gene cluster of A201A antibiotic from *Saccharothrix mutabilis* subsp. *capreolus*. The structure of HA resembles that of A201A in the A and B subunits, and many genes with similar sequences, and possibly similar functions, have been identified in the biosynthetic gene clusters of these two antibiotics [40]. The N-terminal region of Hyg19 specifically shows similarity to MFS proteins involved in drug efflux, such as the tetracycline resistance determinant TetV

from *Mycobacterium smegmatis*, macrolide efflux protein MefA from *Streptococcus pneumoniae*, and chloramphenicol resistance protein from *Streptomyces lividans*. Hydropathy analysis and transmembrane topology prediction suggest that Hyg19 has 12 transmembrane (TM) helices with cytoplasmic N- and C-termini, and thus is a member of the proton gradient-dependent DHA12 family of MFS transporters. Five sequence motifs have been identified in the DHA12 efflux proteins [72]. Hyg19 does not exhibit full conservation of all the motifs but a partially conserved motif C (gxxxGPxxGGrl) in TM5 (positions 163 – 181) and a partially conserved motif G (GxxxGPL) in TM11 (positions 373 – 392) can be clearly distinguished. Based on these observations, Hyg19 is hypothesized to be a proton gradient-dependent efflux protein that confers resistance to *S. hygroscopicus* by exporting HA out of the cell.

The deduced translation product of *hyg28*, with 570 residues and a theoretical molecular mass of 61.47 kDa, shows homology to several ATP binding cassette (ABC) type transporter proteins, including Ard1 from the A201A gene cluster that is known to confer resistance to A201A in *S. lividans* [85]. Two ABC domains containing the Walker A and Walker B motifs characteristic of ATPases are present in Hyg28. The Walker A motif ([AG]-x(4)-G-K-[ST]) is a glycine-rich loop that binds to the phosphates of ATP or GTP [102]. The Walker B motif (hhhhDEPT, where h indicates a hydrophobic residue) coordinates a magnesium ion [102]. Therefore, the *hyg28* gene is predicted to encode a type II ABC transporter protein, which in association with an unidentified membrane component, constitutes the second transporter system for HA efflux and subsequent self-resistance.

### 4.4.2 Effect of *hyg19* and *hyg28* gene disruptions on HA biosynthesis and efflux

In order to determine whether Hyg19 and Hyg28 are involved in antibiotic biosynthesis and efflux, the corresponding genes were individually replaced with apramycin resistance cassette in the *S. hygroscopicus* wild type (FIGURE 27). The resulting mutant strains, Δ*hyg19* and Δ*hyg28*, were cultured, the mycelia were removed by centrifugation, and the filtered supernatants were analyzed by HPLC and LC-MS for antibiotic production. Analysis of fermentation broth of the Δ*hyg28* mutant revealed that the antibiotic production profile was unaffected by *hyg28* disruption. The strain produced nearly the same amount (~1.5 gm/l) of HA as the wild type (data not shown). This clearly indicates that Hyg28 is not essential for antibiotic biosynthesis and efflux. On the other hand, disruption of *hyg19* caused HA production to drop to ~509 mg/l, a three-fold decrease compared to the HA yield in the wild type. The levels of methoxyhygromycin A (**3**) and 5"-dihydromethoxyhygromycin A (**4**) also appeared to be similarly reduced. Interestingly, the yield of 5"-dihydro hygromycin A (**2**) in Δ*hyg19* increased significantly to ~380 mg/l from ~37 mg/l seen in the wild type (FIGURE 28). A slight increase in the amount of 5"-dihydroAB (**7**) was also observed in Δ*hyg19*, which was detected only in trace levels in the wild type. (see FIGURE 3 for structures of compounds).

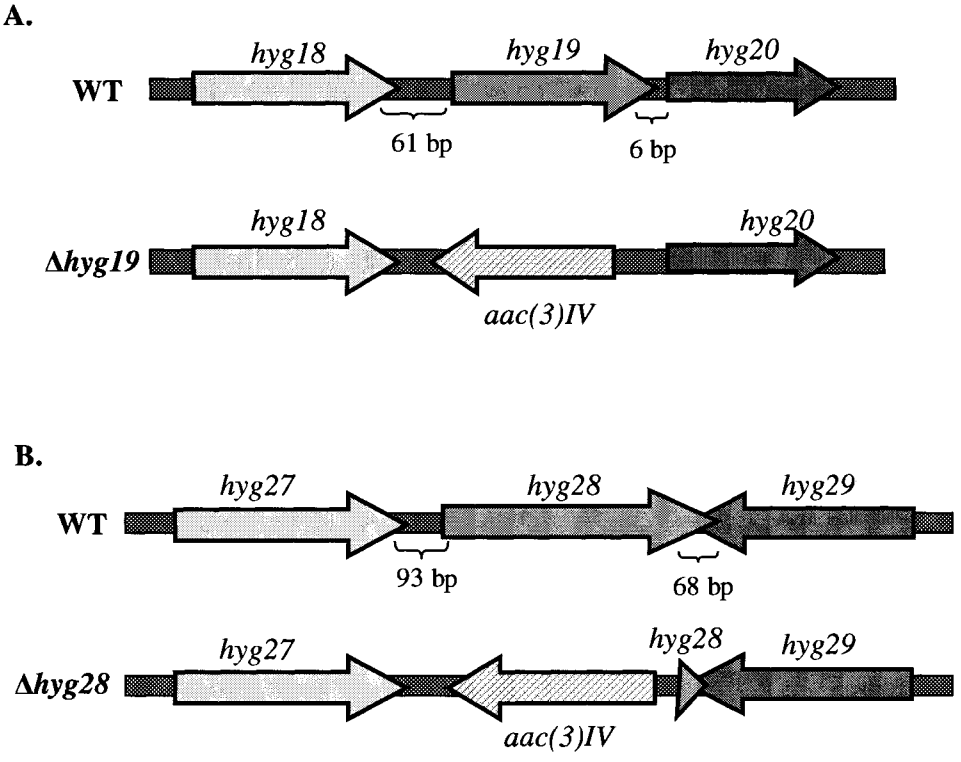


**FIGURE 27. Arrangement of *hyg19* (panel A) and *hyg28* (panel B) in the hygromycin A biosynthetic gene cluster.** The *hyg18* gene in panel A is a *myo*-inositol-1-phosphate synthase homolog while *hyg20* is a transglucosylase homolog. The *hyg27* and *hyg29* genes in panel B are homologous to DAHP synthase and methyltransferase, respectively.

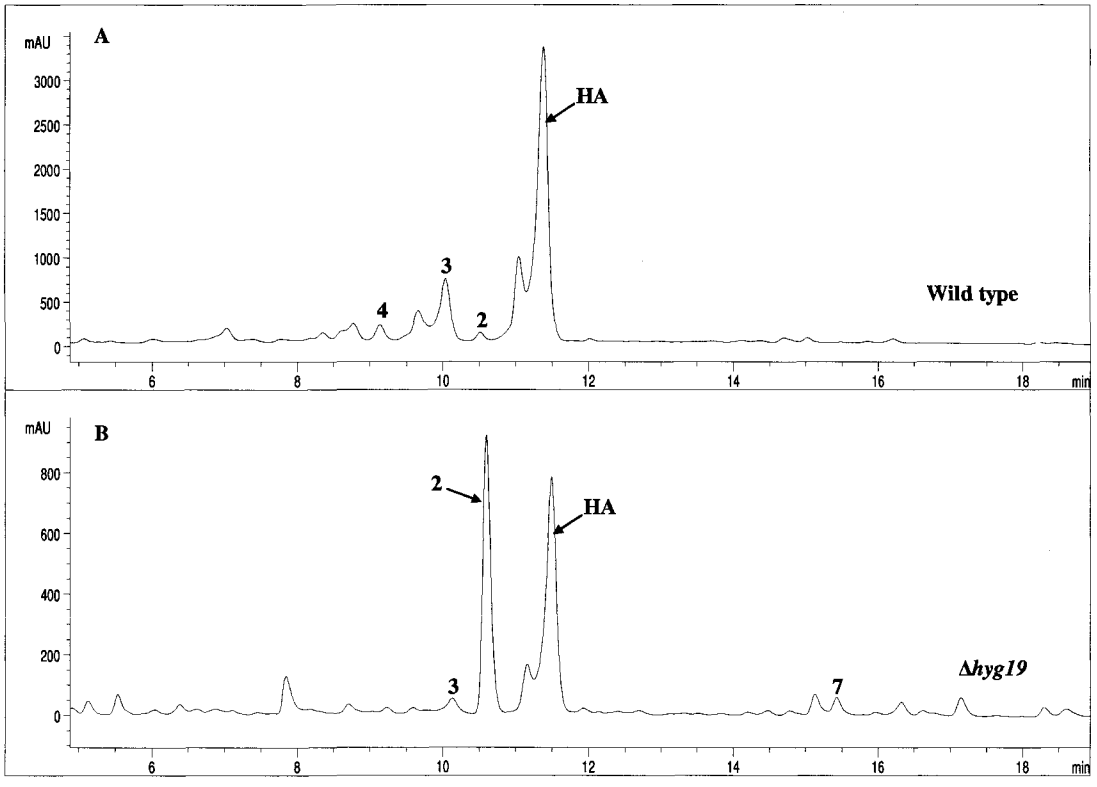


**FIGURE 28. Reverse-phase HPLC analysis of fermentation broths of wild type (panel A) and Δ*hyg19* mutant (panel B).** Reduced HA production and accumulation of 5"-dihydrohygromycin A were observed in Δ*hyg19*.

It was speculated that the reduced amount of HA in the fermentation broth of Δ*hyg19* could be a consequence of intracellular HA accumulation due to impaired transmembrane transport. To test this possibility, the mycelium of Δ*hyg19* was lysed by methanol treatment and the lyaste was analyzed by HPLC. The cell lysates of the wild type and Δ*hyg28* were also examined alongside in the same way. However, HA and related metabolites, including any phosphorylated forms, were not detected in

the cell lysates of any of the strains. These data demonstrate that all detectable HA and related products are outside the cell and that they are exported in the absence of Hyg19.

### 4.4.3 Contribution of *hyg19* and *hyg28* gene products to self-resistance of *S. hygroscopicus*

The wild type and mutant strains were assessed for their sensitivity to HA by growing their spores on agar plates with different antibiotic concentrations. The $MIC_{95}$ of HA for the wild type was found to be 400 μg/ml. The mutants also showed high levels of resistance, with $MIC_{95}$ values of 400 μg/ml and 300 μg/ml for Δ*hyg19* and Δ*hyg28,* respectively. These data indicate that the self-resistance of *S. hygroscopicus* is not entirely conferred by *hyg19* or *hyg28.* Another mutant strain was generated by disrupting *hyg19* together with the *hyg20* and *hyg21* genes present immediately downstream to it (FIGURE 29). The *hyg20* gene encodes a putative transglucosylase/ mutase for generating the A subunit and its disruption was observed to abolish antibiotic production completely (unpublished data). The *hyg21* encodes an antibiotic-modifying *O*-phosphotransferase with a probable role in self-resistance, and loss of this gene results in reduced HA production (chapter 2) [140]. The Δ(*hyg19*+*hyg20*+*hyg21*) strain did not produce HA and showed significantly increased sensitivity with a $MIC_{95}$ of 75 μg/ml. A Δ*hyg20* strain, in which the above mentioned putative transglucosylase/mutase gene alone was disrupted, had a $MIC_{95}$ of 300 μg/ml, which is not significantly lower than that of the wild type. The $MIC_{95}$ of *S. lividans* for HA was determined to be 20 μg/ml. These data suggest that the increased sensitivity

of Δ(*hyg19+hyg20+hyg21*) is due to the loss of *hyg19* and *hyg21*, implying a synergistic role of these two genes in self-resistance.

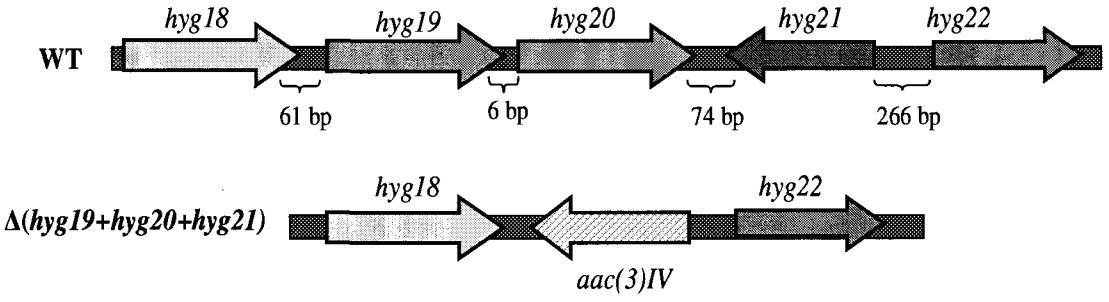


**FIGURE 29. Schematic representation of replacement of *hyg19*, *hyg20*, and *hyg21* genes with the apramycin resistance cassette**

### 4.4.4 Biological activity of C5"-dihydro analogs

Compounds **2**, **4**, and **6** are the C5"-dihydro analogs of HA, methoxyhygromycin A (**3**), and desmethylenehygromycin A (**5**), respectively (FIGURE 3). They were studied for their ability to inhibit growth of Δ*tolC E. coli*, and also for their ability to inhibit protein synthesis in an *E. coli in vitro* coupled transcription-translation system [98, 99]. The $MIC_{90}$ values of **2**, **4**, and **6** were determined to be 20 μg/ml, 150 μg/ml, and 150 μg/ml respectively (TABLE 6). These values are similar to the MIC of the corresponding 5"-oxidized analogs (TABLE 4, chapter 3). The 5"-dihydroAB subunit (**7**) was inactive against Δ*tolC E. coli* even at 250 μg/ml. In the *in vitro* protein synthesis inhibition assay, however, the $IC_{50}$ and $IC_{90}$ values indicated that **2** was 4-7 times more active than HA. Compounds **4** and **6** were less potent protein synthesis inhibitors compared to their oxidized forms **3** and **5**, where as **7** had no activity even at 100 μM (TABLE 6, FIGURE 30).

**TABLE 6. Comparison of $MIC_{90}$ and $IC_{50/90}$ data for 5"-dihydrohygromycin analogs**

| | HA | 2 | 3 | 4 | 5 | 6 |
|---|---|---|---|---|---|---|
| $MIC_{90}$ (μg/ml) | 10 | 20 | 150 | 150 | 150 | 150 |
| $IC_{50}$ (μM) | 2.1 | 0.3 | 1.8 | 7.4 | 0.5 | 2.7 |
| $IC_{90}$ (μM) | 5.2 | 1.5 | 6.2 | 50 | 1.6 | 14.1 |

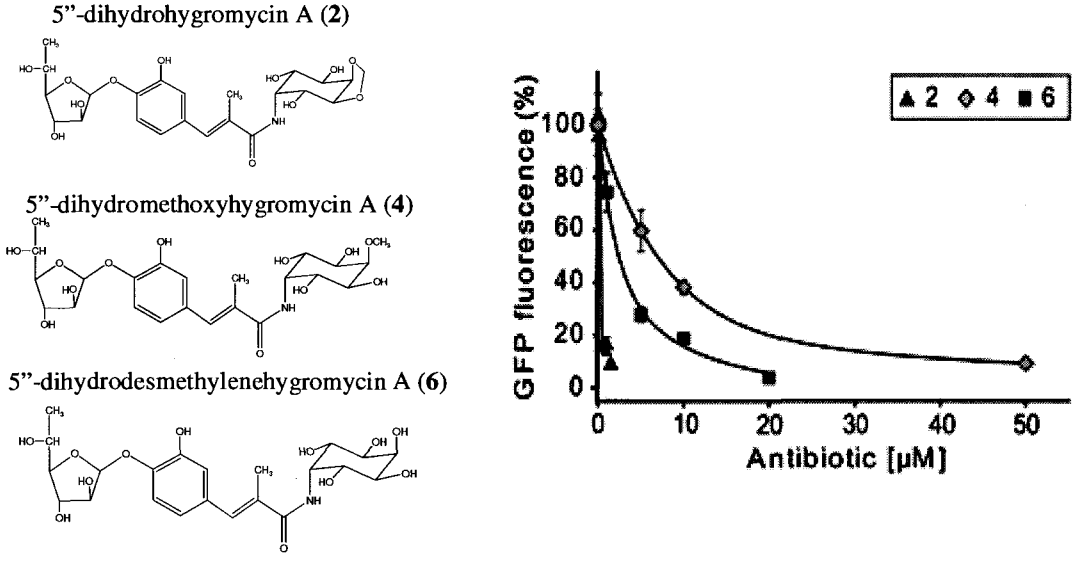


**FIGURE 30. Effect of 5"-dihydro derivatives on *in vitro* synthesis of green fluorescent protein (GFP).** GFP fluorescence is given as a percentage where 100% is defined as the fluorescence detected in the absence of the antibiotic. Activities of HA, **3**, and **5** are reproduced from TABLE 4. Assays were carried out in Munich by Daniel Wilson's group.

### 4.4.5 Enzymatic characterization of a short chain dehydrogenase encoded by *hyg26*

A gene disruption study had unequivocally demonstrated that a short chain dehydrogenase/reductase encoded by the *hyg26* gene is responsible for the C5 dehydrogenation of L-fucofuranose [40]. It was suggested, but not proved, that this biosynthetic step precedes the glycosyltransferase reaction that connects the A subunit

to the B subunit. Enhanced production of **2** in Δ*hyg19* suggests a contrary hypothesis that dehydrogenation of **2** to form HA might be the last step of HA biosynthesis. Compound **2** would, therefore, represent a pathway intermediate and not a shunt metabolite. It was reasoned that if efflux of HA is compromised in the Δ*hyg19* mutant, it would result in longer intracellular HA retention and an inhibitory effect either on the expression of *hyg26* or on the activity of the enzyme, resulting in accumulation of **2**. The presence of HA and **2** only in the fermentation broth would imply the existence of other systems capable of export of these antibiotics. In order to verify this hypothesis *in vitro*, a pET15b-*hyg26* expression vector was constructed and the enzyme was assayed to determine its ability to interconvert HA and **2**. The N-terminal hexahistidine tagged Hyg26 was purified by $Ni^{2+}$ affinity chromatography and showed the expected size of ~30 kDa on SDS PAGE (FIGURE 31). The apparent molecular mass of native recombinant Hyg26 was determined by size-exclusion chromatography to be approximately 64000 Da, suggesting that recombinant Hyg26 is a dimeric protein (FIGURE 32).

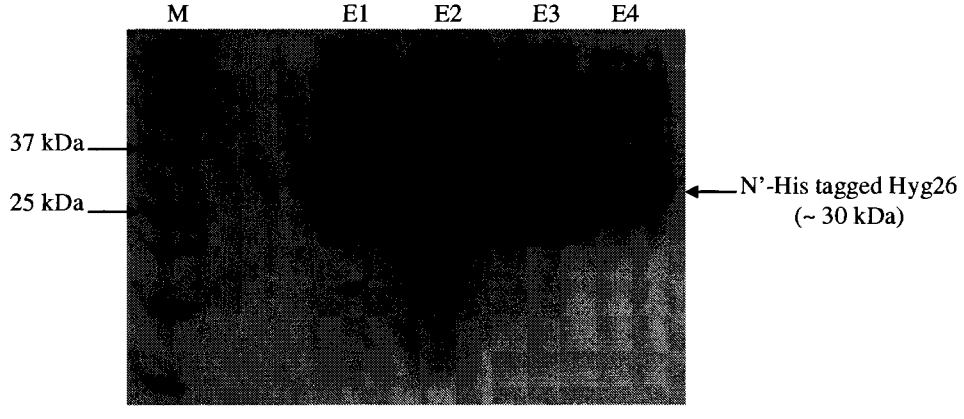


**FIGURE 31. SDS PAGE analysis of Ni-NTA purified Hyg26.**
M – Standard protein marker; E1 – E4 - Hyg26 elution fractions

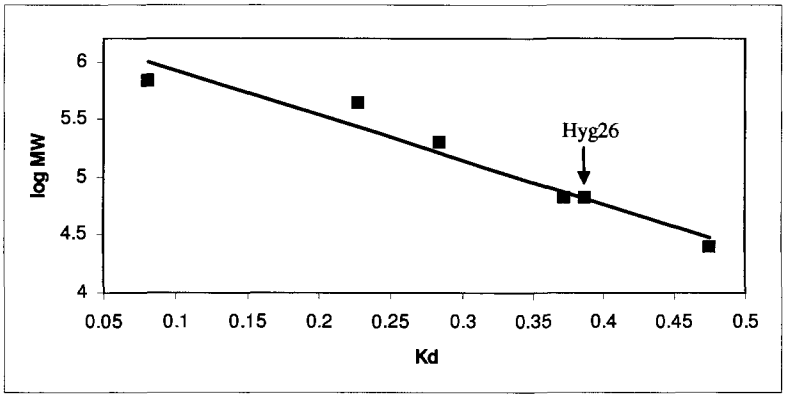


**FIGURE 32. Molecular weight estimation for recombinant Hyg26 by size exclusion chromatography.** Thyroglobulin (669 kDa), apoferritin (443 kDa), β-amylase (200 kDa), bovine serum albumin (66 kDa), and carbonic anhydrase (25 kDa) were used as standards.

The dehydrogenase activity of the enzyme was assayed by incubating it with **2**, **4**, or **6** in the presence of $NAD^+$ or $NADP^+$ as cofactor. Reverse-phase HPLC analysis of each reaction mixture provided with $NAD^+$ showed the appearance of a new peak with longer retention time than the substrate (FIGURE 33 for assay with **2**). This peak was not observed in a control without Hyg26 or in the assay with $NADP^+$. The retention time of the new peak coincided with that of the corresponding C5"-oxidized analog (HA, **3**, and **5**), and therefore, represents the product of Hyg26-dependent dehydrogenation. The very low product formation (1.2 – 1.5 μM from 100 μM of substrate after 2 hr at 30 °C) may reflect Hyg26 inhibition either by the oxidized antibiotic or by the resulting NADH. The oxidized antibiotic could not be removed from the reaction mixture, but coupled enzymatic assays that would regenerate $NAD^+$ were performed using pyruvate and lactate dehydrogenase. However, no increase in product amount was observed even after overnight incubations under these conditions.

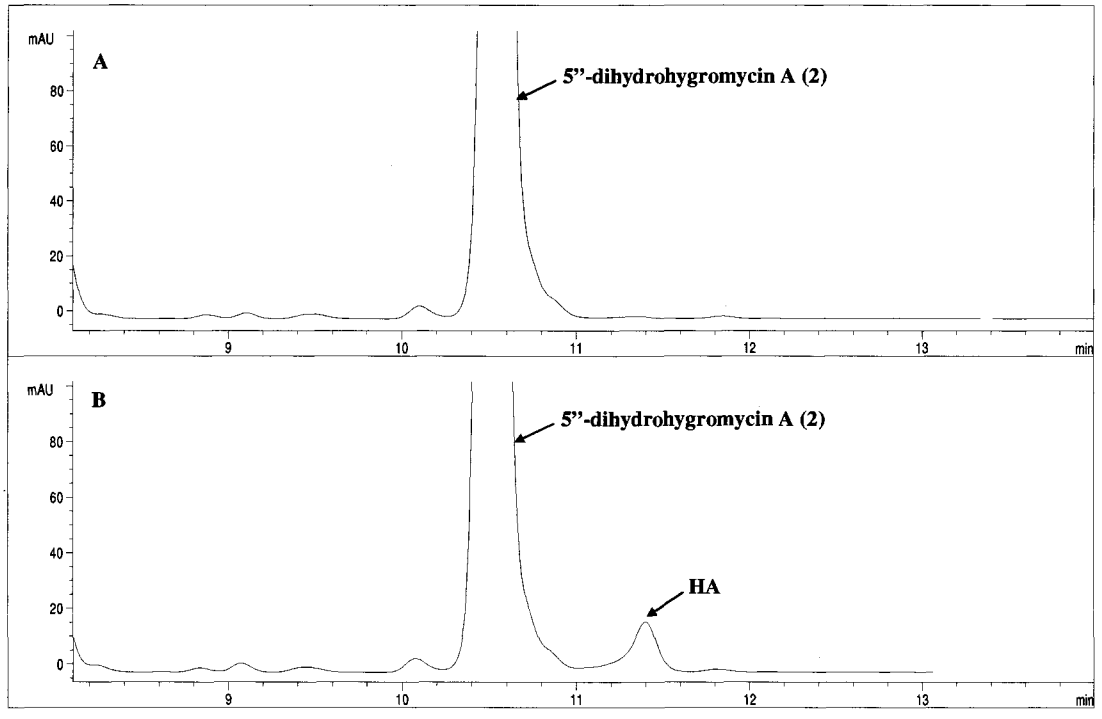


**FIGURE 33. Reverse-phase HPLC analysis of 5"-dihydrohygromycin A (2) dehydrogenation by Hyg26.** (A) Control reaction of **2** and NAD without Hyg26. (B) Reaction of 5"-dihydrohygromycin A (**2**) and NAD after incubation with Hyg26 showing formation of HA.

The ability of Hyg26 to catalyze the reverse reaction (reductase activity) was also investigated. Assays were carried out with HA, **3**, or **5** in the presence of NADH or NADPH, followed by HPLC analyses. Compared to a control without Hyg26, each of the NADH assays showed a significant decrease in the amount of substrate and the appearance of a new peak with shorter retention time than the substrate (FIGURE 34). This peak was not observed in the reaction with NADPH. Mass spectrometric analyses of the NADH reaction mixtures showed that the compounds under the new peaks had an increase in mass by 2 AMU with respect to the substrates, consistent with that

expected for the C5"-reduced analogs. These observations confirm that Hyg26 is an $NAD^+$/NADH-dependent oxidoreductase with broad substrate specificity. These data demonstrated that under the given assay conditions, the enzyme catalyzed the reverse reaction more efficiently than the forward biosynthetic reaction, suggesting that the equilibrium position favors the reduced product.

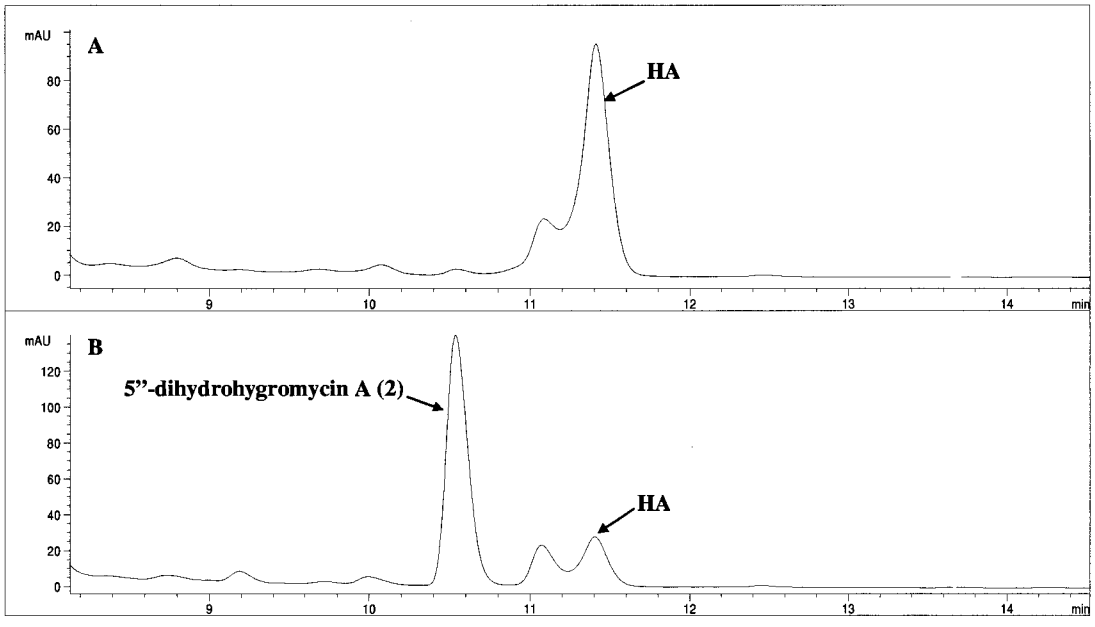


**FIGURE 34. HPLC analysis of hygromycin A (HA) reduction by Hyg26.** (A) Control reaction of HA and NADH without Hyg26. (B) Reaction of HA and NADH after incubation with Hyg26, showing formation of 5"-dihydrohygromycin A (**2**).

The optimal pH for catalysis of the reverse reaction was determined within a 4.0 - 9.0 pH range and was found to be 6.0 (FIGURE 35A). The optimal temperature was 37 °C among temperatures from 23 °C to 42 °C, although no significant difference was observed between the amounts of product formed at 30 °C and 37 °C (FIGURE 35B). The metal-chelating reagent EDTA did not reduce enzyme activity,

suggesting that, like other short chain dehydrogenases, Hyg26 is metal ion-independent (data not shown) [141].

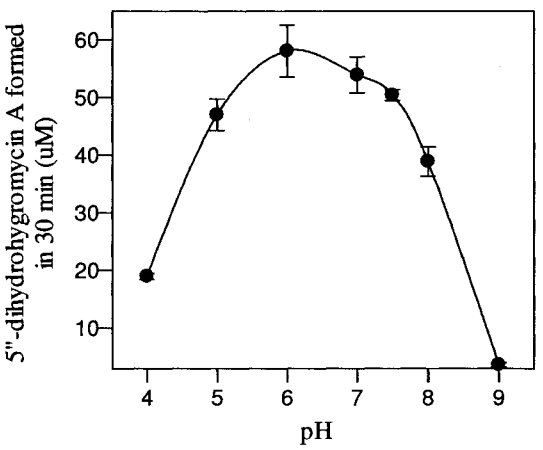


**FIGURE 35A. pH dependence of Hyg26 reductase activity.** Assays were done with 100 μM HA and 1000 μM NADH at 37°C for 30 min and the amount of 5"-dihydrohygromycin A was determined.

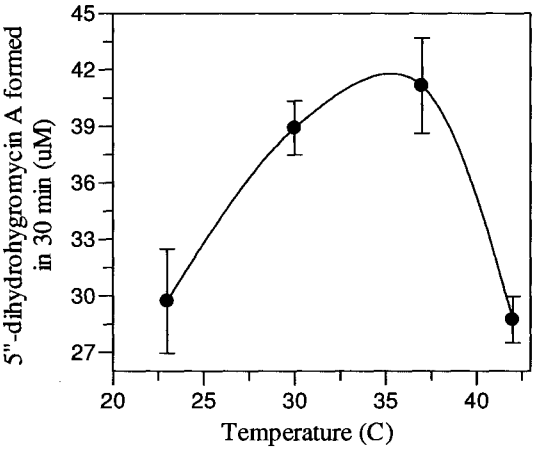


**FIGURE 35B. Temperature dependence of Hyg26 reductase activity.** Assays were done with 100 μM HA and 1000 μM NADH at pH 7.5 for 30 min and the amount of 5"-dihydrohygromycin A was determined.

Analysis of the steady state kinetic parameters for reduction of HA, **3**, and **5** showed that Hyg26 has very low affinity for them as indicated by the high $K_m$ values (in millimolar range, TABLE 7, FIGURE 36). The catalytic efficiency, as indicated by $k_{cat}/K_m$, was found to be comparable for all three substrates. The $K_m$ for NADH was determined to be 399.5 ± 33.7 μM.

**TABLE 7. Kinetic parameters for Hyg26 reductase activity**

| Substrate | $k_{cat}$ ($s^{-1}$) | $K_m$ (mM) | $k_{cat}/K_m$ ($M^{-1}$ $s^{-1}$) |
|---|---|---|---|
| Hygromycin (HA) | 5.1 | 5.8 ± 0.8 | $1.0 \times 10^3$ |
| Methoxyhygromycin A (**3**) | 15.5 | 19.8 ± 1.9 | $0.9 \times 10^3$ |
| Desmethylenehygromycin A (**5**) | 31.7 | 63.6 ± 24.4 | $0.9 \times 10^3$ |

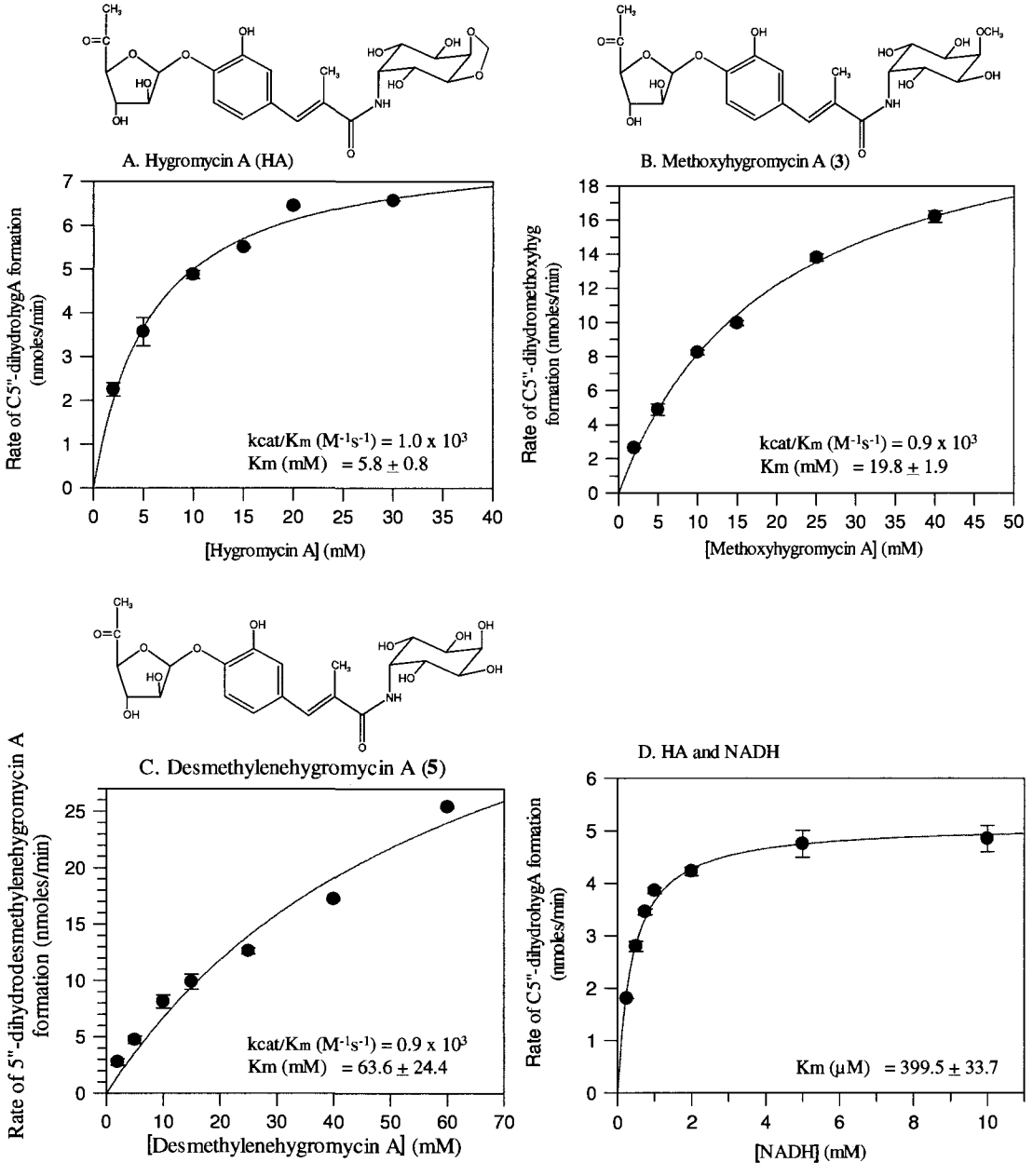


**FIGURE 36. Kinetic analysis of Hyg26 reductase activity using HA, 3, or 5, and NADH**

## 4.5 Discussion

Sequence analysis of the biosynthetic gene cluster of hygromycin A showed that the *hyg19* gene encodes a putative proton gradient-dependent transmembrane protein and the *hyg28* gene encodes a putative type II ABC transporter, and either one or both of these were hypothesized to be involved in HA efflux and self-resistance. The antibiotic production profile and intrinsic resistance of the Δ*hyg28* strain were similar to that of the wild type, which revealed that *hyg28* is not essential for HA efflux and resistance of *S. hygroscopicus*. Disruption of *hyg19* also did not affect resistance, although there were qualitative changes in antibiotic production. Similar observations with regard to resistance have been made in the landomycin E producer *S. globisporus* 1912. Self-resistance was not affected when the proton gradient-dependent transporter gene *lndJ* and the ABC transporter gene *lndW*, both occurring in the landomycin E biosynthetic gene cluster, were independently disrupted. Heterologous expression of these genes, however, conferred resistance to landomycin E, verifying their function as resistance genes [142, 143]. The intrinsic resistance of an antibiotic producer is often due to the synergistic action of multiple gene products [42]. This appears to be the case for HA self-resistance also as simultaneous disruption of two putative HA resistance determinants, *hyg19* and *hyg21*, resulted in a greater decrease in resistance than when either of them was individually disrupted [140]. Sustained resistance of the HA non-producing Δ*hyg20* strain suggests that HA is not essential for inducing the resistance genes.

The Δ*hyg19* strain showed enhanced production of 5"-dihydrohygromycin A (**2**) and a reduction in HA levels. Several examples are known where the final steps of antibiotic biosynthesis are intricately balanced with efflux. In the case of nystatin biosynthesis by *S. noursei*, disrupting the *nysH* and *nysG* genes for a putative type III ABC transporter resulted in accumulation of 10-deoxynystatin, a precursor of nystatin lacking the hydroxyl at C10 [144]. Further, expression in the mutant strains of an additional copy of *nysL*, which presumably encodes a monooxygenase for C10 hydroxylation, increased nystatin production with a concomitant decrease in 10-deoxynystatin. These observations indicated that the process of hydroxylation of the precursor is balanced with efficient efflux of the nystatin formed. Similarly, in landomycin A biosynthesis by *S. cyanogenus*, overexpression of the proton gradient-dependent transporter gene *lanJ* or disruption of the regulatory gene *lanK* that represses *lanJ* prevented completion of landomycin A biosynthesis and led to premature efflux of a precursor landomycin D [145]. A dideacetylated precursor has been suggested to be the true substrate for a type I ABC transporter present in chromomycin A3 biosynthetic gene cluster in *S. griseus* subsp. *griseus*. It was proposed that acetylation of the precursor occurs during transport by a membrane-bound acetyltransferase to form the final product, chromomycin A3 [146].

The results of *hyg19* disruption indicate that compound **2** is the penultimate product of the HA biosynthetic pathway, and that the conversion of **2** to HA by Hyg26 is the final step of HA biosynthesis, prior to efflux. The observed Hyg26 activity

supports this hypothesis. Since HA is the predominant product in the wild type, and as altered antibiotic production is observed only in the Δ*hyg19* mutant, it can also be hypothesized that the *hyg19* gene product is responsible for selective and efficient transport of HA under normal conditions. In the absence of *hyg19*, decreased efficiency of HA efflux would have a negative feedback effect on the biosynthetic pathway, resulting in lower HA yields and accumulation of **2**. The presence of HA and **2** in the fermentation broth of Δ*hyg19* further implies the existence of an alternative system for antibiotic efflux (FIGURE 37). This alternate transporter, which can potentially be the *hyg28*-encoded ABC transporter, would have reduced selectivity (exporting both HA and **2**) relative to the process mediated by Hyg19. It will be interesting to examine if the *hyg28* gene is upregulated in the Δ*hyg19* strain compared to the wild type.

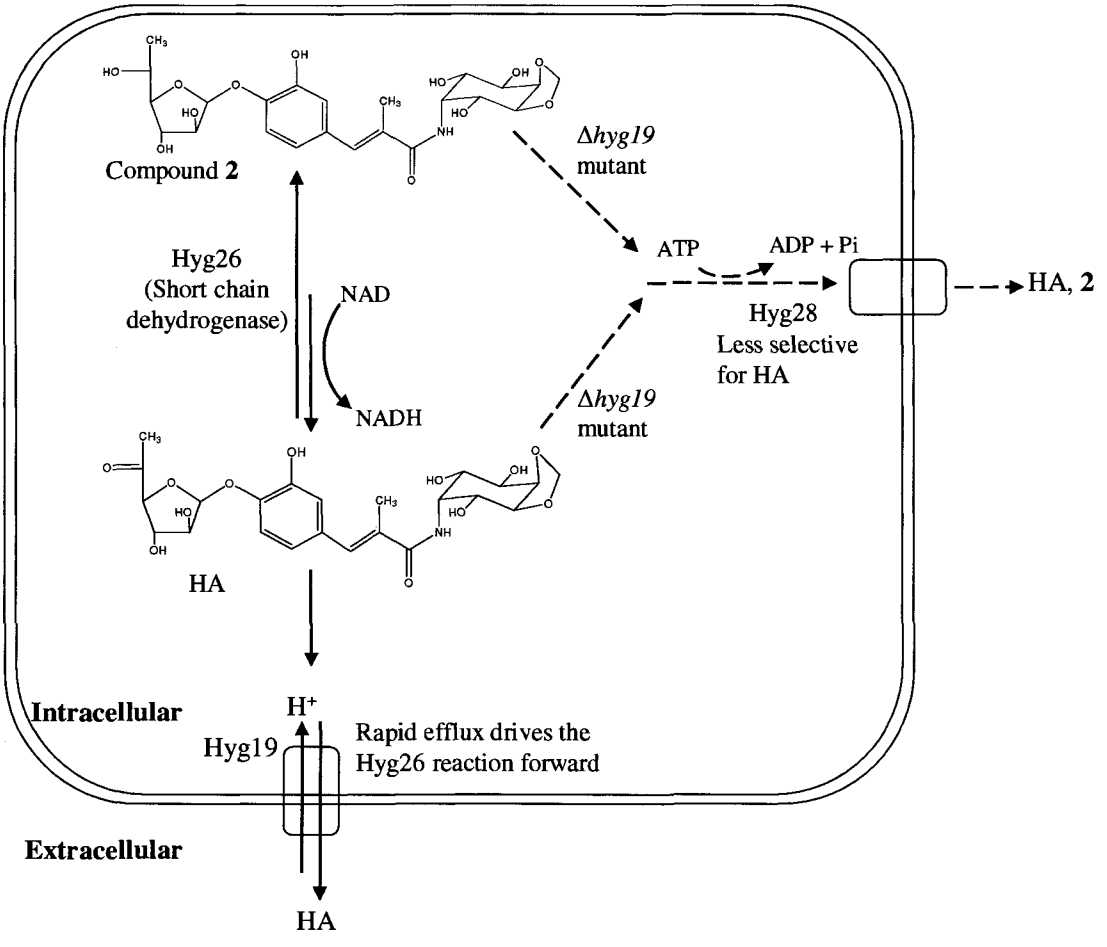


**FIGURE 37. A working hypothesis for the roles of Hyg19 and Hyg28 in antibiotic efflux.** The proton gradient-dependent transporter, Hyg19, is the primary HA transporter in the wild type. Efflux in the Δ*hyg19* strain is presumably brought about by the ABC transporter, Hyg28, which is less selective for hygromycin A.

While compounds **2** and **5** exhibit better *in vitro* activity than HA, the antibacterial activity is highest for HA (although the dataset is limited only to *E. coli* assays). This suggests that the HA biosynthetic process has evolved to produce and export HA as the major product because of some ecological advantage to *S. hygroscopicus* in its environmental niche.

The function of *hyg26* as a gene encoding a short chain dehydrogenase / reductase was already confirmed by gene disruption studies [40]. Most short chain dehydrogenase enzymes are dimers or tetramers and typically do not need a divalent metal ion for activity, unlike the classical metal-dependent 'medium chain' alcohol dehydrogenases [147, 148]. Analyses of Hyg26 in the present study showed that it occurs as a dimer and is metal ion-independent. The enzyme showed an absolute preference for NAD(H) and did not utilize NADP(H) as coenzyme. The coenzyme-binding site of short chain dehydrogenases preferring NAD(H) has an acidic residue (Asp or Glu) that forms hydrogen bonds with the 2'- and 3'- hydroxyl groups of the adenine ribose, whereas the binding site for NADP(H) has two basic residues (Arg or Lys) that interact with the 2'- phosphate and the acidic residue is replaced by a hydrophobic residue (Ala or Thr) [149, 150]. The specificity of Hyg26 for NAD(H) is consistent with the presence of an Asp residue at position 38 in the putative coenzyme-binding region in its sequence. The *in vitro* assays show that Hyg26 has reversible activity, but the reductase reaction (reverse) appears to be more favored than the dehydrogenase reaction (forward) under the given assay conditions. The high $K_m$ values of Hyg26 for HA, **3**, and **5** however indicate that the enzyme binds these substrates very poorly. Such high intracellular concentrations of these compounds are unlikely to exist under physiological conditions, considering the high efflux efficiency of Hyg19. It is possible that, under physiological conditions, removal of intracellular HA by its rapid export drives the Hyg26 reaction in the forward direction.

A gene inactivation experiment targeting all the four putative resistance determinants was also initiated to verify if HA self-resistance is conferred by any genes that are not a part of the HA biosynthetic gene cluster, but could not be accomplished due to technical difficulties. However, the present study has clearly shown that the ABC transporter and the proton gradient dependent transporter are individually dispensable for antibiotic efflux and self-resistance. On the other hand, the final step of HA biosynthesis catalyzed by the short-chain dehydrogenase is coupled with efficient efflux of HA by the proton gradient transporter (Hyg19), and in the absence of Hyg19, there is accumulation of the C5"-reduced precursor.

## 5. Conclusions and recommendations for future work

The work presented in this thesis describes the functional characterization of putative self-resistance genes in the biosynthetic gene cluster of hygromycin A (HA). The results have provided significant insights into the intrinsic resistance mechanisms of the HA-producer, *Streptomyces hygroscopicus* NRRL 2388, and have also revealed essential details about the biosynthesis of HA. The present data have also raised important questions and opened up new opportunities for further studies on HA biosynthesis and self-resistance.

**Conclusion 1:** The *hyg21* gene in the HA biosynthetic gene cluster encodes an ATP/GTP-dependent *O*-phosphotransferase that modifies the C5"-OH of HA and related compounds. Phosphorylation of HA abolishes its *in vivo* biological activity and *in vitro* translation inhibition activity. Disruption of *hyg21* also decreases HA production significantly, but the self-resistance of *S. hygroscopicus* is not affected.

**Future work:** The function of *hyg21* as a resistance gene can be verified by cloning the gene into a HA-susceptible *Streptomyces* strain such as *S. lividans* and examining it for acquired resistance to HA. Determining the HA resistance of the *E. coli* strain expressing Hyg21 versus a control *E. coli* will also validate the role of this gene in HA modification-mediated resistance. Genetic complementation of the Δ*hyg21* strain is expected to restore HA production, thereby confirming that the decrease in antibiotic yields is due to loss of *hyg21* and not due to polar effects arising from gene disruption.

Further, growing the Δ*hyg21* strain in the presence of phosphorylated HA (HA-P) and quantitating the antibiotic yields will reveal if HA-P has a regulatory effect on HA biosynthesis.

**Conclusion 2:** The *hyg6* gene encodes an *O*-methyltransferase that introduces the methylene group in the C4-C5 methylenedioxy bridge of HA. Loss of the methylenedioxy bridge reduces the antibacterial activity of HA. Disruption of the second methyltransferase homolog, *hyg29*, does not affect antibiotic production profile or self-resistance.

**Future work:** *In vitro* enzyme assays using recombinant Hyg6 and the proposed structural intermediates in the aminocyclitol biosynthetic sequence as substrates will determine the exact timing for *O*-methylation event in this pathway. Desmethylene hygromycin A can serve as starting material for the synthesis of HA derivatives with novel C4-C5 alkyl groups, thereby generating antibiotics with potentially improved activity. Ligand docking studies can be carried out to analyze the differences in binding of HA and related compounds to the 50S ribosomal subunit, and this information can subsequently be used to design better ribosome-binding analogs. In order to verify the proposed role of *hyg29* as an rRNA methyltransferase gene, the rRNA from the wild type and the Δ*hyg29* disruption strain can be examined for differences in methylation. The predicted role of *hyg29* can also be confirmed by *in vitro* rRNA methylation assays using the recombinant enzyme. Drug binding assays using ribosomes from the wild type and the Δ*hyg29* strain will also verify the

existence of target site modification as a self-resistance mechanism in *S. hygroscopicus.*

**Conclusion 3:** The *hyg28* gene, which encodes a putative ATP binding cassette transporter, is dispensable for HA biosynthesis and efflux. The *hyg19* gene, which encodes a putative proton gradient-dependent transporter, is essential for complete progression through the biosynthetic pathway and for optimal levels of antibiotic production. The dehydrogenation of 5"-dihydrohygromycin A by the NAD-dependent Hyg26 is the last step of HA biosynthesis and is interlinked with efficient efflux of HA by Hyg19. Self-resistance in *S. hygroscopicus* is a synergistic effect of more than one resistance determinant.

**Future work:** The proposed roles of *hyg19* and *hyg28* gene products as resistance determinants can be confirmed by expressing them in HA-sensitive strains and determining their levels of resistance. It will be informative to compare the expression levels of *hyg28* in the wild type and the Δ*hyg19* mutant, because upregulation of *hyg28* in the Δ*hyg19* strain will identify it as the alternate transporter gene in the absence of *Hyg19*. It will also be interesting to study the effects of disrupting both *hyg19* and *hyg28* on antibiotic production and efflux. Complementing the Δ*hyg19* strain with the disrupted gene is expected to restore the antibiotic production profile, which will verify that the accumulation of 5"-dihydrohygromycin A is an effect of gene disruption, and that the efficient conversion of 5"-dihydrohygromycin A to HA by the Hyg26 enzyme is dependent on the presence of Hyg19.

## References


1. Kieser, T., et al., *Practical Streptomyces Genetics.* 2000, Norwich, United Kingdom: The John Innes Foundation.
2. Omura, S., *The bacteria.* 1986. **IX**: p. xvii-xxi, Academic Press Inc., New York.
3. Vining, L.C., *Functions of secondary metabolites.* Annu Rev Microbiol, 1990. **44**: p. 395-427.
4. Martin, M.F. and P. Liras, *Organization and expression of genes involved in the biosynthesis of antibiotics and other secondary metabolites.* Annu Rev Microbiol, 1989. **43**: p. 173-206.
5. Vining, L.C., *Secondary metabolism, inventive evolution and biochemical diversity--a review.* Gene, 1992. **115**(1-2): p. 135-40.
6. Tropf, S., et al., *Heterologously expressed acyl carrier protein domain of rat fatty acid synthase functions in Escherichia coli fatty acid synthase and Streptomyces coelicolor polyketide synthase systems.* Chem Biol, 1998. **5**(3): p. 135-46.
7. Crump, M.P., et al., *Conserved secondary structure in the actinorhodin polyketide synthase acyl carrier protein from Streptomyces coelicolor A3(2) and the fatty acid synthase acyl carrier protein from Escherichia coli.* FEBS Lett, 1996. **391**(3): p. 302-6.
8. Revill, W.P., M.J. Bibb, and D.A. Hopwood, *Relationships between fatty acid and polyketide synthases from Streptomyces coelicolor A3(2): characterization of the fatty acid synthase acyl carrier protein.* J Bacteriol, 1996. **178**(19): p. 5660-7.
9. Shen, B., *Polyketide biosynthesis beyond the type I, II and III polyketide synthase paradigms.* Curr Opin Chem Biol, 2003. **7**(2): p. 285-95.
10. Staunton, J. and K.J. Weissman, *Polyketide biosynthesis: a millennium review.* Nat Prod Rep, 2001. **18**(4): p. 380-416.
11. Rix, U., et al., *Modification of post-PKS tailoring steps through combinatorial biosynthesis.* Nat Prod Rep, 2002. **19**(5): p. 542-80.
12. Donadio, S. and M. Sosio, *Strategies for combinatorial biosynthesis with modular polyketide synthases.* Comb Chem High Throughput Screen, 2003. **6**(6): p. 489-500.
13. Katz, L., *Manipulation of Modular Polyketide Synthases.* Chem Rev, 1997. **97**(7): p. 2557-2576.
14. Watve, M.G., et al., *How many antibiotics are produced by the genus Streptomyces?* Arch Microbiol, 2001. **176**(5): p. 386-90.
15. Bentley, S.D., et al., *Complete genome sequence of the model actinomycete Streptomyces coelicolor A3(2).* Nature, 2002. **417**(6885): p. 141-7.
16. Ikeda, H., et al., *Complete genome sequence and comparative analysis of the industrial microorganism Streptomyces avermitilis.* Nat Biotechnol, 2003. **21**(5): p. 526-31.

17. Oliynyk, M., et al., *Complete genome sequence of the erythromycin-producing bacterium Saccharopolyspora erythraea NRRL23338.* Nat Biotechnol, 2007. **25**(4): p. 447-53.
18. Ohnishi, Y., et al., *Genome sequence of the streptomycin-producing microorganism Streptomyces griseus IFO 13350.* J Bacteriol, 2008. **190**(11): p. 4050-60.
19. Taubes, G., *The bacteria fight back.* Science, 2008. **321**(5887): p. 356-61.
20. Levy, S.B. and B. Marshall, *Antibacterial resistance worldwide: causes, challenges and responses.* Nat Med, 2004. **10**(12 Suppl): p. S122-9.
21. Norrby, S.R., C.E. Nord, and R. Finch, *Lack of development of new antimicrobial drugs: a potential serious threat to public health.* Lancet Infect Dis, 2005. **5**(2): p. 115-9.
22. Pittenger, R.C., et al., *Hygromycin. I. Preliminary studies in the production and biologic activity on a new antibiotic.* Antibiot Chemother, 1953. **3**: p. 1268-78.
23. Yoshida, M., et al., *Hygromycin A and methoxyhygromycin A, novel inhibitors of K88 antigen synthesis of enterotoxic Escherichia coli strain.* Agric Biol Chem, 1986. **50**: p. 143-9.
24. Omura, S., et al., *Hygromycin A, an antitreponemal substance. I. Screening method and therapeutic effect for Treponema hyodysenteriae-caused infection in CF-1 mice.* J Antibiot (Tokyo), 1987. **40**(11): p. 1619-26.
25. Nakagawa, A., et al., *Hygromycin A, an antitreponemal substance. II. Therapeutic effect for swine dysentery.* J Antibiot (Tokyo), 1987. **40**(11): p. 1627-35.
26. Uyeda, M., et al., *Pentalenolactone I and hygromycin A, immunosuppressants produced by Streptomyces filipinensis and Streptomyces hygroscopicus.* Biosci Biotechnol Biochem, 2001. **65**(5): p. 1252-4.
27. Lee, H.B., et al., *A bleaching herbicidal activity of methoxyhygromycin (MHM) produced by an actinomycete strain Streptomyces sp. 8E-12.* Lett Appl Microbiol, 2003. **36**(6): p. 387-91.
28. Kim, S.D., et al., *Hygromycin, a plant growth inhibitor.* Korean Biochem. J., 1990. **23**(1): p. 23-25.
29. Jana, S. and J.K. Deb, *Molecular understanding of aminoglycoside action and resistance.* Appl Microbiol Biotechnol, 2006. **70**(2): p. 140-50.
30. Guerrero, M.D. and J. Modolell, *Hygromycin A, a novel inhibitor of ribosomal peptidyltransferase.* Eur J Biochem, 1980. **107**(2): p. 409-14.
31. Poulsen, S.M., C. Kofoed, and B. Vester, *Inhibition of the ribosomal peptidyl transferase reaction by the mycarose moiety of the antibiotics carbomycin, spiramycin and tylosin.* J Mol Biol, 2000. **304**(3): p. 471-81.
32. Mann, R.L., R.M. Gale, and R.F. Van Abeele, *Hygromycin. II. Isolation and properties.* Antibiot Chemother, 1953. **3**: p. 1279-82.
33. Jaynes, B.H., N.C. Elliott, and D.L. Schicho, *Semisynthetic hygromycin A analogs: synthesis and anti-bacterial activity of derivatives lacking the furanose moiety.* J Antibiot (Tokyo), 1992. **45**(10): p. 1705-7.

34. Hayashi, S.F., et al., *Structure-activity relationships of hygromycin A and its analogs: protein synthesis inhibition activity in a cell free system.* J Antibiot (Tokyo), 1997. **50**(6): p. 514-21.
35. Hecker, S.J., et al., *Semisynthetic modification of Hygromycin A. 2. Synthesis and antibacterial activity of aryl analogs.* Bioorg Med Chem Lett, 1993. **3**(2): p. 289-94.
36. Chida, N., et al., *Total synthesis of methoxyhygromycin and its 5-epimer.* Chem Lett, 1990: p. 423-26.
37. Hecker, S.J., et al., *Semisynthetic modification of Hygromycin A. 3. Synthesis and antibacterial activity of aminocyclitol analogs.* Bioorg Med Chem Lett, 1992. **2**(9): p. 1015-18.
38. Hecker, S.J., S.C. Lilley, and K.M. Werner, *Hygromycin A: preparation of aminocyclitol analogs defining the minimum functionality required for biological activity.* Bioorg Med Chem Lett, 1992. **2**(9): p. 1043-1046.
39. Habib el, S.E., J.N. Scarsdale, and K.A. Reynolds, *Biosynthetic origin of hygromycin A.* Antimicrob Agents Chemother, 2003. **47**(7): p. 2065-71.
40. Palaniappan, N., et al., *Production of hygromycin A analogs in Streptomyces hygroscopicus NRRL 2388 through identification and manipulation of the biosynthetic gene cluster.* Chem Biol, 2006. **13**(7): p. 753-64.
41. Gust, B., et al., *PCR-targeted Streptomyces gene replacement identifies a protein domain needed for biosynthesis of the sesquiterpene soil odor geosmin.* Proc Natl Acad Sci U S A, 2003. **100**(4): p. 1541-6.
42. Cundliffe, E., *How antibiotic-producing organisms avoid suicide.* Annu Rev Microbiol, 1989. **43**: p. 207-33.
43. Thompson, C.J., et al., *Biochemical characterization of resistance determinants cloned from antibiotic-producing streptomycetes.* J Bacteriol, 1982. **151**(2): p. 678-85.
44. Perez-Gonzalez, J.A., et al., *Biochemical characterization of two cloned resistance determinants encoding a paromomycin acetyltransferase and a paromomycin phosphotransferase from Streptomyces rimosus forma paromomycinus.* J Bacteriol, 1989. **171**(1): p. 329-34.
45. Miller, A.L. and J.B. Walker, *Accumulation of streptomycin-phosphate in cultures of streptomycin producers grown on a high-phosphate medium.* J Bacteriol, 1970. **104**(1): p. 8-12.
46. Walker, J.B. and M.S. Walker, *Streptomycin biosynthesis. Enzymatic synthesis of O-phosphorylstreptidine from streptidine and adenosinetriphosphate.* Biochim Biophys Acta, 1967. **148**(2): p. 335-41.
47. Mansouri, K. and W. Piepersberg, *Genetics of streptomycin production in Streptomyces griseus: nucleotide sequence of five genes, strFGHIK, including a phosphatase gene.* Mol Gen Genet, 1991. **228**(3): p. 459-69.
48. Vara, J., J.A. Perez-Gonzalez, and A. Jimenez, *Biosynthesis of puromycin by Streptomyces alboniger: characterization of puromycin N-acetyltransferase.* Biochemistry, 1985. **24**(27): p. 8074-81.

49. Fierro, J.F., C. Hardisson, and J.A. Salas, *Resistance to oleandomycin in Streptomyces antibioticus, the producer organism.* J Gen Microbiol, 1987. **133**(7): p. 1931-9.
50. Vilches, C., et al., *Role of glycosylation and deglycosylation in biosynthesis of and resistance to oleandomycin in the producer organism, Streptomyces antibioticus.* J Bacteriol, 1992. **174**(1): p. 161-5.
51. Quiros, L.M., et al., *Two glycosyltransferases and a glycosidase are involved in oleandomycin modification during its biosynthesis by Streptomyces antibioticus.* Mol Microbiol, 1998. **28**(6): p. 1177-85.
52. Zhao, L., et al., *Beta-glucosylation as a part of self-resistance mechanism in methymycin/pikromycin producing strain Streptomyces venezuelae.* Biochemistry, 2003. **42**(50): p. 14794-804.
53. Zhang, Q., et al., *Reevaluation of the final steps in the biosynthesis of blasticidin S by Streptomyces griseochromogenes and Identification of a novel self-resistance mechanism.* Tetrahedron, 2000. **56**: p. 693-701.
54. Cundliffe, E., *Mechanism of resistance to thiostrepton in the producing-organism Streptomyces azureus.* Nature, 1978. **272**(5656): p. 792-5.
55. Thompson, J., F. Schmidt, and E. Cundliffe, *Site of action of a ribosomal RNA methylase conferring resistance to thiostrepton.* J Biol Chem, 1982. **257**(14): p. 7915-7.
56. Zalacain, M. and E. Cundliffe, *Methylation of 23S rRNA caused by tlrA (ermSF), a tylosin resistance determinant from Streptomyces fradiae.* J Bacteriol, 1989. **171**(8): p. 4254-60.
57. Zalacain, M. and E. Cundliffe, *Cloning of tlrD, a fourth resistance gene, from the tylosin producer, Streptomyces fradiae.* Gene, 1991. **97**(1): p. 137-42.
58. Wilson, V.T. and E. Cundliffe, *Molecular analysis of tlrB, an antibiotic-resistance gene from tylosin-producing Streptomyces fradiae, and discovery of a novel resistance mechanism.* J Antibiot (Tokyo), 1999. **52**(3): p. 288-96.
59. Liu, M. and S. Douthwaite, *Resistance to the macrolide antibiotic tylosin is conferred by single methylations at 23S rRNA nucleotides G748 and A2058 acting in synergy.* Proc Natl Acad Sci U S A, 2002. **99**(23): p. 14658-63.
60. Holmes, D.J. and E. Cundliffe, *Analysis of a ribosomal RNA methylase gene from Streptomyces tenebrarius which confers resistance to gentamicin.* Mol Gen Genet, 1991. **229**(2): p. 229-37.
61. Levine, C., H. Hiasa, and K.J. Marians, *DNA gyrase and topoisomerase IV: biochemical activities, physiological roles during chromosome replication, and drug sensitivities.* Biochim Biophys Acta, 1998. **1400**(1-3): p. 29-43.
62. Maxwell, A., *The interaction between coumarin drugs and DNA gyrase.* Mol Microbiol, 1993. **9**(4): p. 681-6.
63. Steffensky, M., et al., *Identification of the novobiocin biosynthetic gene cluster of Streptomyces spheroides NCIB 11891.* Antimicrob Agents Chemother, 2000. **44**(5): p. 1214-22.

64. Pojer, F., S.M. Li, and L. Heide, *Molecular cloning and sequence analysis of the clorobiocin biosynthetic gene cluster: new insights into the biosynthesis of aminocoumarin antibiotics.* Microbiology, 2002. **148**(Pt 12): p. 3901-11.
65. Wang, Z.X., S.M. Li, and L. Heide, *Identification of the coumermycin A(1) biosynthetic gene cluster of Streptomyces rishiriensis DSM 40489.* Antimicrob Agents Chemother, 2000. **44**(11): p. 3040-8.
66. Thiara, A.S. and E. Cundliffe, *Cloning and characterization of a DNA gyrase B gene from Streptomyces sphaeroides that confers resistance to novobiocin.* Embo J, 1988. **7**(7): p. 2255-9.
67. Thiara, A.S. and E. Cundliffe, *Interplay of novobiocin-resistant and -sensitive DNA gyrase activities in self-protection of the novobiocin producer, Streptomyces sphaeroides.* Gene, 1989. **81**(1): p. 65-72.
68. Thiara, A.S. and E. Cundliffe, *Expression and analysis of two gyrB genes from the novobiocin producer, Streptomyces sphaeroides.* Mol Microbiol, 1993. **8**(3): p. 495-506.
69. Frohlich, K.U., et al., *Substitution of a pentalenolactone-sensitive glyceraldehyde-3-phosphate dehydrogenase by a genetically distinct resistant isoform accompanies pentalenolactone production in Streptomyces arenae.* J Bacteriol, 1989. **171**(12): p. 6696-702.
70. Krab, I.M. and A. Parmeggiani, *EF-Tu, a GTPase odyssey.* Biochim Biophys Acta, 1998. **1443**(1-2): p. 1-22.
71. Cappellano, C., et al., *Natural kirromycin resistance of elongation factor Tu from the kirrothricin producer Streptomyces cinnamoneus.* Microbiology, 1997. **143 ( Pt 2)**: p. 617-24.
72. Paulsen, I.T., M.H. Brown, and R.A. Skurray, *Proton-dependent multidrug efflux systems.* Microbiol Rev, 1996. **60**(4): p. 575-608.
73. Pao, S.S., I.T. Paulsen, and M.H. Saier, Jr., *Major facilitator superfamily.* Microbiol Mol Biol Rev, 1998. **62**(1): p. 1-34.
74. Tercero, J.A., R.A. Lacalle, and A. Jimenez, *The pur8 gene from the pur cluster of Streptomyces alboniger encodes a highly hydrophobic polypeptide which confers resistance to puromycin.* Eur J Biochem, 1993. **218**(3): p. 963-71.
75. Caballero, J.L., et al., *Organisation and functions of the actVA region of the actinorhodin biosynthetic gene cluster of Streptomyces coelicolor.* Mol Gen Genet, 1991. **230**(3): p. 401-12.
76. Jones, P.M. and A.M. George, *The ABC transporter structure and mechanism: perspectives on recent research.* Cell Mol Life Sci, 2004. **61**(6): p. 682-99.
77. Mendez, C. and J.A. Salas, *ABC transporters in antibiotic-producing actinomycetes.* FEMS Microbiol Lett, 1998. **158**(1): p. 1-8.
78. Guilfoile, P.G. and C.R. Hutchinson, *A bacterial analog of the mdr gene of mammalian tumor cells is present in Streptomyces peucetius, the producer of daunorubicin and doxorubicin.* Proc Natl Acad Sci U S A, 1991. **88**(19): p. 8553-7.

79. Linton, K.J., et al., *An ABC-transporter from Streptomyces longisporoflavus confers resistance to the polyether-ionophore antibiotic tetronasin.* Mol Microbiol, 1994. **11**(4): p. 777-85.
80. Fernandez, E., et al., *An ABC transporter is essential for resistance to the antitumor agent mithramycin in the producer Streptomyces argillaceus.* Mol Gen Genet, 1996. **251**(6): p. 692-8.
81. Rodriguez, A.M., et al., *Streptomyces antibioticus contains at least three oleandomycin-resistance determinants, one of which shows similarity with proteins of the ABC-transporter superfamily.* Mol Microbiol, 1993. **8**(3): p. 571-82.
82. Schoner, B., et al., *Sequence similarity between macrolide-resistance determinants and ATP-binding transport proteins.* Gene, 1992. **115**(1-2): p. 93-6.
83. Rosteck, P.R., Jr., P.A. Reynolds, and C.L. Hershberger, *Homology between proteins controlling Streptomyces fradiae tylosin resistance and ATP-binding transport.* Gene, 1991. **102**(1): p. 27-32.
84. Olano, C., et al., *A second ABC transporter is involved in oleandomycin resistance and its secretion by Streptomyces antibioticus.* Mol Microbiol, 1995. **16**(2): p. 333-43.
85. Barrasa, M.I., et al., *The ard1 gene from Streptomyces capreolus encodes a polypeptide of the ABC-transporters superfamily which confers resistance to the aminonucleoside antibiotic A201A.* Eur J Biochem, 1995. **228**(3): p. 562-9.
86. Peschke, U., et al., *Molecular characterization of the lincomycin-production gene cluster of Streptomyces lincolnensis 78-11.* Mol Microbiol, 1995. **16**(6): p. 1137-56.
87. Calcutt, M.J. and F.J. Schmidt, *Gene organization in the bleomycin-resistance region of the producer organism Streptomyces verticillus.* Gene, 1994. **151**(1-2): p. 17-21.
88. Beyer, S., J. Distler, and W. Piepersberg, *The str gene cluster for the biosynthesis of 5'-hydroxystreptomycin in Streptomyces glaucescens GLA.0 (ETH 22794): new operons and evidence for pathway-specific regulation by StrR.* Mol Gen Genet, 1996. **250**(6): p. 775-84.
89. Martinez, J.L. and F. Baquero, *Mutation frequencies and antibiotic resistance.* Antimicrob Agents Chemother, 2000. **44**(7): p. 1771-7.
90. Davies, J., *Inactivation of antibiotics and the dissemination of resistance genes.* Science, 1994. **264**(5157): p. 375-82.
91. Benveniste, R. and J. Davies, *Aminoglycoside antibiotic-inactivating enzymes in actinomycetes similar to those present in clinical isolates of antibiotic-resistant bacteria.* Proc Natl Acad Sci U S A, 1973. **70**(8): p. 2276-80.
92. Marshall, C.G., et al., *Glycopeptide antibiotic resistance genes in glycopeptide-producing organisms.* Antimicrob Agents Chemother, 1998. **42**(9): p. 2215-20.

93. Hopwood, D.A., *How do antibiotic-producing bacteria ensure their self-resistance before antibiotic biosynthesis incapacitates them?* Mol Microbiol, 2007. **63**(4): p. 937-40.
94. Hawkey, P.M., *The origins and molecular basis of antibiotic resistance.* BMJ, 1998. **317**(7159): p. 657-60.
95. D'Costa, V.M., et al., *Sampling the antibiotic resistome.* Science, 2006. **311**(5759): p. 374-7.
96. Altschul, S.F., et al., *Basic local alignment search tool.* J Mol Biol, 1990. **215**(3): p. 403-10.
97. Hulo, N., et al., *The PROSITE database.* Nucleic Acids Res, 2006. **34**(Database issue): p. D227-30.
98. Dinos, G., et al., *Dissecting the ribosomal inhibition mechanisms of edeine and pactamycin: the universally conserved residues G693 and C795 regulate P-site RNA binding.* Mol Cell, 2004. **13**(1): p. 113-24.
99. Szaflarski, W., et al., *New features of the ribosome and ribosomal inhibitors: non-enzymatic recycling, misreading and back-translocation.* J Mol Biol, 2008. **380**(1): p. 193-205.
100. Barrasa, M.I., J.A. Tercero, and A. Jimenez, *The aminonucleoside antibiotic A201A is inactivated by a phosphotransferase activity from Streptomyces capreolus NRRL 3817, the producing organism. Isolation and molecular characterization of the relevant encoding gene and its DNA flanking regions.* Eur J Biochem, 1997. **245**(1): p. 54-63.
101. Saraste, M., P.R. Sibbald, and A. Wittinghofer, *The P-loop--a common motif in ATP- and GTP-binding proteins.* Trends Biochem Sci, 1990. **15**(11): p. 430-4.
102. Walker, J.E., et al., *Distantly related sequences in the alpha- and beta-subunits of ATP synthase, myosin, kinases and other ATP-requiring enzymes and a common nucleotide binding fold.* Embo J, 1982. **1**(8): p. 945-51.
103. Fralick, J.A., *Evidence that TolC is required for functioning of the Mar/AcrAB efflux pump of Escherichia coli.* J Bacteriol, 1996. **178**(19): p. 5803-5.
104. Butler, A.R., S.A. Flint, and E. Cundliffe, *Feedback control of polyketide metabolism during tylosin production.* Microbiology, 2001. **147**(Pt 4): p. 795-801.
105. Hansen, J.L., et al., *The structures of four macrolide antibiotics bound to the large ribosomal subunit.* Mol Cell, 2002. **10**(1): p. 117-28.
106. Wahab, H.A., et al., *Refinement of a low-resolution crystal structure to better understand erythromycin interactions on large ribosomal subunit.* J Biomol Struct Dyn, 2008. **26**(1): p. 131-46.
107. Schlunzen, F., et al., *Structural basis for the interaction of antibiotics with the peptidyl transferase centre in eubacteria.* Nature, 2001. **413**(6858): p. 814-21.
108. Gandecha, A.R., S.L. Large, and E. Cundliffe, *Analysis of four tylosin biosynthetic genes from the tylLM region of the Streptomyces fradiae genome.* Gene, 1997. **184**(2): p. 197-203.
109. Kreuzman, A.J., J.R. Turner, and W.K. Yeh, *Two distinctive O-methyltransferases catalyzing penultimate and terminal reactions of macrolide*

*antibiotic (tylosin) biosynthesis. Substrate specificity, enzyme inhibition, and kinetic mechanism.* J Biol Chem, 1988. **263**(30): p. 15626-33.
110. Bauer, N.J., et al., *Purification, characterization, and kinetic mechanism of S-adenosyl-L-methionine:macrocin O-methyltransferase from Streptomyces fradiae.* J Biol Chem, 1988. **263**(30): p. 15619-25.
111. Decker, H., H. Motamedi, and C.R. Hutchinson, *Nucleotide sequences and heterologous expression of tcmG and tcmP, biosynthetic genes for tetracenomycin C in Streptomyces glaucescens.* J Bacteriol, 1993. **175**(12): p. 3876-86.
112. Summers, R.G., et al., *Nucleotide sequence of the tcmII-tcmIV region of the tetracenomycin C biosynthetic gene cluster of Streptomyces glaucescens and evidence that the tcmN gene encodes a multifunctional cyclase-dehydratase-O-methyl transferase.* J Bacteriol, 1992. **174**(6): p. 1810-20.
113. Ikeda, H., et al., *Cloning of the gene encoding avermectin B 5-O-methyltransferase in avermectin-producing Streptomyces avermitilis.* Gene, 1998. **206**(2): p. 175-80.
114. Chen, Z., et al., *[Effect of gene disruption of aveD on avermectins production in Streptomyces avermitilis].* Wei Sheng Wu Xue Bao, 2001. **41**(4): p. 440-6.
115. Motamedi, H., et al., *Characterization of methyltransferase and hydroxylase genes involved in the biosynthesis of the immunosuppressants FK506 and FK520.* J Bacteriol, 1996. **178**(17): p. 5243-8.
116. Charan, R.D., et al., *Dioxapyrrolomycin biosynthesis in Streptomyces fumanus.* J Nat Prod, 2006. **69**(1): p. 29-33.
117. Guy T. Carter, G.T., et al., *Biosynthetic origin of the carbon skeleton of simaomicin .alpha., a hexacyclic xanthone antibiotic.* J Org Chem, 1989. **54**(18): p. 4321-4323.
118. Staley, A.L. and K.L. Rinehart, *Biosynthesis of the streptovaricins: 3-amino-5-hydroxybenzoic acid as a precursor to the meta-C7N unit.* J Antibiot (Tokyo), 1991. **44**(2): p. 218-24.
119. Koda, S., et al., *Studies on a new antibiotic FR-900109. 2. X-ray structure determination of FR-900109 p-bromophenyl ester.* J Antibiot (Tokyo), 1983. **36**(9): p. 1237-8.
120. Blum, S., et al., *Biosynthetic capacities of actinomycetes. 5. Dioxolides, novel secondary metabolites from Streptomyces tendae.* J Basic Microbiol, 1996. **36**(1): p. 19-25.
121. Cui, C.B., et al., *Pseudoverticin, a novel benzoquinone-derived ansamycin antibiotic obtained as new cell cycle inhibitor from Streptomyces pseudoverticillus YN17707.* Tetrahedron Lett, 2007. **48**: p. 4839-43.
122. Chida, N., et al., *Total synthesis of methoxyhygromycin and its 5-epimer.* Chem. Lett., 1990. **19**(3): p. 423-426.
123. Flatt, P.M. and T. Mahmud, *Biosynthesis of aminocyclitol-aminoglycoside antibiotics and related compounds.* Nat Prod Rep, 2007. **24**(2): p. 358-92.
124. Higgins, C.F., *ABC transporters: from microorganisms to man.* Annu Rev Cell Biol, 1992. **8**: p. 67-113.

125. van Veen, H.W. and W.N. Konings, *Multidrug transporters from bacteria to man: similarities in structure and function.* Semin Cancer Biol, 1997. **8**(3): p. 183-91.
126. Bouige, P., et al., *Phylogenetic and functional classification of ATP-binding cassette (ABC) systems.* Curr Protein Pept Sci, 2002. **3**(5): p. 541-59.
127. van Veen, H.W., et al., *The homodimeric ATP-binding cassette transporter LmrA mediates multidrug transport by an alternating two-site (two-cylinder engine) mechanism.* Embo J, 2000. **19**(11): p. 2503-14.
128. Saier, M.H., Jr., et al., *The major facilitator superfamily.* J Mol Microbiol Biotechnol, 1999. **1**(2): p. 257-79.
129. Guilfoile, P.G. and C.R. Hutchinson, *Sequence and transcriptional analysis of the Streptomyces glaucescens tcmAR tetracenomycin C resistance and repressor gene loci.* J Bacteriol, 1992. **174**(11): p. 3651-8.
130. Liras, P., *Biosynthesis and molecular genetics of cephamycins. Cephamycins produced by actinomycetes.* Antonie Van Leeuwenhoek, 1999. **75**(1-2): p. 109-24.
131. Sheldon, P.J., et al., *Mitomycin resistance in Streptomyces lavendulae includes a novel drug-binding-protein-dependent export system.* J Bacteriol, 1999. **181**(8): p. 2507-12.
132. Zhang, H.Z., H. Schmidt, and W. Piepersberg, *Molecular cloning and characterization of two lincomycin-resistance genes, lmrA and lmrB, from Streptomyces lincolnensis 78-11.* Mol Microbiol, 1992. **6**(15): p. 2147-57.
133. Ma, Y., J. Patel, and R.J. Parry, *A novel valanimycin-resistance determinant (vlmF) from Streptomyces viridifaciens MG456-hF10.* Microbiology, 2000. **146 ( Pt 2)**: p. 345-52.
134. Blanc, V., et al., *Molecular characterization and transcriptional analysis of a multidrug resistance gene cloned from the pristinamycin-producing organism, Streptomyces pristinaespiralis.* Mol Microbiol, 1995. **17**(5): p. 989-99.
135. Tahlan, K., et al., *Initiation of actinorhodin export in Streptomyces coelicolor.* Mol Microbiol, 2007. **63**(4): p. 951-61.
136. Sambrook, J. and D.W. Russell, *Molecular cloning: A laboratory manual, Third Edition.* Third ed. 2001, Cold Spring Harbor, NY: Cold Spring Harbor Laboratory Press.
137. Kyte, J. and R.F. Doolittle, *A simple method for displaying the hydropathic character of a protein.* J Mol Biol, 1982. **157**(1): p. 105-32.
138. Saier, M.H., Jr., et al., *The Transporter Classification Database: recent advances.* Nucleic Acids Res, 2008.
139. Jones, D.T., *Improving the accuracy of transmembrane protein topology prediction using evolutionary information.* Bioinformatics, 2007. **23**(5): p. 538-44.
140. Dhote, V., S. Gupta, and K.A. Reynolds, *An O-phosphotransferase catalyzes phosphorylation of hygromycin A in the antibiotic-producing organism Streptomyces hygroscopicus.* Antimicrob Agents Chemother, 2008. **52**(10): p. 3580-8.

141. Persson, B., M. Krook, and H. Jornvall, *Characteristics of short-chain alcohol dehydrogenases and related enzymes.* Eur J Biochem, 1991. **200**(2): p. 537-43.
142. Ostash, I., et al., *Proton-dependent transporter gene lndJ confers resistance to landomycin E in Streptomyces globisporus.* Genetika, 2007. **43**(8): p. 1032-7.
143. Ostash, I., et al., *An ABC transporter encoding gene lndW confers resistance to landomycin E.* Arch Microbiol, 2008. **190**(1): p. 105-9.
144. Sletta, H., et al., *Nystatin biosynthesis and transport: nysH and nysG genes encoding a putative ABC transporter system in Streptomyces noursei ATCC 11455 are required for efficient conversion of 10-deoxynystatin to nystatin.* Antimicrob Agents Chemother, 2005. **49**(11): p. 4576-83.
145. Ostash, I., et al., *Coordination of export and glycosylation of landomycins in Streptomyces cyanogenus S136.* FEMS Microbiol Lett, 2008. **285**(2): p. 195-202.
146. Menendez, N., et al., *Involvement of a chromomycin ABC transporter system in secretion of a deacetylated precursor during chromomycin biosynthesis.* Microbiology, 2007. **153**(Pt 9): p. 3061-70.
147. Jornvall, H., et al., *Short-chain dehydrogenases/reductases (SDR).* Biochemistry, 1995. **34**(18): p. 6003-13.
148. Oppermann, U., et al., *Short-chain dehydrogenases/reductases (SDR): the 2002 update.* Chem Biol Interact, 2003. **143-144**: p. 247-53.
149. Tanaka, N., et al., *Crystal structure of the ternary complex of mouse lung carbonyl reductase at 1.8 A resolution: the structural origin of coenzyme specificity in the short-chain dehydrogenase/reductase family.* Structure, 1996. **4**(1): p. 33-45.
150. Kallberg, Y., et al., *Short-chain dehydrogenases/reductases (SDRs).* Eur J Biochem, 2002. **269**(18): p. 4409-17.